"AN *IN-VIVO* AND *IN-VITRO* STUDY OF HEPATOCELLULAR CARCINOMA COMPLICATIONS IN DIABETES MELLITUS"

Thesis submitted to

The KLE Academy of Higher Education and Research,

Belagavi

(KLE DEEMED UNIVERSITY)

[Declared as Deemed-to-be-University u/s 3 of the UGC Act, 1956 vide Govt. of India Notification No.F.9-19/2000-U.3 (A)]

(Accredited 'A' Grade by NAAC) (2nd Cycle)

[Placed in Category 'A' by MHRD (GoI)]

For the award of the degree of

Doctor of Philosophy

in the

Faculty of Pharmacy

By

Mr. Bhrigu Kumar Das M. Pharm.

(Registration No: KLEU/Ph.D/16-17/DO1216006)

KLE

EMPOWERING PROFESSIONALS

Under the Guidance of

Dr. P. C. GADAD M. Pharm., Ph.D.

KLE College of Pharmacy, Hubballi-580 031,
Karnataka, India

December-2021

UNDERTAKING

I, **Mr. Bhrigu Kumar Das** hereby declare that the information and the data mentioned in my thesis entitled **"An *in-vivo* and *in-vitro* study of hepatocellular carcinoma complications in diabetes mellitus"** belongs to me and is original.

I am aware of definition of plagiarism as detailed below:

- An act or instance of using or closely imitating the language and thoughts of another author without authorization and the representation of that author's work as one's own, as by not crediting the original author.
- A piece of writing or other work reflecting such unauthorized use or imitation.
- The deliberate or reckless representation of another's words, thoughts or ideas as one's own without attribution in connection with submission of academic work, whether graded or otherwise.

I hereby declare that the thesis prepared by me is original-one and does not involve plagiarism anywhere. In case at a later stage it is found that I have indulged in plagiarism, then I am solely responsible for the same and the Institution is at liberty to take any disciplinary action against me including cancellation of dissertation or any other penalties imposed by the University.

Place: Hubballi
Date:

Bhrigu Kumar Das
Full time Ph.D Research Scholar
Registration No.: DO1216006
KLE College of Pharmacy,
Hubballi.

PLAGIARISM REPORT

KLE ACADEMY OF HIGHER EDUCATION AND RESEARCH
(Formerly known as KLE University)
(Deemed-to-be-University established u/s 3 of the UGC Act, 1956)
ಕೆ.ಎಲ್.ಇ. ಎಕ್ಯಾಡಮಿ ಆಫ್ ಹಾಯರ್ ಎಜ್ಯುಕೇಶನ ಆ್ಯಂಡ್ ರಿಸರ್ಚ್
(ಕೆ.ಎಲ್.ಇ. ವಿಶ್ವವಿದ್ಯಾಲಯವೆಂದು ಮುಂಚೆ ಗುರುತಿಸಿದ)
(ವಿ.ಧ.ಆ.ಕಲಂ 3ರಡಿ ಸ್ವಾಯತ್ತ ವಿಶ್ವವಿದ್ಯಾಲಯವೆಂದು ಸ್ಥಾಪಿಸಲ್ಪಟ್ಟಿದೆ)
KLE EMPOWERING PROFESSIONALS
Accredited 'A' Grade by NAAC (2nd Cycle) Placed in Category 'A' by MHRD (GoI)

Ref. No. KAHER/AA/21-22/D- 231021003 2nd December 2021

Sir,

The soft copy of Ph.D. research thesis of **Mr. Bhrigu Kumar Das, Faculty of Pharmacy** of KAHER, Belagavi has been submitted for anti-plagiarism check at the office of the undersigned through "Turn-it-in" package. The scan has been carried out and the scanned output reveals a match percentage of **9%** which is within the acceptable limit of 10%.

To obtain the comprehensive report of the plagiarism test, research scholar can send a mail to **diracademic@kledeemeduniversity.edu.in** along with the Registration Number, Name of the Scholar, Name of Guide/Co-guide and title of the thesis.

DIRECTOR Deemed-to-be University ACADEMIC AFFAIRS

Dr.(Mrs.) Roopa M. Bellad
Director, Academic Affairs

To,

Mr. Bhrigu Kumar Das
Full-Time Ph.D. Scholar, 2016-17 Batch
Faculty of Pharmacy,
College of Pharmacy,
Hubballi.

Cc to :
1. The Principal, College of Pharmacy, KAHER, Bengaluru
2. Dr. P. C. Gadad, Associate Professor of Pharmacology, College of Pharmacy, Hubballi– Guide

KLE ACADEMY OF HIGHER EDUCATION AND RESEARCH,

(KLE DEEMED UNIVERSITY)

[Declared as Deemed-to-be-University u/s 3 of the UGC Act, 1956 1956 vide

Govt. of India Notification No.F.9-19/2000-U.3 (A)]

[Accredited 'A' Grade by NAAC (2nd Cycle)]

[Placed in Category 'A' by MHRD (GoI)]

BELAGAVI

Copyright Declaration

We hereby declare that **KLE ACADEMY OF HIGHER EDUCATION AND RESEARCH, BELAGAVI, KARNATAKA,** *shall have the rights to preserve, use and disseminate this thesis in print or electronic format for academic/research purpose.*

Bhrigu Kumar Das
Full time Ph.D Research Scholar
Registration No.: DO1216006
KLE College of Pharmacy,
Hubballi.

Dr. P. C. Gadad
Professor
Department of Pharmacology
KLE College of Pharmacy,
Hubballi.

Place: Hubballi
Date:

KLE ACADEMY OF HIGHER EDUCATION AND RESEARCH,

(KLE DEEMED UNIVERSITY)

[Declared as Deemed-to-be-University u/s 3 of the UGC Act, 1956 1956 vide

Govt. of India Notification No.F.9-19/2000-U.3 (A)]

[Accredited 'A' Grade by NAAC (2nd Cycle)]

[Placed in Category 'A' by MHRD (GoI)]

BELAGAVI

Declaration

I hereby declare that the thesis entitled **"An *in-vivo* and *in-vitro* study of hepatocellular carcinoma complications in diabetes mellitus"** *is a bonafide and original research carried out by me under the guidance of* ***Dr. P. C. Gadad****, Professor, Department of Pharmacology, KLE College of Pharmacy, Hubballi. The thesis or any part thereof has not formed the basis for the award of any degree/fellowship or similar title to any candidate of any University.*

Place: Hubballi
Date:

Bhrigu Kumar Das
Full time Ph.D Research Scholar
Registration No.: DO1216006
KLE College of Pharmacy,
Hubballi.

KLE ACADEMY OF HIGHER EDUCATION AND RESEARCH,

(KLE DEEMED UNIVERSITY)

[Declared as Deemed-to-be-University u/s 3 of the UGC Act, 1956 1956 vide

Govt. of India Notification No.F.9-19/2000-U.3 (A)]

[Accredited 'A' Grade by NAAC (2nd Cycle)]

[Placed in Category 'A' by MHRD (GoI)]

BELAGAVI

KLE
EMPOWERING PROFESSIONALS

Certificate

This is to certify that the thesis entitled **"An *in-vivo* and *in-vitro* study of hepatocellular carcinoma complications in diabetes mellitus"** is *a bonafide and genuine research carried out by* ***Mr. Bhrigu Kumar Das*** *under the guidance of* ***Dr. P. C. Gadad,*** *Professor, Department of Pharmacology, KLE College of Pharmacy, Hubballi.*

Place: Hubballi
Date:

Prof. (Dr.) M. S. Ganachari
Dean, Faculty of Pharmacy,
KLE College of Pharmacy,
Belagavi.

KLE ACADEMY OF HIGHER EDUCATION AND RESEARCH,

(KLE DEEMED UNIVERSITY)

[Declared as Deemed-to-be-University u/s 3 of the UGC Act, 1956 1956 vide

Govt. of India Notification No.F.9-19/2000-U.3 (A)]

[Accredited 'A' Grade by NAAC (2nd Cycle)]

[Placed in Category 'A' by MHRD (GoI)]

BELAGAVI

Certificate

This is to certify that the thesis entitled **"An *in-vivo* and *in-vitro* study of hepatocellular carcinoma complications in diabetes mellitus"** is *a bonafide and genuine research carried out by* ***Mr. Bhrigu Kumar Das*** *under the guidance of* ***Dr. P. C. Gadad,*** *Professor, Department of Pharmacology, KLE College of Pharmacy, Hubballi.*

Place: Hubballi
Date:

Prof. (Dr.) A. H. M. V. Swamy
Principal
KLE College of Pharmacy,
Hubballi.

KLE ACADEMY OF HIGHER EDUCATION AND RESEARCH,

(KLE DEEMED UNIVERSITY)

[Declared as Deemed-to-be-University u/s 3 of the UGC Act, 1956 1956 vide

Govt. of India Notification No.F.9-19/2000-U.3 (A)]

[Accredited 'A' Grade by NAAC (2nd Cycle)]

[Placed in Category 'A' by MHRD (GoI)]

BELAGAVI

Certificate

This is to certify that the thesis entitled **"An *in-vivo* and *in-vitro* study of hepatocellular carcinoma complications in diabetes mellitus"** *is a bonafide record of original research carried out by* ***Mr. Bhrigu Kumar Das*** *for the award of degree of* ***Doctor of Philosophy*** *in faculty of* ***Pharmacy*** *under my supervision and guidance.*

Place: Hubballi
Date:

Dr. P. C. Gadad
Professor
Department of Pharmacology
KLE College of Pharmacy,
Hubballi.

ACKNOWLEDGMENT

I want to express my thanks and acknowledge all the people that supported, encouraged, and helped me either directly or indirectly throughout my Ph.D. journey in many ways for the feat of the proposed work. In particular, I am grateful to:

My research guide, Respected Dr. P. C. Gadad sir for his valuable guidance, support, time, and constant encouragement. His practical knowledge, positive approach, stimulating discussion, and unending enthusiasm made my experience interesting, fruitful, and pleasing. I am highly obliged for his unconditional support that allowed me for timely presentation of this work in a true perspective.

Prof. (Dr.) A.H.M.V. Swamy, Principal, KLE College of Pharmacy, Hubballi, for his support and providing all the necessary facilities for completion of the research work.

Prof. (Dr.) V. G. Jamakandi, Former Principal, KLE College of Pharmacy, Hubballi and Prof. (Dr.) B. C. Koti, Former Vice-Principal, and Head, Department of Pharmacology, for their co-operation, motivation, and suggestion during the project.

The KLE Academy of Higher Education and Research, Belagavi, for grant of financial assistance (scholarship & contingency) to the full-time research scholars for two years to accomplish this project.

Dr. S. M. Choukimath, Department of Pathology, Karnataka Institute of Medical Sciences (KIMS), Vidyanagar, Hubballi, for his guidance and valuable support during the histopathological study.

Dr. K. Jayalakshmi, Department of Chemistry, Karnatak Science College, Dharwad, for generously sharing her expertise during the ^{1}H-NMR study.

The Sophisticated Analytical Instrument Facilities (SAIF) of Karnatak University, Dharwad for providing the instrumentation facility to carry out the NMR study.

The Cell Kraft Biotech Pvt. Ltd. Bangalore, for their support and guidance, to carry out the flow cytometry study.

I also wish to extend my deep gratitude to all the teaching, technical, and non-teaching staff members of KLE College of Pharmacy, Hubballi, for their generous support throughout my research work and for making every moment enjoyable.

It’s my privilege to express my heartful thanks for the efforts of eminent senior faculty members of KLE Academy of Higher Education and Research, Belagavi including the external resource persons for their mentorship during the course work of Ph.D.

A special thanks to Angels Pharma India Pvt. Ltd. Hyderabad, for providing the gift sample of metformin for my research work.

I am incredibly grateful to the editors, reviewers, and publishing team of Life Sciences, Heliyon, Future Journal of Pharmaceutical Sciences (FJPS), Indian Journal of Pharmaceutical Education and Research (IJPER), and the Diabetes Epidemiology and Management for their efforts and sparing their valuable time to identify our work and to publish the same in their revered journals.

I am indebted to all the family members, seniors, juniors, and friends for their constant cheer and for providing me with the forte and enthusiasm to reach my goals. I am grateful for them who stood by me over all these years for their love, affection, continuous encouragement, co-operation, and support that made me come to this stage.

I want to say thanks and express regret to anyone whose contributions were missed a special remark on this thesis.

Above all, I wish to express my gratitude and dedicate my thesis to the ***“God-almighty”***, who gave me the strength and courage to accomplish my dream and has showered upon me with their choicest blessings.

Thankfully I ever remain.

Bhrigu Kumar Das

TABLE OF CONTENTS

LIST OF ABBREVIATIONS

^{0}C	Degree celsius
%	Percentage
µg	Microgram
µl	Microliter
µM	Micromolar
α	Alpha
β	Beta
AFP	Alpha-fetoprotein
Akt	Protein kinase B (PKB)
ALP	Alkaline phosphatase
ALT	Alanine aminotransferase
AMPK	5´adenosine monophosphate-activated protein kinase
ANOVA	Analysis of variance
AST	Aspartate aminotransferase
ATP	Adenosine triphosphate
b.w.	Body weight
CAT	Catalase
CPCSEA	Committee for the Purpose of Control and Supervision of Experiments on Animals
d	Day
DB	Direct bilirubin
DEN	Diethylnitrosamine
DM	Diabetes mellitus
DMEM	Dulbecco's modified eagle medium
DMSO	Dimethyl sulfoxide
DNA	Deoxyribonucleic acid
DNPH	2,4-dinitrophenyl hydrazine
DTNB	5,5´-dithiobis (2-nitrobenzoic acid)
ELISA	Enzyme-linked immunosorbent assay
FBS	Fetal bovine serum

FITC	Fluorescein isothiocyanate
g	Gram
GGT	Gamma-glutamyl transferase
GMFI	Geometric mean fluorescence intensity
GPx	Glutathione peroxidase
GSH	Reduced glutathione
h	Hour
H_2O_2	Hydrogen peroxide
HbA_1c	Glycosylated hemoglobin
HCl	Hydrochloride
HCC	Hepatocellular carcinoma
HDL-c	High-density lipoprotein-cholesterol
H&E	Hematoxylin and eosin
HG	Hyperglycemia/high glucose
HI	Hyperinsulinemia/high insulin
IAEC	Institutional Animal Ethical Committee
IC_{50}	Inhibitory concentration-50
IDF	International Diabetes Federation
IFCC	International Federation of Clinical Chemistry and Laboratory Medicine
i.p.	Intraperitoneal
IR	Insulin resistance
IU	International Unit
kg	Kilogram
LDL-c	Low-density lipoprotein-cholesterol
LPO	Lipid peroxidation
M	Molar
MDA	Malondialdehyde
mg	Milligram
M.HCl	Metformin hydrochloride
min	Minute

ml	Milliliter
mm	Millimeter
mM	Millimolar
MTT	Methyl thiazolyl tetrazolium
NaCl	Sodium chloride
NG	Normoglycemic/normal glucose
nm	Nanometer
nM	nanomolar
NMR	Nuclear Magnetic Resonance
p	Probability
p.o.	Per oral
PBS	Phosphate buffer saline
PEPCK	Phosphoenolpyruvate carboxykinase
PI	Propidium iodide
RNA	Ribonucleic acid
ROS	Reactive oxygen species
rpm	Rotation per minute
SEM	Standard error of the mean
sec	Seconds
SGOT	Serum glutamic oxaloacetic transaminase
SGPT	Serum glutamic pyruvic transaminase
SOD	Superoxide dismutase
SREBP-1	Sterol regulatory element-binding protein-1
STZ	Streptozotocin
TB	Total bilirubin
TC	Total cholesterol
TG	Triglycerides
v/v	Volume by volume
W	Week
w/v	Weight by volume

LIST OF TABLES

LIST OF FIGURES

ABSTRACT

Background: Diabetes mellitus (DM) is a lifelong epidemic condition that has become one of the most significant global health emergencies in the 21st century, especially in developing countries. The increased levels of blood glucose or hyperglycemia for an extended period can lead to the development of serious life-threatening conditions such as neuro (nerve damage), nephron (kidney damage), retino (eye disease), and vascular complications. Beyond these classical complications, epidemiologic evidence suggests that the DM is correlated with a higher incidence of cancer of various organs, including liver. The probability of incidence and progression of malignant hepatocellular carcinoma (HCC) is high in the patients of DM as suggested by numerous case-control, cohort, and retrospective data-based studies. The complex association between DM and HCC is manifold. It may be attributed to metabolic alteration (hyperglycemia), hormonal disorders [insulin, adipokines, insulin-like growth factor (IGF)-1], obesity, immunological process (cytokines in inflammation) and even the treatment for diabetes (insulin analogs, secretagogues as sulfonylureas and incretins). Majority of reports clarify the association between high insulin level and HCC, and few epidemiological studies supports hyperglycemia as a cause for the progression of HCC. Moreover, the mechanistic link with the progression of HCC during diabetic condition may also be due to disturbances in the cell signaling pathways by stimulating the cancer proliferation factors. The DM pose as one of risk factors for development and progression of hepatic cancer either independently or synergistically for uncontrolled proliferation, mutations, invasion, migration, and survival of the tumor cells.

The results based on numerous epidemiological and experimental studies suggest that the biguanide class of anti-diabetic drug, metformin HCl has been associated with reduced cancer risk through inhibition of the growth of the tumor cells. On the other hand, two main bioactive aromatic phytoconstituents isolated from the rhizomes of *Acorus calamus*, alpha,

and beta-asarone as well as its extract has been reported for its cytotoxic effects as well as hypoglycemic effects. However, the asarone effect as cytotoxic agents in diabetic condition remains unexplored.

Objectives: This study aims to develop an animal model to replicate the clinical evidence for diabetic-HCC conditions and to evaluate the beneficial effects of asarone and metformin HCl in controlling the progression of HCC. The objectives of the present study are:

1. To investigate the role of hyperglycemia in aiding the progression of hepatocellular carcinoma.
2. To evaluate the role of asarone and metformin HCl in controlling the progression of hepatocellular carcinoma during hyperglycemia, and understand the underlying molecular mechanism.

Methodology: Experimental diabetes was induced in 6 to 8 h fasted rats by a single injection of freshly prepared streptozotocin (STZ) (55 mg/2 ml/kg b.w. *i.p.* prepared in 0.05 M citrate buffer, pH 4.5). The hepatocarcinogenesis in rats was induced by the administration of single injection of carcinogenic chemical agent diethylnitrosamine (DEN) (200 mg/ml/kg b.w. *i.p.* prepared in 0.9% w/v NaCl). Further, two weeks later, after confirmation of diabetes, another group received DEN to simulate the diabetic-HCC condition. The treatment group received a combination dose of α-and β-asarone (50 µg/1.5 ml/kg b.w., *p.o.*) prepared in 0.5% w/v sodium carboxymethyl cellulose were given in the ratio of 1:1 and metformin HCl (250 mg/1.5 ml/kg b.w.) for five days per week after two weeks of STZ+DEN injections. The blood/serum and liver samples were collected at the end of the experimental period (12 and 18-weeks) and subjected for the measurement of various biochemical parameters and histopathological observation of the liver.

The human HepG2 HCC cell line was used for the *in-vitro* study. A colorimetric based methyl thiazolyl tetrazolium (MTT) assay was used to predict the cytotoxicity of metformin HCl, α-asarone, and β-asarone on the HepG2 cell line. Further, the flow cytometry technique was used to measure the expression of the intracellular markers (AMPKα1, Akt, PCK-2, and SREBP-1) and cell cycle analysis in hyperglycemic (25 mM) condition.

Results: The STZ induced diabetic animals with severe hyperglycemia did not show the development of HCC until the end of 12-weeks. Conversely, hepatocarcinogenesis was observed in the DEN alone and STZ+DEN-induced animals. Whereas, the pre-administration of the diabetogenic agent (STZ) before initiation of DEN leads to the occurrence of HCC at least by a few weeks early as supported by all biochemical and histo-morphological changes. Further, the asarone and metformin-treated group either reduced or reversed the severity of hepatocarcinogenesis during the diabetic condition, indicating their chemo-preventive effect. This was supported by all the biochemical parameters (glucose, insulin, glycosylated hemoglobin, liver dysfunction markers, lipid profile and HCC bio-markers), ^{1}H-NMR based metabolomics (glycolysis, valine degradation and alanine, lipid and glutamate metabolism), oxidant-antioxidant imbalance, and histo-morphological evidence (inflammation score, hepatocyte ballooning score, Sirius-red positive area, nodule incidence, nodule multiplicity, relative nodular size,).

The results of the *in-vitro* study suggest that asarone and metformin treatment reduces (concentration-dependent manner) the proliferation and modifies the morphology of HepG2 cells. A time-dependent increase in the cell proliferation or viability was observed when the HepG2 cell was incubated with a high concentration of glucose (25 mM) compared to the cells cultured in normal glucose (5 mM) as measured by MTT assay, indicating that the glucose-rich condition enhances the proliferation of HepG2 cells. Further, asarone and metformin treatment reduce the cell proliferation through arresting the cell cycle at the G_0/G_1

phase during hyperglycemic condition. This was mediated by the activation of 5´adenosine monophosphate-activated protein kinase (AMPK) and inhibition of protein kinase B/Akt signaling pathways. This study also proved that the inhibition of phosphoenolpyruvate carboxykinase-2 (PCK-2) and sterol regulatory element-binding protein-1 (SREBP-1) indicate a link between the glucose metabolic pathway and HepG2 cell proliferation.

Conclusion: The present study concluded that the streptozotocin (STZ)-induced diabetogenic agent developed hepatic fibrosis as assessed by the Sirius red staining in study design II, but failed to progress to hepatocarcinogenesis (HCC) till the end of the study period. At the same time, the pre-administration of the diabetogenic agent (STZ) before initiation of DEN leads to the occurrence of HCC at least by a few weeks early. This suggests that hyperglycemia due to STZ alone has no impact on HCC development, but can precipitate the development of HCC when combined with DEN. Furthermore, oral administration of asarone and metformin HCl exhibited chemo-preventive activity in diabetic conditions as confirmed through *in-vivo* and *in-vitro* study.

Keywords: Diabetes mellitus, Hepatocellular carcinoma, Streptozotocin, Diethylnitrosamine, Asarone, Metformin HCl, HepG2 cells.

1. INTRODUCTION

1.1. BACKGROUND

Diabetes mellitus (DM) is a lifelong epidemic condition that has become one of the most significant global health emergencies in the 21st century, especially in developing countries. The International Diabetes Federation (IDF) predicts an estimated rise of 700 million people (20–79 years) with diabetes worldwide by 2045 than 463 million in 2019, with the highest rate in the Western Pacific, Middle-East, South-East Asia and North Africa. The United States of America, China and India were the top three countries with the most significant number of adults with diabetes in 2019 among the age group 20 to 79 years, and this is expected to continue till 2045.[1]

The DM, a chronic metabolic disorder with increased blood glucose levels, causes abnormal carbohydrate, protein and fat metabolism because of beta-cells' insufficient insulin utilization or secretion.[2] With an effort to reduce mortality due to the severe consequences from its complications, world leaders, as part of the 2030 agenda, have set diabetes among the four priorities of non-communicable diseases (NCDs).[3] The increased levels of blood glucose or hyperglycemia for an extended period can lead to the development of severe life-threatening conditions such as neuro (nerve damage), nephron (kidney damage), retino (eye disease), and vascular complications.[4] Despite the various treatment approach and awareness for diabetes, it is estimated that half of the populations with high glucose are unaware of the disease and subsequently are more prone to diabetic associated-complications.[5] As noted, beyond these classical complications, epidemiological evidence suggests that diabetes is linked to an increased risk of cancer in various organs, including the stomach, liver,

colorectal, reproductive organs, breast, pancreas, and urinary tract.[6] The chance of malignant hepatocellular carcinoma (HCC) development and progression is high in diabetic patients among these cancers, as evidenced in numerous cohorts, case-control and retrospective data-based studies. Furthermore, diabetes is also likely to be an independent risk factor for the HCC progression, along with others such as viral hepatitis, heavy alcohol consumption, exposure to aflatoxin-contaminated food, non-alcoholic steatohepatitis (NASH) and cirrhosis.[7-9]

The liver is a vital organ and plays a crucial role in glucose metabolism. High glucose-associated diabetes has been linked with a spectrum of liver diseases involving alteration of the liver enzymes leading to acute liver failure, fatty liver, chronic hepatitis, and cirrhosis. During diabetes, the liver undergoes various changes with the biochemical and histopathological profile, as observed in experimentally induced *in-vivo* models. The liver injury with the induction of experimental diabetes can be initially correlated with the changes observed in lipid risk ratios and increased liver function enzymes, such as alkaline phosphatase (ALP), aspartate aminotransferase (AST), and alanine aminotransferase (ALT). The deposition of fat or glycogen in the hepatic cells results in hypertrophy, which is considered a significant histopathological shift. Besides these, there are signs of increased mitochondrial volume fractions, damaged nuclear membrane, a considerable decrease in the endoplasmic reticulum, and reduced concentrations of pyknotic nuclei at the subcellular level.[10-12] Furthermore, these modifications combined with other pathological factors affect the collagen balance of the liver, contributing to fibrosis and cirrhosis development.[13-15]

Several epidemiological studies indicate a significant association between DM and HCC.[8] The complex association between DM and HCC is manifold. It may be

attributed to metabolic alteration (hyperglycemia), hormonal disorders [insulin, adipokines, somatomedin C], immunological process (inflammatory cytokines), obesity, and even on treatment for diabetes (insulin analogs, secretagogues as sulfonylureas and incretins). Many reports establish a connection between increased insulin and liver cancer, and a small number of observational studies favor high glucose as a factor for HCC progression.[16-19] Moreover, the mechanistic link with the progression of HCC during diabetic conditions may also be due to disturbances in the cell signaling pathways by stimulating the cancer hallmarks. These hallmarks of DM pose risk factors for the development and progression of hepatic cancer either independently or synergistically for uncontrolled proliferation, mutation, invasion, migration, and survival of the tumor cells.[20]

The current approaches used in the treatment of diabetes include drugs that can either overcome insulin resistance (metformin, thiazolidinediones) or improve insulin availability (insulin, sulfonylureas). The primary goal of managing diabetes is to reduce diabetes-associated complications through appropriate glucose control.[21] Remarkably, various reports of *in-vitro* and *in-vivo* studies have suggested that drugs used to treat diabetes are associated with cancer risk. Several reports suggest that insulin, incretin-based therapies, and insulin secretagogues are associated with increased cancer prevalence and cancer-related mortality. Whereas, evidence from numerous epidemiological and experimental-based studies indicates that metformin HCl, a biguanide class of anti-diabetic medication, is associated with a lower risk of cancer by inhibiting the growth of the tumor cells. The reported mechanism of action from various studies includes reduced insulin-like growth factor, inhibition of energy metabolism, partial cell cycle arrest, inhibition of angiogenesis, apoptosis, and 5′

adenosine monophosphate-activated protein kinase (AMPK) activation thereby inhibiting mammalian target of rapamycin (mTOR) signaling.[6,22-26]

Studies have endeavored that anti-proliferative agent derived from traditional medicine offer efficacy with mild side effects and strong chemotherapeutic effects. Therefore, these anti-proliferative derived compounds from plants are used in alternative and evidence-based medical systems along with conventional chemo and/or radiation therapy.[27] *Acorus calamus* (L.) (Sweet flag) has generated significant interest and is widely used in Indian and Chinese folk medicine to treat various diseases, either alone or with other herbs. The cytotoxic and anti-hyperglycemic effects of the two biologically active aromatic phytoconstituents extracted from the rhizomes of *A. calamus*; alpha or beta-asarone, or its extract, have been documented.[28,29] Nevertheless, the impact of asarone as cytotoxic agents in diabetic condition have yet to be investigated.

Given the above, this research aimed to look into high glucose or hyperglycemia in aiding the progression of hepatocarcinogenesis (HCC). In addition, it also focused on how the combined effects of alpha (α)-and beta (β)-asarone and metformin HCl in regulating the disease progression on the chemically induced *in-vivo* model and human hepatocellular carcinoma HepG2 cells.

1.2. LITERATURE REVIEW

1.2.1. Diabetes mellitus (DM)

Diabetes mellitus (DM) is frequently considered diabetes, a clinically heterogeneous group of syndromes of disordered metabolism with unusually high blood glucose levels (hyperglycemia) sharing glucose intolerance in common. It is a chronic condition due to a defect in insulin utilization and/or secretion by the pancreas' beta (β)-cells. The β-ells of the pancreas secreting insulin play an essential role in glucose homeostasis and increases the metabolic process of glycolysis, lipogenesis, protein synthesis, and glycogenesis and decrease gluconeogenesis. The β–cells fail to compensate for the stress of insulin resistance in peripheral tissue, leading to a gradually rising blood glucose level and developing hyperglycemia. The prolonged effect of chronic hyperglycemia over time results in the onset of DM.[30,31]

The two most important types of DM are insulin-dependent type 1 diabetes mellitus (ID-T1DM) with defective insulin production and noninsulin-dependent type 2 diabetes mellitus (NID-T2DM) with poor utilization of insulin (insulin resistance). Besides these, the other types of DM include gestational diabetes (detected any time during pregnancy), genetically modified monogenic diabetes observed among the youngs and neonates, secondary diabetes (resultant of complication of other diseases as due to disturbances of hormone includes acromegaly or Cushing’s disease or pancreatic disorders) and chemical/drug-induced diabetes (Glucocorticoids, Niacin, Pentamidine, etc.) as summarized in the table 1.[1,32]

The T1DM is an auto-immune response in which the body's immune system targets the β-cells of the pancreas, resulting in decreased insulin production. It usually occurs in young adults or children who need insulin therapy every day to control their

blood glucose levels. Henceforth, based on etiology, TIDM is widely used to describe insulin-dependent diabetes mellitus (IDDM).[1,32]

The T2DM is the most predominant form of diabetes (around 90%) and is caused by a defect in insulin utilization and/or secretion, leading to high blood glucose levels. It usually occurs in adults, although increasing cases in adolescents and children are also observed. The β-cells of the pancreas producing insulin become resistant and cannot be utilized, and after that, the insulin levels may become insufficient over time. Henceforth, based on etiology, T2DM is widely used to describe noninsulin-dependent diabetes mellitus (NIDDM).[1,32]

The symptoms of both types of diabetes are similar, although their severity varies. These include hyperglycemia, polydipsia (extreme thirst), polyphagia (extreme eating), polyuria (excessive amounts of urine), weight loss (unintentional), fatigue, abnormalities in vision and changes in energy metabolism.[1]

Table 1: Classification of Diabetes: The classification is based on the associated factors, diagnostic criteria and the treatment/management of diabetes.[1,32,33]

Diabetes mellitus (DM)	**Old terminology**	**Associated factors**	**Diagnostic criteria**	**Treatment/Management***
Insulin-dependent type 1 diabetes mellitus.	Juvenile-onset diabetes, Ketosis-prone diabetes.	Genetic, environmental, acquired factors, auto-immune reactions (type 1a), or idiopathic (type 1b; no evidence of autoimmunity) leading to immunological destruction of pancreatic β–cells with little or no endogenous insulin production.	When the fasting glucose level is more than 126 mg/dl. *or* more than 200 mg/dl following 2 hr after a 75 g oral glucose load.	Daily insulin therapy, monitoring of blood glucose levels regularly, and maintaining a healthy lifestyle and diet.
Non-insulin-dependent type 2 diabetes mellitus.	Adult/Maturity-onset diabetes, Ketosis-resistant diabetes.	Evidence on past family cases of diabetes indicates genetic factors and other factors like lack of physical activity, obesity, and poor nutrition, leading to defect in insulin utilization and/or secretion.		Oral hypoglycemic agents, regular physical activity, and maintenance of a healthy diet.

Gestational diabetes mellitus (GDM; onset of glucose intolerance during pregnancy).	Gestational diabetes.	Changes in metabolic and hormonal levels; being incompletely understood. Also, insulin resistance (IR) may be responsible for GDM.	When the fasting glucose level is between 92–125 mg/dl. *or* more than 180 mg/dl following 1 hr after a 75 g oral glucose load. *or* in between 153–199 mg/dl following 2 hr after a 75 g oral glucose load.	Blood glucose monitoring, maintenance of a healthy diet, and gentle exercise. In a few cases, insulin therapy or oral medication may also be prescribed.
Other specific types related to certain syndromes (Genetic syndromes, pancreatic disease, abnormalities	Secondary diabetes.	The etiologic association of secondary diabetes is related to pancreatic disease or hormonal (hypo or hyperinsulinemic) or intake of certain drugs [hormonally active agents like	The diagnostic criteria and regimen for secondary diabetes can be made as described above for the T1 and T2DM and associated syndromes/conditions.	

in insulin receptor, chemical or drug-induced/hormonal).		glucocorticoids, oral contraceptives, thyroid hormones, psychoactive agents (Chlorpromazine, Amitriptyline, Lithium carbonate, Haloperidol), anti-neoplastic agents like Alloxan (ALX), Streptozotocin (STZ) and others drugs like Isoniazid, Nicotinic acid, etc.]. Besides these, it is also suspected because of a higher frequency of association of diabetes with genetic syndromes [Glycogen-storage disease-(GSD) type I, hyperlipidemia, etc.].	

* People who have any diabetes may need other medication classes to maintain lipid profile and blood pressure.

1.2.1.1. Pathophysiology of DM

Based on the associated factors of DM, an increase in the blood glucose level may result from reduced endogenous insulin production or defect in insulin utilization. Physiologically, insulin produced by the pancreatic β-cells stored within the vacuoles are found in the islets of Langerhans and is regulated by an elevation of blood glucose level. After a meal, an increase in the plasma glucose concentrations stimulates glucose transport into β-cells via glucose transporter proteins, GLUT1 and GLUT2. Furthermore, the islet transcription factor glucokinase catalyzes glucose to glucose-6-phosphate, which metabolizes and produces cellular ATP levels. The generation of ATP modifies the activity of the ions, thus inhibiting the K^+-dependent ATP-sensitive channel (K^+ATP) on the membrane resulting in membrane depolarization due to the accumulation of intracellular potassium. This, in turn, opens the voltage-gated Ca^{2+} channel ensuing in the influx of calcium ions, which stimulates insulin release.[34,35]

The pathogenesis concerning the T1DM is due to pancreatic β-cells mass destruction, typically leading to endogenous insulin deficiency. Type 1a diabetes is auto-immune mediated, while type 1b diabetes remains idiopathic. The pathogenesis of T1DM can be explained based on the following mechanism.[34]

1. The autoreactive T-cell mediated cytotoxicity selectively targets pancreatic β-cells while leaving the other islet cell types unaffected, resulting in immunological abnormalities.

2. The presence of islet cell antibodies against insulin, the role of CD8+T-lymphocytes, along with a variable number of macrophages and CD4+T-lymphocytes (insulitis), can also lead to auto-immunity.

3. In about 10–20% of cases, type 1a diabetes with other auto-immune diseases such as Addison's disease (adrenal insufficiency), Graves' disease (hyperthyroidism), Hashimoto's thyroiditis (chronic lymphocytic thyroiditis), etc. can also lead to auto-immunity.

4. If one of the identical twins has type 1a diabetes, the chance of the second twin developing the same is about 50%, but not all, as some other additional aspects are involved with the progression of the disease.

5. Besides these, the involvement of environmental factors may trigger the development of diabetes after several years. The experimentally induced diabetes mellitus can be achieved with chemicals like Alloxan (ALX), Streptozotocin (STZ), and Pentamidine. Other possible associations are early exposure to bovine milk proteins, certain viral infections as cytomegalovirus, measles, etc. can increase type 1a diabetes.[34]

The pathogenesis concerning T2DM is due to a defect in the utilization of insulin (insulin resistance) by the peripheral tissues (skeletal muscle, fat, and liver) and/or secretion of insulin relative to glucose load with a progressive decline in the pancreatic β–cell function. The pathogenesis of T2DM can be explained based on the following mechanism.[34,35]

1. The lack of insulin sensitivity by the peripheral tissues due to obesity is one of the prominent metabolic factors strongly associated with the defect in insulin utilization (IR; insulin resistance), thereby leading to T2DM. Henceforth, the mechanisms behind the increased blood glucose levels in T2DM (insulin resistance) can be explained as:

- Insulin resistance impairs the proper utilization of glucose.
- Increase in the hepatic synthesis of glucose.
- Obesity-related cytokines (adiponectin and tumor necrosis factor-alpha) and free fatty acids affect the peripheral tissues, thereby playing IR.
- The mechanism of polymorphism may be one of the defects for IR in various post-receptor intracellular signal pathways.

2. The impaired insulin secretion is also interlinked with T2DM in response to IR. During the initial phase of the disease, there is a compensatory rise in insulin secretion (hyperinsulinemia) to balance the normal blood glucose levels in the body. Furthermore, the pancreatic β-cells partially fail to secrete an adequate quantity of insulin for its action. The possible mechanisms behind the increased blood glucose levels in T2DM (impaired insulin secretion) can be explained as:
    - The fibrillar protein accumulation in islets of the pancreas due to amylin in T2DM may be one reason for the impaired function of pancreatic β-cells of the islet.
    - Glucose toxicity due to long-standing hyperglycemia act as a suitable metabolic environment for impaired β-cell function.
    - The lipo-toxicity due to increased free fatty acid levels may also worsen the β-cell function.
3. If one of the identical twins develops T2DM, the chance of the second twin developing the same is about 80%. Furthermore, the risk for developing

diabetes in the offspring rises to 40% if both parents have T2DM. Although there is a more significant role in genetic inheritance, no definite and consistent genes have been identified. Few genes found to be associated with T2DM are Transcription factor 7-like (TCF7L2) gene, Calpain-10 gene, Maturity onset diabetes of young (MODY) genes [hepatocyte nuclear factor-(HNF-4a and HNF-1β)] and Peroxisome proliferator geneγ2.

4. Besides these, the involvement of certain environmental factors such as hypertension, obesity, or lack of physical activity may trigger the phenotyping of the disease.[34,35]

1.2.1.2. Experimental models for assessing DM

Various *in-vivo* and *in-vitro* models have been used extensively in research to study the pathogenesis of human diabetes. However, due to different factors and uncertain etiology of diabetes, numerous models are employed, where the induction of disease is due to different mechanisms with a wide range of advantages. The commonly used animal models of diabetes mellitus are explained in table 2.

Table 2: The major animal models of diabetes mellitus (DM).

A. Pharmacological induction of DM (Chemically-induced models): The commonly used *in-vivo* chemically-induced diabetic models are classified based on the administration, mechanism, and significance.[36-40]

Drugs/Chemicals	Administration	Mechanism	Significance
Streptozotocin (STZ)	subcutaneous (*s.c.*), intra-venous (*i.v.*), intraperitoneal (*i.p.*).	The STZ enters the GLUT2 receptor and causes deoxyribonucleic acid (DNA) alkylation in the pancreatic β–cells. Furthermore, due to the activation of polyadenosine diphosphate ribosylation and nitric oxide secretion, the β-cells become necrotic.	Syndromes similar to either T1DM or T2DM can be simulated according to the administered dose of STZ/ALX. Thus, it offers a better understanding of the effect of various compounds within 20–30 days.
Alloxan (ALX)		Dialuric acid, the reduced ALX product, begins a redox cycle with superoxide radical's production. Furthermore, these radicals undergo dismutation due to the massive increase in cytosolic calcium concentration, where the pancreatic β-cells are destroyed.	

B. Genetic models of DM: The commonly used genetic models of diabetes are classified based on the description and significance.[40-42]

Animal models	Description of the model	Significance
db/db mouse (C57BL/KSJ strain)	The inherited autosomal recessive mutation on chromosome 4 of the strain is in the db gene encoding leptin receptors.	They are spontaneously hyperphagic and obese, exhibiting insulin resistance (IR) within the first month of age and progress to hyperglycemia (HG) and hyperinsulinemia (HI) later between 3rd and 4th months of age. Furthermore, the disease advances to diabetic nephropathy and ketosis, similar to the T2DM of humans.
ob/ob mouse (C57BL/6J strain)	The inherited autosomal recessive mutation on chromosome 6 of the strain is in the leptin gene encoding leptin protein.	They are hyperphagic and obese, exhibiting diabetes-like syndrome with mild HG, severe HI, mild insulin glucose tolerance (IGT), IR, and impaired wound healing.
Zucker fatty rat (fa/fa) or obese rat	The simple autosomal recessive (fa) gene on chromosome 5 of the strain encodes for leptin receptors.	They are hyperphagic and obese, mimicking the early T2DM stage similar to humans within four weeks with increased fat deposition, mild HG, mild glucose intolerance, IR, hyperlipidemia, HI, and moderate hypertension.

NOD (Non-obese diabetic) mouse	It was developed from a strain (the JcI-ICR mouse) through selective breeding, which was used for the first time in the study of cataract development.	At the age of 4–5 weeks, the mice develop insulitis, followed by pancreatic β-cells damage (through immune attack with macrophages, natural killer, T and B cells) and decreased insulin levels. They are remarkably analogous to the T1DM of humans.
BB (Bio-breeding) rat	It was first recognized in Bio-Breeding Laboratories in Ottawa. The mechanism of developing insulitis is the same as the NOD mouse.	At around 12 weeks, the rat develops weight loss, polydipsia, polyuria, HG, and insulinopenia.

C. Surgical models of DM: The effects of natural products have been screened for the anti-diabetic activity through complete removal of the pancreas with species like rats, dogs, pigs, and primates to obtain hyperglycemia. But, limitations to this technique have opted for a better alternative. Few limitations are:

- The availability of technical expertise due to major surgery and the risk of animal infection.
- The requirement and maintenance of an adequate surgical room environment.
- The suitable administration of antibiotics and analgesia post-operation, and
- Intake of pancreatic enzymes (for malabsorption).[40]

1.2.2. Hepatocellular carcinoma (HCC)

The HCC is the most frequent malignant type of primary cancer and accounts for nearly 75% of all liver cases.[43] Globally, it represents the fourth most frequent cause of cancer-related deaths with high prevalence rates predominantly in South-Eastern/Eastern Asia and Africa, followed by intermediate rates in Southern Europe and low rates in most high-income countries.[43-45] Furthermore, male patients are at higher risk than females, increasing with age.[43] The clinical signs and symptoms in patients with HCC include gastrointestinal hemorrhage, abdominal discomfort, jaundice, weight loss, fatigue, loss of appetite, ascites, blood in the stool, fluid in the abdomen, fever, hepatomegaly, nausea, and vomiting.[46,47] The global burden of HCC are probably resultant of:

1. Failure to identify people at risk of viral infections (as hepatitis B and/or C).
2. The population has a high prevalence of common etiological factors.
3. Lack of medical skills and facilities for early detection.
4. Lack of operative treatment options among the patients with an advanced stage of hepato-carcinoma after diagnosis.
5. Poor responsiveness, with inadequate or ambiguous attendance in HCC surveillance programs.[46,47]

The various risk accompanying HCC factors are chronic hepatitis B and/or C virus infection (HBV and/or HCV), cirrhosis, dietary (nutritional) and toxic factors, heavy alcohol drinking, non-alcoholic fatty liver disease (NAFLD), tobacco smoking, hormones and chemicals, race/ethnicity and gender as explained in detail in table 3.[43,45,48]

Table 3: The major risk factors for hepatocellular carcinoma (HCC).[43,45,46,48-53]

Risk factors	Examples	Characteristic features/Mechanisms
Infection with the hepatitis B/C virus (HBV/HCV).	**HBV:** A small DNA virus (Hepatotropic DNA viruses) known as hepadnaviruses.	▪ The HBV infection increases the inflammatory cell turnover in the hepatocytes leading to the release of cytokines and ultimately leads to lysis of the infected cells. ▪ Incorporating the hepatitis B DNA genome into the host genome disrupts the regulatory elements of DNA methylation, cell cycling, histone modifications, and RNA interference. ▪ Transmission: Up to 90% of infected people, including mothers of newborns, have a chronic infection.
	HCV: Single-stranded RNA genome.	▪ The direct role of HCV infection in the pathogenic mechanisms of HCC is less understood. ▪ However, DNA methylation, histone modifications, and RNA interference may be frequently associated with HCC.
Dietary (Nutritional)	**Aflatoxin:** A mycotoxin	▪ It thrives on foods like peanuts (kept in damp and warm conditions),

and toxic factors.	produced by *Aspergillus parasiticus* and *Aspergillus flavus*.	corn, or consuming the animal's meat fed with aflatoxin-contaminated cereals. ▪ It is converted to aflatoxin B-exo-8, 9-epoxide, an activated substrate that can interact with DNA and cause damage.
	Alcohol: It is a leading cause of the chronic liver disease (CLD) and liver cirrhosis.	▪ It acts as a co-factor (synergistic effect) and increases the risk of HCC in patients who have hepatitis by promoting cirrhosis more aggressively.
	Tobacco smoking	▪ There is a strong connection between tobacco use and the risk of HCC. ▪ It acts due to synergism between cigarette smoking and HBV and/or HCV infection.
Hormones/Chemicals.	**Steroidal sex hormones** **Nitrosamines**	▪ It may lead to severe consequences like liver adenomas and HCC. ▪ When ingested, tinned foods or other stored products containing nitrites further converts to nitrates and finally reacts with amines and cause cancer (liver, stomach cancer, etc.).

	Polycyclic hydrocarbons	▪ Derivatives of car exhaust, cigarette smoke and fumes interact with the base pairs of cellular DNAs, impose changes, and result in cancer.
	Aromatic amines and azo dyes	▪ Benzidine and beta-naphthyl amine react with the liver cells, and once excreted from the liver, they are meant to reach the urinary bladder and may lead to cancer.
Race/ethnicity.	▪ Asians are two times more prone to get HCC than African Americans.	
Gender.	▪ Males are more prone than females for the incidence of HCC, with approximately three times higher frequency and mortality among men than women. ▪ Experimental studies suggest that sex hormones play a pivotal role in tumor progression. For example, it was observed from the endocrine ablation experiments that ovarian estrogens protect against tumor progression. In contrast, testicular androgens promote tumorigenesis administered with a potent carcinogen.	

The non-specific HCC laboratory findings parameters include the rise in various liver enzyme levels such as alkaline phosphatase (ALP), aspartate aminotransferase (AST), alanine aminotransferase (ALT) and bilirubin levels. However, specific serum protein diagnostic bio-markers strongly suggest that it gets elevated in hepatocarcinoma conditions. They include alpha-fetoprotein (AFP), des-gamma-carboxyprothrombin (DCP), and gamma-glutamyl transferase (GGT). Besides these, for the detection, staging and localization of HCC, imaging techniques are also effective for patient management. They include ultrasonography, computed tomography (CT), lipiodol CT, angiography, and magnetic resonance imaging techniques. Further, especially in AFP-negative patients, liver biopsy guided by ultrasound or CT usually provides sufficient tissue for a conclusive diagnosis. But, in patients with significantly increased AFP levels, a liver biopsy is not permitted, as they are potentially eligible for resection or liver transplantation to eliminate the greater risk of cancerous cells spreading before surgery.[46]

1.2.2.1. Pathophysiology of HCC

The HCC is heterogeneous with alterable molecular features at the histo-molecular level based on transcriptome analysis, exome sequencing, and genomic characterization.[45] The initial step towards the neoplastic progression of HCC involves forming hyperplastic nodules in the regenerating hepatocytes with regular cytological features. This, in turn, progresses to premalignant dysplastic nodules where anomalous liver features are noted with nuclear crowding, enlarged trabeculae thickening, and apparent cell changes. Further, these premalignant dysplastic nodules attack the adjacent fibrous stroma and blood vessels, and metastasis is achieved.[49,54-56] Here, during this process of evolution of HCC, several oncogenes and tumor-

suppressor genes are deregulated through many genetic and epigenetic alterations, which are explained in detail in table 4.[49]

The macroscopic features of most HCCs cases associated with liver cirrhosis show characteristic expanding types of the tumor with intra-tumoral septa and a fibrous capsule. Whereas those without cirrhosis tend to be present as massive and non-encapsulated.[46] Grossly, different degrees of morphological changes observed in HCC can be classified into three patterns of growth as follows:[34]

1. Multifocal type: It is observed less often, where the nodules of 3 to 5 cm in diameter are spread throughout the liver.
2. Expanding type: It is most frequently observed with a large mass of tumors, most often in the right lobe of the liver, accompanied by necrosis, hemorrhage, and occasional bile staining.
3. Spreading type: It is infiltrating tumor mass observed rarely.

Further, microscopically, the tumor cells of HCC can be classified based on patterns as follows:[34]

1. Sinusoidal or trabecular pattern: The most common pattern where sinusoids separate the trabeculae of 2–8 extensive layers of cancerous cells.
2. Acinar or pseudo-glandular pattern: This pattern is sometimes observed where the tumor cells are disposed around the central cystic space.
3. Compact pattern: This pattern resembles a trabecular form with large tumor solid masses and fine sinusoids.
4. Scirrhous pattern: The presence of abundant fibrous stroma characterizes this pattern.

Table 4: The molecular alterations identified during the pathogenesis of hepatocellular carcinoma (HCC).

Molecular features	Summary of molecular alterations in HCC
Methylation[49,57-60]	▪ During the early stages of human HCC tumor development, DNA methylation is critical. ▪ Initially, apoptosis-related markers [deleted in liver cancer 1 (DLC1), E-cadherin, p16 (INK4α)] are targeted due to specific hypermethylation events. This leads to abnormal apoptotic activity, both intrinsically or extrinsically. ▪ During HCC, anti-apoptotic signal molecules like B-catenin, Ras/extracellular receptor kinase (Ras/ERK), and Snail are overexpressed. In contrast, few pro-apoptotic molecules like phosphatase and tensin homolog (PTEN), Bax and p^{53} are downregulated, leading to imbalance and evasion of apoptosis.
Tyrosine-protein kinase receptor Met or c-Met and hepatocyte growth factor receptor (HGFR)[60-63]	▪ Reports of over-expression of Met receptors have been confirmed in an advanced stage of HCC through activation of cell proliferation, angiogenesis, and survival. ▪ The deterioration of tumors due to apoptosis and cell proliferation resulted from the hepatic-driven expression and termination of transgene expression activates the tyrosine-protein kinase transgene Met, leading to HCC.
ErbB receptor family[64-66]	▪ The ErbB family (ERBB1-ERBB4) is implicated in a variety of cancers.

	▪ Over-expression of these receptors is confirmed in HCC cases. ▪ The HCC progression can be correlated with the ErbB receptor family as confirmed through a high rate of proliferation, intrahepatic metastasis, de-differentiation and tumor size.
p^{53} tumor suppression[67,68]	▪ The p^{53} deficiency plays a part in the development of HCC. ▪ It works as a transcript factor in the growth, differentiation, and cell cycle processes of cells. ▪ The genetic mutations of p^{53} detected in larger HCCs are related to the development of late-stage disease. An association with p^{53} changes and advanced malignancies in HCV and/or HBV-related HCCs cases is confirmed.
β-catenin[69-72]	▪ It's a downstream part of the Wnt cancer signaling pathway connected to one-third of all HCC cases. ▪ Reports indicate that over-expression and mutations related to β-catenin have been correlated to early-stage HCC progression.
p^{16} (CDKN2A; Cyclin-dependent kinase inhibitor 2A)[49]	▪ A tumor suppresser gene and a powerful modulator of cell cycle progression during the G_1 phase.

	▪ Mutations primarily mediate the decreased expression of p^{16} in HCC in CDKN2A or homozygous deletions in chromosome 9.
Axis inhibition proteins (AXIN1 and 2)[49]	▪ They are tumor suppressor proteins that play an essential role in the transduction of Wnt-mediated through β-catenin.
Vascular endothelial growth factor A (VEGFA)[49]	▪ An efficient angiogenesis controller that influences tumorigenesis by encouraging endothelial development and redistribution. ▪ The over-expression of the VEGFA gene, tumor size and density of arteries and veins has been expressed in HCC cases.
Phosphatase and tensin homolog (PTEN)[49]	▪ It functions as a specific gene by decreasing the PI3K/AKT/mTOR pathway involved in various biological processes such as differentiation, growth and metabolism. ▪ It also aids in the progression and advancement of hepatocarcinogenesis, where reduced expression of the PTEN gene has been identified.

Abbreviations: PI3K, Phophoinositide 3-kinase; AKT, Protein kinase B; mTOR, Mammalian target of rapamycin.

1.2.2.2. Experimental models for assessing HCC[73,74]

The experimental models of hepato-carcinogenesis are being developed to initiate inflammation and the progression from fibrosis to cancer. In addition, numerous *in-vivo* models have been used extensively in research to define HCC pathogenesis and assess potential drug targets. The different available animal models used in HCC research are categorized as:

1. **Chemically induced models:** The chemical models of HCC involve the usage of varying chemical reagents for the induction of tumors in animals (Table 5). Generally, there are two known carcinogens: (a) Genotoxic substances that eventually cause DNA modifications and (b) Promoting substances that do not cause DNA changes but can increase tumor development after hepatotoxic agents have been used. Hereafter, an example of two-stage chemically induced models often involves initiation by a genotoxic substance as diethylnitrosamine (DEN) influenced by a promoting agent as phenobarbital (PB) for inducing HCC.[73-76]

   The most commonly used hepatocarcinogen in rodents is diethylnitrosamine (DEN), a genotoxic compound of the nitrosamine family, which produces reactive oxygen species (ROS). The ethyl radical metabolite ($CH_3CH_2^+$) is formed when cytochrome p450 enzymes metabolize the DEN. It causes damage to the liver by eliciting ROS production and interacting with the nucleophilic sites in DNA. It is widely reported in the environment, tobacco smoke, varieties of foods as smoked meat, fermented and preserved fish, dairy products, groundnut, nitrate-rich groundwater, and alcoholic drinks. The duration required to develop HCC after a single injection of DEN depends on various factors as dose, route of administration, age, gender, and strain of the rodents. This related variation in the

animal species may be due to enzymatic and metabolic reactions in different organs. The mechanism of action of various stages of DEN-induced hepato-carcinoma is being illustrated with the help of a flow diagram (Figure 1).

Carbon tetrachloride (CCl_4) induces hepatotoxicity by producing reactive trichloromethyl radical metabolite during oxidative metabolism by eliciting ROS production membrane-phospholipids damage. The extent of the liver damage can be further progressed to necrosis through microsomal cytochrome p450 enzymes by compounds like ethanol, acetone, and phenobarbital.

Peroxisome proliferators (PPs), such as ciprofibrate, fenofibrate, clofibrate, or methyl clofenapate, induce liver tumors in rodents. After a repetitive long-term, the peroxisome proliferator-activated receptor α is stimulated. This receptor protein is responsible for the regulation of cell proliferation and apoptosis. Well-defined trabecular histological patterns characterize the tumors induced by PPs.

Aflatoxin B_1 (AFB_1) is a well-known hepatic carcinogen produced by a particular genus of the fungi, *Aspergillus*, such as *Aspergillus flavum*. The liver microsomal enzymes metabolized the AFB to an Exo-8,9-epoxide substrate, which binds specifically to DNA's guanine residues, resulting in DNA mutations.

Choline/methionine-deficient diet (CDD) induces cirrhosis and hepato-carcinogenesis in rodents due to the depletion of the anti-oxidant mechanisms of the hepatocytes. It ultimately leads to inflammation, necrosis, fatty liver changes, fibrosis, followed by infrequent cirrhosis and HCC as observed with the histological changes in CDD-fed rodents. Further, Thioacetamide (TAA), a

hepatotoxin, induces rodent fibrosis due to the compound's oxidation abilities and hepatic stress.[73-80]

2. **Xenograft models:** The primary basis of the xenograft models includes that tumor could develop from cancer cells grown in a lab when implanted subcutaneously or intraperitoneally in athymic (nude) mice. It offers advantages where the tumors are easily and rapidly induced and have a negligible effect on animal well-being. The different kinds of xenograft models are orthotopic implantation, ectopic implantation, and hollow fiber model.

   The orthotopic implantation model describes how cancer cells are implanted into mice intra-hepatically. It offers advantages and provides information about the metastatic state of the tumors and is more appropriate for extrapolation to humans. Besides these, it also allows the possibility to implant HCC cells in chemically induced-fibrotic livers, where fibrosis is induced initially with the help of chemical agents (Thioacetamide or CCl_4 or Alcohol).

   The tumor cells are administered subcutaneously into the mice in the ectopic implantation model. Generally, the fast occurrence of tumors can be achieved within 5 to 20 weeks, and it is easy to perform. It is weakly extrapolatable to humans, and several cell lines need to be tested as a significant difference is observed between the cell lines.

   Further, the hollow fiber model explains cancer cell lines placed in small polyvinylidene semi-permeable tubes cultured for 24 to 48 h *in-vitro* are implanted intraperitoneally or subcutaneously in nude mice. It offers fast results within 1 to 2 weeks. Besides this, the retrieval of cancer cells after experimentation can be

helpful for subsequent analysis. At the same time, no direct interaction with the liver tissue occurs and subsequently, metastasis cannot be tested.[73-82]

3. **Genetically modified models:** It is the most sophisticated model where genetically engineered animals mimic the molecular and pathophysiological conditions of HCC. It helps in the thorough investigation of the oncogenic signaling pathway, in which the effects of cancerous cells alone or in association with other carcinogens are evaluated.

The transgenic models involving the overexpression of oncogenes explain where the alteration of the oncogenes such as β-catenin or myc protein influences tumor development. Likewise, transgenic models involved with the incorporation of hepatitis B or C virus genes promote hepatitis induced-HCC. Further, the growth factor involvement can also augment cell proliferation to induce HCC in animals. Besides these, through the creation of an ideal tumor environment, this model helps to mimic and develop inflammation, steatosis, fibrosis and tumors alike to human non-alcoholic steatohepatitis.[73-80,83-85]

Table 5: The commonly used *in-vivo* chemically-induced HCC models are classified based on the usual routes of administration, mechanism of action, and significance.[73-80]

Drugs/Chemicals	Common routes	Mechanism of action	Significance
Diethylnitrosamine (DEN)	Intraperitoneal (*i.p.*) injection.	It is a genotoxic hepatocarcinogen that acts by ethylating at the nucleophilic sites of DNA.	100% HCC in males; 30% in females.
Dimethylnitrosamine (DMN)	Intraperitoneal (*i.p.*) injection or per oral (*p.o.*).	It acts by methylation and covalent binding of nucleic acids and proteins in hepatocytes.	100% HCC.
Carbon tetrachloride (CCl_4)	Through drinking water, inhalation, or intraperitoneal (*i.p.*) injection.	It acts through the production of ROS and by damage of membrane phospholipids.	50–94% (dose-dependent) in both males and females.
Peroxisome proliferators (PPs)	In the form of diet.	It is a non-genotoxic carcinogen that causes the peroxisome proliferator-activated receptor to become activated.	100% HCC.

Aflatoxin B_1 (AFB_1)	Bolus injection.	It binds selectively with the guanine residues of DNA, hence causing DNA mutations.	Inter-strain differences are observed.
Choline/methionine-deficient diet (CDD)	In the form of diet.	It acts through DNA injury, inflammation and chromosomal heterogeneity.	100% HCC.
Thioacetamide (TAA)	Intraperitoneal (*i.p.*) injection.	Metabolites induce hepatic oxidative stress.	70–100% HCC.

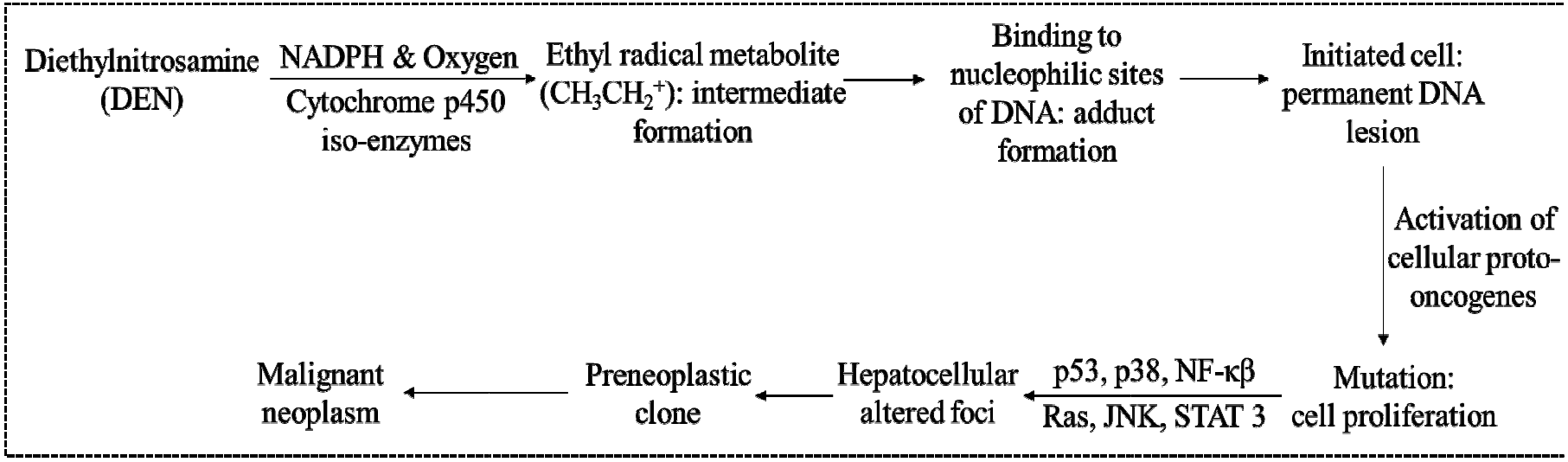

Figure 1: The mechanism of action of various stages of diethylnitrosamine-induced hepato-carcinoma.

NADPH: Nicotinamide adenine dinucleotide phosphate; NF-κB: Nuclear factor-κB; JNK:c-Jun N-terminal kinase; STAT-3: Signal transducers and activator of transcription 3.

1.2.3. Correlation between diabetes and hepatocellular carcinoma

A large number of cohorts, retrospective, observational and case-control reports indicate that people with diabetes are more likely to develop site-specific tumors, such as hepatic cancer, and their mortality rate is higher.[6,7,9,86-88] The first possible connection was reported by Lawson *et al*. They documented that irrespective of the well-known factors of HCC as viral hepatitis, cirrhosis (alcoholic), or other factors, diabetes is also more predominant in the patients with hepatic cancer.[89] The complicated relationship between these two diseases makes it challenging to understand the exact pathophysiological mechanisms of diabetes and HCC. Nevertheless, various ongoing studies in recent years have suggested the pathophysiology of HCC in diabetic conditions. It may be attributed to hyperglycemia (HG), hyperinsulinemia (HI), insulin resistance (IR), obesity and enhanced inflammatory processes or treatment for diabetes.[88,90,91]

1.2.3.1. Evidence for a biological link between DM and HCC

The underlying mechanisms that link diabetes to hepatic cancer depend on the following factors:

1. **Hyperglycemia (HG) and hepatic cancer**: The connection between hyperglycemia (HG) and hepatic cancer is still unknown. Nonetheless, several epidemiological studies have revealed that high glucose levels can be a factor in tumor development and progression. Hyperglycemia, the major metabolic abnormality, characterizes all types of diabetes diagnosed under impaired glucose tolerance (IGT) and/or resultant increase in blood glucose level.[6,16,92-94] According to the American Diabetes Association guidelines, if the blood glucose level is greater than seven mmol/l, it is regarded as diabetic. The persistent HG results in glucose toxicity, which is considered one of the significant causes of organ

impairment.[95] The high glucose serves as a subordinate cause that triggers several direct and indirect mechanisms for the proliferation of cancer cells, migration, invasion, and immunological escape. The production of free radicals (ROS) and DNA damage increases due to high energy consumption or glucose toxicity, indicating a role in developing oxidative stress and inflammatory response. Changes in the levels of both enzymatic and non-enzymatic anti-oxidants levels are observed. It also includes the stimulation of polyol and hexosamine biosynthetic pathways and changes in gene expression. Besides that, increased formation of advanced glycation end products (AGEs), oxidative phosphorylation, glucose auto-oxidation process and protein kinase C (PKC) activation could also promote carcinogenesis.[16,96-99] The WNT/β-catenin activation in HG cells has recently been linked to cancer cell proliferation, survival, and senescence.[20,100]

The well-known metabolic hallmark of the cancer cells, unlike the normal cells, predominantly metabolizes glucose uptake through glycolysis even in the presence of oxygen and results in lactate production, termed as the Warburg effect.[101] Hence, hyperglycemia favored the cancer cells to fuel survival and proliferation through this altered metabolism. Moreover, due to the overproduction of lactate, the acidic environment supports the adjacent cancer cells by suppressing the cytotoxic immune response.[102] Besides these, the cancer cells also play a critical role in synthesizing lipid, protein, DNA, and RNA through aerobic glycolysis, thereby augmenting cell proliferation via different signaling pathways.[103,104] Thus, the increased utilization of glucose by cancerous cells and the association between the rise of hepatic cancer and hyperglycemia due to diabetes may not be a coincidence. As a result, high glucose should not be overlooked as a factor that aids in developing hepatic cancer.

2. **Hyperinsulinemia (HI), insulin resistance (IR), and hepatic cancer**: Insulin sensitivity and hyperinsulinemia (HI) are essential aspects in the progress of diabetes in people who have hepatic cancer. Early HI is seen in type II diabetic patients compared to HG levels, and it can also be seen in type I patients with diabetes receiving insulin supplements. Enhanced insulin levels increase the growth factor receptors of insulin, resulting in a vast network in which most cancerous cells express these receptors through multiple pathways. Further, they can stimulate insulin-facilitated mitogenesis by increasing protein synthesis, decreased mitochondrial oxidation of fatty acids, cellular proliferation, invasion, metastasis, and apoptosis suppression which are considered essential factors for the progression of tumor cells. Taken together, these may be associated with hepatic injury, inflammation, followed by fibrosis, cirrhosis and finally, hepatic cancer.[6,105-108] Moreover, insulin receptors are overexpressed during hepatic cancer.

   Insulin, a potent metabolic hormone and growth factor, may interact with hepatocytes, thereby activating Akt (Protein kinase B) phosphorylation, thus contributing to the progression of cancerous cells. This signaling pathway is mediated via several mechanisms through increased uptake of glucose by the hepatocytes (through translocation of glucose transporters), suppression of apoptosis by inhibition of pro-apoptotic proteins and by regulating the cell cycle (from G_1 to S phase).[109]

3. **Obesity, inflammation, and hepatic cancer**: Type II diabetes mellitus associated with obesity characterized by chronic inflammation appears to be another linking factor for tumor progression. The increase in the production of the free radicals mediated through oxidative stress affects different cancer signaling pathways. It starts with the disruption of the insulin signaling pathway leading to DNA

mutations being favored by the free radicals.[110,111] The DNA mutations (single/double-strand break in DNA, oxidized DNA) are formed when the hydroxyl free radicals interact with the DNA. Further, following the DNA mutations, our body's repair system can prevent DNA damage or undergo apoptosis. The cells escaping from apoptosis and undergoing DNA changes contribute to the promotion of hepatic cancer.[112] The adiponectin and leptin by the visceral adipose tissue and pro-inflammatory cytokines markers regulate the apoptotic markers, promoting hepatic cancer.[113-115] Besides these, the heritable phenotypic changes such as histone modification, DNA methylation, and RNA interference also affect the cytokine-mediated cell signaling pathway. The proteins and pro-inflammatory gene nuclear factor kappa B (NF-*κ*B) involved in the cytokine-mediated cell signaling pathway leads to the metabolic deregulation followed by hepatocyte changes.[116,117] Furthermore, ROS may influence extracellular signal-regulated kinases or mitogen-activated protein kinases (MAPK) transcription factors, ensuing in the proliferation of the hepatic cells.[118]

1.2.4. Molecular mechanism for hyperglycemia increasing the risk of HCC: Cancer-associated pathways

1.2.4.1. Effect of 5´adenosine monophosphate-activated protein kinase (AMPK) metabolic alteration in HCC and diabetes

The AMPK is one of the central metabolic and cellular regulators in all eukaryotic cells. It is a highly complex and conserved heterotrimeric threonine/serine protein kinase composed of catalytic subunits designated as alpha (α) along with two regulatory subunits as beta (β) and gamma (γ). Furthermore, each catalytic and regulatory subunit has two or three subunits, α_{1-2}, β_{1-2} and γ_{1-3}, represented by

different genes.[119,120] It plays multiple roles in the physiology and pathology of various diseases, notably the HCC and diabetes.[121-123]

Hepatocellular carcinoma (HCC): The dysregulation and malfunction of AMPK mediate a particular type of regulatory process in the pathological condition of HCC progression. It is coordinated through various mechanisms such as modulation of the apoptosis, cell cycle, autophagy, *de novo* fatty acid synthesis, inhibition of protein synthesis and cell metabolism. Several direct and indirect AMPK activators possess anti-HCC activity suggesting a reduction in cell proliferation in tumor cells and animal studies. The direct activators such as 5-aminoimidazole-4-carboxamide riboside (AICAR), benzimidazole derivatives interact with the protein and lead to conformational changes of AMPK. On the other hand, indirect activators such as metformin HCl or berberine don't require any direct interaction with the protein. They are the modulators of calcium or AMP levels.[124-126]

Diabetes mellitus (DM): High free fatty acids (FFAs), which are the driving factors for insulin resistance (IR) in diabetic populations, resulted in decreased AMPK activity. These results in impairment of the insulin signaling pathway. AMPK-activators have been shown in studies to increase insulin sensitivity by inhibiting protein synthesis or lipogenesis. As a result, AMPK inhibits anabolism by regulating ROS-mediated stress as well as lipid and protein metabolism, which may be effective in preventing and treating IR and diabetes.[125]

1.2.4.2. Targeting Akt or Protein kinase B (PKB) signaling pathway in HCC

The Akt or Protein kinase B (PKB) dysfunction is an essential pathway in various pathological conditions, including HCC and diabetes. A serine/threonine-protein kinase family includes three classes, each encoded by a different gene, namely $Akt_{1-3,}$ in mammalian cells.[127]

The Akt, known as a proto-oncogene, is increasingly implicated in hepato-carcinogenesis. It serves as a significant pathway by triggering a cascade of responses that links from increased cell proliferation and growth, apoptosis, migration, survival to metastasis of tumor cells. Besides these, Akt also regulates the glucose metabolism pathway. According to evidence, increased activity of the Akt transcription factor is frequently observed in the development of hepato-carcinogenesis. It is clearly explained in response to the stimuli of specific growth factors (GFs) such as IGFs, tyrosine-protein kinase or human epidermal growth factors, all of which are over-expressed in several cases of HCC. Besides these, viral hepatitis infection also contributes to the increased expression of Akt. These altogether activate the Akt. Studies related to both pre-clinical and clinical studies have shown promising anti-HCC activity targeting the Akt signaling pathway through regulation of multiple down-stream molecules.[124,128-130]

1.2.4.3. Role of phosphoenolpyruvate carboxykinase (PCK/PEPCK) genes in cancer

In mammalian cells, the gluconeogenic enzyme PCK is classified into two isoforms: cytoplasmic PEPCK-c or PCK-1 and mitochondrial PEPCK-m or PCK-2. It forms phosphoenolpyruvate (PEP) by catalyzing the oxaloacetate (OAA) in the liver, the rate-limiting step of gluconeogenesis.[131,132] Evidence indicates the increased expression of PCK-genes in various types of cancer, including skin, colon, bladder, breast, kidney, and lung. It is linked with the increase in the anabolic metabolism and the growth and differentiation of the tumor cells. It also indicates that the altered expression has been linked to insulin resistance (IR), diabetes, obesity, fatty liver and other metabolic states.[132-134]

1.2.4.4. Targeting sterol regulatory element-binding protein-1 (SREBP-1) regulated pathway to treat cancer

The SREBP-1, which plays a significant part in oncogenic signaling-mediated glucose metabolism to *de novo* lipogenesis, is regulated by AMPK and PI3K/Akt. The levels of SREBP-1 are observed to be elevated in various types of cancer and animal models of diabetes. Further, the pharmacological targeting of SREBP-1 has been correlated with decreased tumor growth. The development of specific inhibitors by targeting SREBP-1 mediated through AMPK and the Akt signaling pathway could act as a possible strategy to treat cancer.[135-138]

1.2.5. Metformin HCl

Metformin, a guanidine derivative, was first discovered in the 1920s from plant extract *Galega officinalis* (French lilac) and isoamylene guanidine (Galegine). The metformin, chemically known as 1,1-dimethyl biguanide, is the most widely used first-line oral therapy to treat hyperglycemia in diabetic patients (Figure 2). Patients with polycystic ovary syndrome, gestational diabetes, diabetes-related cardiovascular complications, or metabolic syndrome may also benefit from it. It also reduces body weight by involving adipose tissue and suppressing food intake by involving hormones or cytokines such as leptin, insulin, or ghrelin. Also, it can reduce fatty liver in animals, impact specific inflammatory markers or cardiovascular markers and possibly decreases the risk of certain types of human cancers.[139,140]

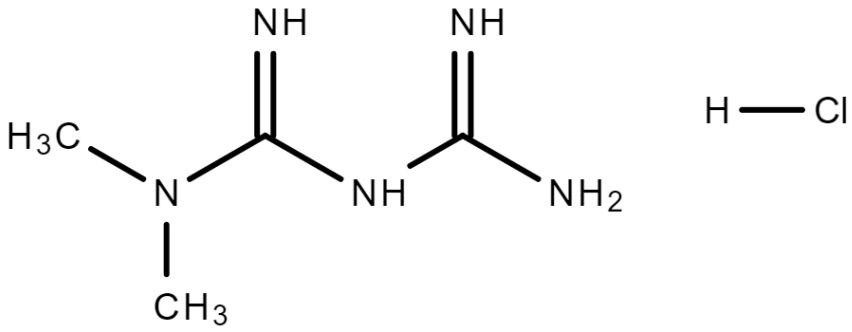

Figure 2: Chemical structure of metformin HCl.

1.2.5.1. Metformin in diabetes mellitus: Anti-diabetic actions

Metformin is an anti-hyperglycemic medication that reduces blood sugar levels by suppressing liver gluconeogenesis or increasing glucose absorption in skeletal muscle without inducing hypoglycemia. It is also known as an insulin-sensitizing agent acting through decreased plasma insulin levels or reducing insulin resistance (IR). The AMPK, a principal energy sensor of multiple metabolic pathways, gets activated due to metformin that lowers hepatic glucose production. Besides these, various *in-vitro* and *in-vivo* experiments showed the glucose-lowering effects of metformin by decreasing the glucagon concentrations. The inhibition of the glucagon signaling reduces the activation of adenylate cyclase (ACs) and further prevents the phosphorylation of downstream molecules. This leads to a decrease in the hepatic glucose production through inhibition of glycogenolysis, gluconeogenesis or ketogenesis and by the promotion of glycolysis or glycogenesis.[139-141]

1.2.5.2. Metformin in cancer: Potential molecular mechanism of actions

The impact of metformin therapy on the reduced risk of cancer and cancer-related mortality was associated with several findings. The *clinicaltrials.gov,* a clinical trial database, reports that 353 clinical trial studies on cancer and metformin have been reported as of 2020.[142] The therapeutic and preventive benefits of metformin in

lowering cancer risk, including hepatic cancer in diabetic patients, have been demonstrated in several observational studies.[143,144] The first reported case-control study by Evans *et al*. in 2005 reported that metformin minimizes the chances of cancer in people with diabetes.[144] Furthermore, Franciosi *et al*. validated the previous findings using 18 retrospective studies in the liver, pancreas, and colon cancers, followed by Zhang *et al.* overall progress and survival outcome in the liver, colorectal, breast, and pancreatic cancers.[145,146] The underlying molecular mechanisms of metformin in cancer remain unclear. Nonetheless, numerous studies have identified reduced insulin-like growth factor or insulin, inhibition of angiogenesis and AMPK activation, thereby inhibiting mTOR signaling, cell cycle arrest, and apoptosis as mechanisms of action.

Cell growth inhibition (LKB1/AMPK/mTOR and IGF-1 signaling pathway): Metformin inhibits tumor cell growth by activating 5´AMP-activated protein kinase programmed in the presence of small interfering RNAs. The presence of liver kinase B1 (LKB1) is needed for AMPK activation. The AMPK activation also interrupts the mTOR (mammalian target of rapamycin) signal transduction pathway, inhibiting cell proliferation.[25,147] The inhibition of mTOR thereby affects the growth-factor-dependent signaling pathways as phosphoinositide 3-kinases (PI3K) and mitogen-activated protein kinase (MAPK) along with the oxygen-dependent signaling pathways. The mTOR phosphorylation regulates the downstream signaling mediators to control cell growth, cycle progression, and angiogenesis.[148] Furthermore, LKB1/AMPK activation disrupts the insulin signaling pathway, resulting in insulin/IGF-1 factor inhibition, a common route for diabetes and cancer. In addition, metformin inhibits the fatty acid enzyme, a key enzyme in tumor progression.[149]

Cell cycle arrest: The cell cycle arrest by metformin in the malignant cell via activated AMPK is another potential mechanism of action. The reduced expression of cyclin D1 and the subsequent activation of p21CIP and p27KIP are linked to AMPK activation. It can also induce cell cycle arrest and apoptosis in the cells by downregulation of cyclin D1 via activating the tumor suppressor gene p53. Furthermore, metformin has been shown to disrupt the cell proliferation of various tumors, notably hepatic tumors, by up-regulating the let-7 family, as observed in the pre-clinical studies.[150-152]

AMPK independent signaling pathways: Metformin protects the oxidative mediated DNA damage by blocking the mitochondrial respiratory chain. It can also activate the signal transducers pathway of apoptosis and autophagy. Furthermore, metformin inhibits glucose uptake by the tumor cells through direct influence on the enzyme hexokinase II.[153-155]

1.2.6. *Acorus calamus* Linn. (Sweet flag)

Table 6: Details of *Acorus calamus* Linn.[156,157]

Name of the plant	***Acorus calamus*** Linn.
Family	Acoraceae.
Common name	Sweet flag, Calamus, Calamus root, Sweet calomel, Myrtle grass, Vacha, Bach, Vaj.
Part of plant used	Leaves, stems, and roots (rhizomes).
Traditional uses	In Chinese and Indian herbal remedies, it is commonly used alone or associated with several other plants.

1.2.6.1. Botanical classification

Table 7: Botanical classification of *Acorus calamus* Linn.[156,157]

Kingdom	Plantae
Sub kingdom	Tracheobionta
Superdivision	Spermatophyta
Division	Magnoliophyta
Class	Liliopsida
Order	Arales
Family	Acoraceae
Genus	*Acorus*
Species	*Calamus*

1.2.6.2. Botanical description and habitat/geographical distribution

The *Acorus calamus*, frequently known as the Sweet flag in the traditional system of medicine, is a tall herbaceous perennial plant with creeping rhizomes that are highly branched, bitter in taste, citrus in odor and pale green or pinkish. It is a semi-aquatic and terrestrial plant present in a moist environment such as rivers, swamp areas, streams, or banks of the pond. The distichously alternate or sympodial radiant green leaf is within 0.7 to 1.7 cm in width. The long cylindrical, greenish-brown flowers (3 to 8 cm long) are covered with rounded spikes. The fruits of the plant containing few seeds are berry-like and small in appearance. Most species of the plant are widely cultivated in various regions of the globe, including India, China, Burma, Japan, Sri Lanka, the northern USA, Mongolia, and Russia.[156,157]

1.2.6.3. Chemical constituents[156-159]

Several studies have investigated the plant *A. calamus* phytochemical constituents from the leaves, rhizomes, and stems. It has reported numerous phytoconstituents such as glycosides (xanthone), steroids, flavonoids, volatile oil, monoterpenes, saponins, polyphenolic compounds, sesquiterpenes, lignin, an alkaloid (glucoside),

mucilage and tannins. It also includes calameon, calamen, and calamenol, as well as other essential oils. It has also reported bitter glycosides such as pinene, acorine, acoretin, camphene, and eugenol. Studies have also revealed the presence of two predominant bioactive aromatic phytoconstituents from rhizomes of the plant. They are alpha (α)-and beta (β)-asarone (Figure 3). Some other constituents have also been identified in the extracts of the plant, such as safrole, β-sitosterol, myrcene, phellandrene-β, thujane, terpinen-α, terpinolene, para-cymene, elemicin, camphor, linalool, calacorene, spathulenol, and α-and β-pinenes.

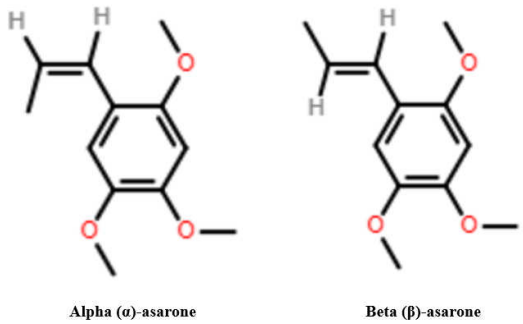

Figure 3: Chemical structures of (α)-asarone (1,2,4-trimethoxy-5-[(E)-prop-1-enyl] benzene) and (β)-asarone (1, 2, 4-trimethoxy-5-[(Z)-prop-1-enyl] benzene) obtained from *A. calamus*.

1.2.6.4. Ethnomedicinal/Traditional uses[156-160]

It has been found that the different parts of the plant are used for various medicinal purposes in Indian Ayurvedic and Traditional Chinese Systems. The herbaceous perennial plant is used externally as a paste for alleviating the pain and swelling in people suffering from inflamed joints, rheumatism, or rheumatic fever. Further, it is effective for digestive complaints, namely loss of appetite, worms, flatulence, abdominal pain, constipation, and digestive system problems. The natives of Albertans use it to treat hangovers, headaches, and toothaches, as well as disinfectants.

Some of the popularly marketed formulations prepared in India such as Janma Ghunti Honey for diarrhea and constipation (Dabur India Limited), Scavon Vet cream as anti-fungal and anti-bacterial agents (The Himalaya Drug Company, Bangalore, India), Vacha powder as a brain tonic and for prevention of nausea (Bixa Botanical), Calamus root powder for mental health problems (Heilen Biopharm), Pigmento tablets for leukoderma (Charak Pharma), Kankayan Bati for dyspepsia and flatulence (Baidyanath Pvt. Ltd.) and many others are used for numerous purposes. It is being used to cure various ailments like cough, skin diseases, diarrhea, asthma, bronchitis, mental retardation, insomnia, depression, fever, hemorrhoids, epilepsy, kidney and liver problems, dysentery, and hysteria.

1.2.6.5. Pharmacological uses[28,156,157]

The pharmacologically active ingredients present in the leaves, rhizomes or stems have been studied extensively and reported to be useful for various biological activities, including anti-oxidant, anti-bacterial, anti-fungal, insecticidal, pesticidal, anti-ulcer, anti-allergic, anti-asthmatic, cardioprotective effects, anti-spasmodic, anti-diarrheal, anti-diabetic, immunosuppressant, radioprotective, anti-cancer, neuroprotective, analgesic, anti-inflammatory, curing of wounds and others. Furthermore, the number of publications as a chemopreventive agent/s is increasing, indicating the future interest in *A. calamus* and its key phytoconstituents. Figure 4 and Table 8 offer a quick overview of the anti-cancer activities of *A. calamus* or its pharmacologically active constituents.

Figure 4: *In-vivo* anti-cancer activity: The anti-cancer effects of *A. calamus* or its pharmacologically active constituents (asarone) are explained in terms of dosage, animal/model used, and potential targets or effects.[161-166]

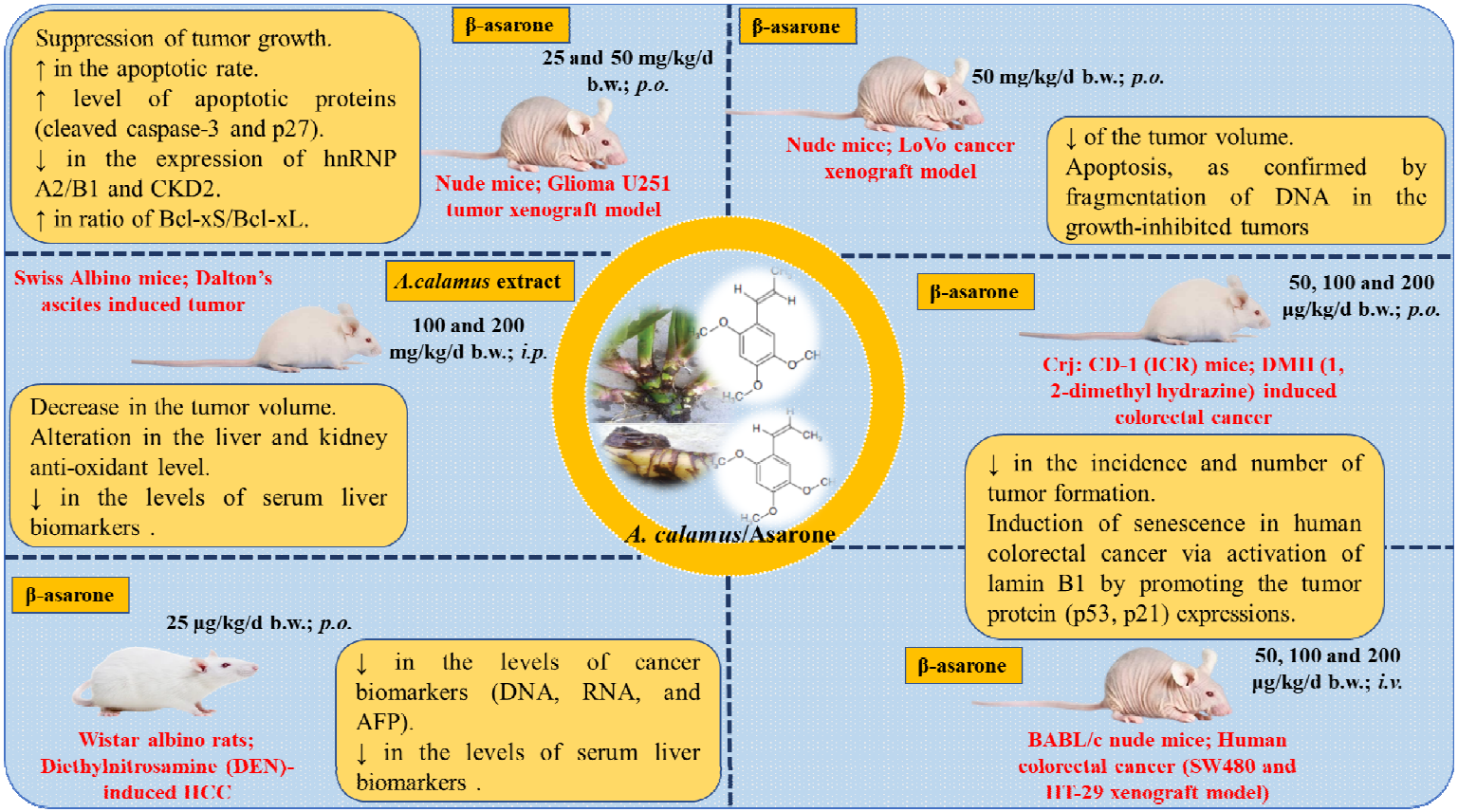

Abbreviations: ↓: decrease; ↑: increase; *b.w.*: body weight; *p.o.*: per oral route; *i.p.*: intraperitoneal route; *i.v.*: intravenous route; hnRNP A2/B1: heterogeneous nuclear ribonucleoproteins; CKD2: cyclin-dependent kinase-2; AFP: Alfa-fetoprotein.

Table 8: *In-vitro* anti-cancer activity: The anti-cancer effects of *A. calamus* or its pharmacologically active constituents (asarone) are explained in dosage, cell lines used, and possible molecular events or targets.

Treatment	Dose	Cell lines; Cancer	Potential molecular events/targets	References
β-asarone	200 and 400 µM	LoVo cells; Colon cancer.	↓ in the rate of cell viability (MTT assay). Ultra-structure changes of the LoVo cells indicating apoptosis (Hoechst staining). Apoptosis (Annexin V-FITC/PI staining). ↓ in mitochondrial membrane potential (MMP). ↑ pro-apoptotic proteins (Bax expression) and ↓ anti-apoptotic regulators (Bcl-2, Bcl-xL, and survivin). ↓ in the Bcl-2/Bax ratio and ↑ of the executer apoptosis enzyme caspase-9 and caspase-3 cascades.	[165]
β-asarone	0, 10, 30 and	HT29 and SW480	↓ in cell proliferation (MTT assay).	[166]

	100 nM	cells; Colorectal cancer.	Induces cell senescence (SA-β-Gal activity). ↑ in the levels of lamin B1, as well as p53, p21, and p15.	
β-asarone	60, 120, 240 and 480 μM	U251 cells; Glioblastoma.	Apoptosis (Annexin V/Pi staining). Cell cycle arrest at the G_1 phase. ↓ in the expression of hnRNP A2/B1 in a concentration and time-dependent way. The ratio of Bcl-xS/Bcl-xL ↑ by β-asarone in both mRNA and protein levels by the inhibition of the hnRNP A2/B1-mediated signaling pathway. Promoted the activation of the death receptor proteins TRAIL and FasL. Cleavage of caspase 8 and caspase 3. ↑ in the expression of cleaved-BID and cellular protein cytochrome C. ↑ in the expression of cell cycle-related proteins p21 and p27 and ↓ an expression of cyclin D, cyclin E, Cdc25A, and CDK2.	[161]

β-asarone	0.12 and 0.24 mM	SGC-7901, BGC-823 and MKN-28 cells; Gastric cancer.	↓ in the cell viability (MTT assay). Apoptosis (Annexin V-FITC/PI staining). Ultra-structure changes of the cells indicating apoptosis (Hoechst 33342 staining). Inhibited the migration, invasion, and adhesion (Wound-healing, transwell, and matrix-cell adhesion assay). Activates caspase-3, 8, and 9 levels. ↑ pro-apoptotic proteins (Bax and Bak expression) and ↓ anti-apoptotic regulators (Bcl-2, Bcl-xL, and survving activity). ↑ in the expression of RECK, E-cadherin, and ↓ MMP-2, MMP-9, MMP-14, and N-cadherin expression.	[167]
Ethanolic extract of *A. calamus*	250, 500 and 750 µg/ml	LNCaP cells; Prostate cancer.	↓ in the cell viability (XTT assay). Induces apoptotic cell death (↑ in cleaved poly (ADP-ribose) polymerase/PARP). ↓ in VEGF mRNA expression.	[168]

Green silver nanoparticles synthesized from *A. calamus*	25, 50, 75, 100, 125, 150, 175 and 200 µg/ml	HeLa cells; Cervical cancer. A549 cells; Adenocarcinoma.	Anti-proliferative effect (% inhibition of cell proliferation through MTT assay). Apoptotic cell death (Acridine orange/ethidium bromide (AO/EB) and annexinV-Cy3 staining and TUNEL assay). Nuclear changes as fragmentation and condensation [propidium iodide (PI) and 4´,6-diamidino-2-phenylindole dilactate (DAPI) staining].	[169]

Abbreviations: ↓: decrease; ↑: increase; MTT assay: methyl thiazolyl tetrazolium assay; FITC: fluorescein isothiocyanate; PI: propidium iodide; hnRNP A2/B1: heterogeneous nuclear ribonucleoproteins; TRAIL: TNF-related apoptosis-inducing ligand; FasL: Fas ligand; CCK-8: cell counting kit 8; MMP-14, Matrix metalloproteinase-14; Oct-1,4: octamer-binding protein-1,4; TUNEL: terminal deoxynucleotidyl transferase dUTP nick end labeling; RECK: reversion-inducing-cysteine-rich protein; VEGF: vascular endothelial growth factor.

1.2.6.6. Toxicology of *A. calamus* or asarone

Table 9 summarises the toxic assessment of *A. calamus* or asarone, which was proven safe at lower levels. A study performed in male BALB/c mice by Morales *et al*. for fourteen days reported the median lethal dose (LD_{50}) of α-asarone to be 245.2 mg/kg b.w.; *i.p*. Dyspnea, ataxia, ptosis, and piloerection were among the clinical symptoms reported in the animals.[170] Liu *et al*. assessed the preliminary toxic profile of β-asarone on BALB/c mice. They conducted this experiment for 24 h and did not exhibit any behavioral changes when administered intra-venously at dosages 0.5, 0.75, 1, 1.25, 1.5, 1.75, and 2 g/kg b.w. Further, a long-term toxicity profile with a dosage of 10, 20, and 50 mg/kg/d was carried out for 90 days. A dose-dependent toxic profile was reported, where a decrease in the counts of red blood cells (RBCs) along with a rise in the counts of white blood cells (WBCs) at 10 mg/kg was observed. Moreover, at 20 mg/kg, decreased levels of serum K^+ and increased levels of Cl^- at 50 mg/kg was observed.[166]

In another study, the sub-acute toxic profile of β-asarone on Sprague Dawley rats showed a decrease in body weight and food intake at a dose of 100 mg/kg/d b.w. when administered intra-peritoneally. Moreover, the increased weight of the adrenals and decreased weight of the thymus and heart were also observed. No such statistical significance was observed for the other biochemical and hematological parameters indicating the hepatotoxic potential. Further, another study in Osborne-Mendel fed male rats for two years either with calamus oil or β-asarone at a dose of 400, 800, or 2000 mg/kg develops leiomyosarcomas in the small intestine. The microscopic investigation showed fatty infiltration, cardiac atrophy, and fibrotic heart. The administration of Jammu oil of calamus for two years to rats at a dose of 5000 mg/kg develops liver and heart lesions and early mortality.[171]

Table 9: Toxic profile of *A. calamus* or asarone: The table explains the test compound's median lethal dose (LD_{50}).[166,170-172]

Animal species/strain/gender	**The median lethal dose (LD_{50})**	
	α-asarone	**β-asarone**
Rat	--	1010 mg/kg b.w.; *p.o.*
Mice	--	184 mg/kg b.w.; *i.p.*
BALB/c mice (both gender)	--	1.56 g/kg b.w.; *i.v.*
Swiss mice (male)	>1000 mg/kg b.w.; *p.o.*	--
BALB/c mice (male)	245.2 mg/kg b.w.; *i.p.*	--

Abbreviations: *b.w.*: body weight; *p.o.*: per oral route; *i.p.*: intraperitoneal route; *i.v.*: intravenous route.

1.3. JUSTIFICATION

Epidemiologic studies suggest that a strong association co-exists between diabetes mellitus (DM) and hepatocellular carcinoma (HCC). Some of the risk factors related to diabetes (namely insulin, IGF-1, or inflammation) have been broadly studied with the progression of cancer and consider as a major link. However, less attention has been paid to how hyperglycemia promotes tumorigenesis in cancer, specifically HCC. It is well-known that the liver is the fundamental metabolic organ mainly involved in maintaining the regulation of glucose metabolism, and high glucose is considered one of the main characteristics of diabetes. High glucose or hyperglycemia (HG) has been implicated as a causal factor, and enhanced glucose uptake is a hallmark of cancer cells. High glucose supply to the cancer cells favors the anabolic metabolism for tumor growth via different cancer-related signaling pathways. However, there is substantial information in the research literature on how diabetes facilitates hepatocarcinogenesis in animals. As a result, this research aims to create an animal model that can reproduce the scientific proof for the diabetic-HCC condition.

Furthermore, evidence from various observational and clinical studies suggests that metformin HCl, a member of the biguanide class of anti-diabetic agents, is linked to lower cancer risk by inhibiting tumor cell development. Separately, the cytotoxic and anti-hyperglycemic effects of the *Acorus calamus* or biologically active phytoconstituent (asarone) have been reported. The α-and β-asarone are the two major active constituents present in volatile oils of the plant *Acorus calamus* Linn. Nevertheless, the role of asarones as cytotoxic agents in diabetic conditions has yet to be investigated. Henceforth, the study aimed to evaluate the collective role of α-and β-asarone and metformin HCl in regulating cancer growth on the chemically induced *in-vivo* model and human hepatocellular carcinoma HepG2 cells.

This study aims to develop an animal model that can reproduce the scientific proof for the diabetic-HCC condition and evaluate the beneficial effects of asarone and metformin HCl in regulating tumor growth. The objectives of the proposed study are:

1. To investigate the role of hyperglycemia in aiding the progression of hepatocellular carcinoma.
2. To evaluate the role of asarone and metformin HCl in controlling the progression of hepatocellular carcinoma during hyperglycemia and understand the underlying molecular mechanism.

SCHEME FOR THE STUDY

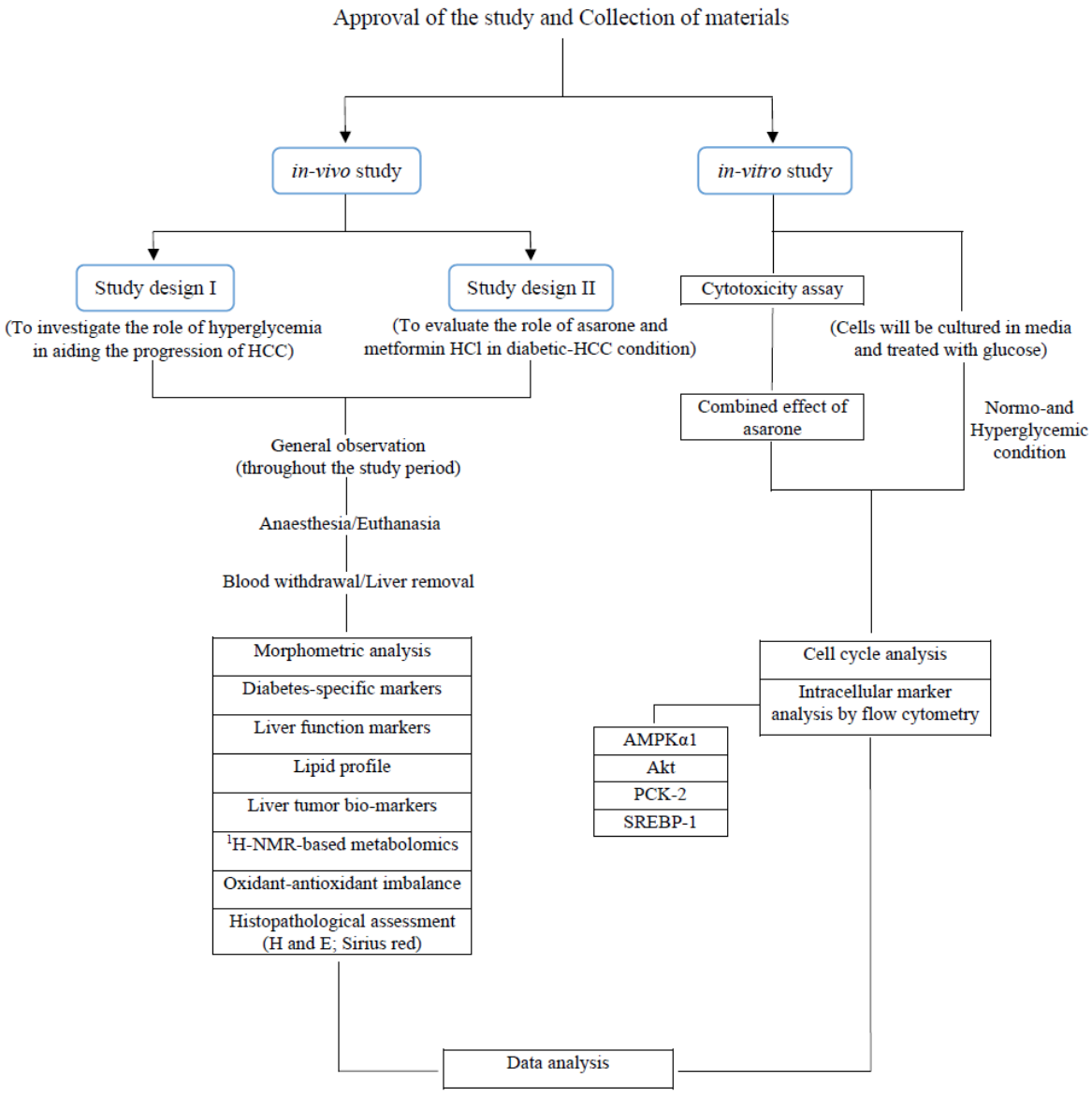

2. MATERIALS AND METHODS

2.1. *In-vivo* study

2.1.1. List of chemicals and instruments/equipment used in the study

Table 10: List of inducing agents (carcinogenic and diabetogenic) used in the study.

Sl. No.	Particulars	Company/Manufacturer
[1]	Diethylnitrosamine (DEN) (Purity ≥99% w/w; Lot # BCBP8749V; PubChem CID: 5921)	Sigma Aldrich Chemical Company, USA.
[2]	Streptozotocin (STZ) extra pure (Purity 98% w/w; Lot No: 2582459; PubChem CID: 29327)	Sisco-Research Laboratories (SRL) Pvt. Ltd., Mumbai, India.

Table 11: List of drugs (treatment) used in the study.

Sl. No.	Particulars	Company/Manufacturer
[1]	Alpha-asarone (Purity 98% w/w; Lot # S18779; PubChem CID: 636822)	Sigma Aldrich Chemical Company, USA.
[2]	Beta-asarone (Purity 70% w/w; Lot # STBF-1179V; PubChem CID: 5281758)	Sigma Aldrich Chemical Company, USA.
[3]	Metformin HCl (Lot No: METI-1710010; PubChem CID: 14219)	Angels Pharma India Pvt. Ltd. Hyderabad, India.

Table 12: List of test kits used in the study.

Sl. No.	Particulars	Company/Manufacturer
[1]	Glucose estimation kit, liver function test kits, lipid profile kits, tumor biomarker gamma-glutamyl transferase (GGT) test kit	Erba Transasia Bio-Medicals Ltd., Baddi, H.P, India.

[2]	Glycated hemoglobin (HbA_1c) test kit	NycoCard^{TM} (HbA_1c) test kit.
[3]	Insulin estimation kit	Mercodia, Sweden.
[4]	Alfa-fetoprotein (AFP) test kit (for hepatocarcinoma)	LifeSpan BioSciences, USA.

Table 13: List of chemicals/solvents/reagents/feed used in the study.

Sl. No.	Particulars	Company/Manufacturer
[1]	Sirius red stain/Direct red 80 (dye content 25%; PubChem CID: 124203941)	Sigma Aldrich Chemical Company, USA.
[2]	D_2O (deuterium oxide)	Sigma Aldrich Chemical Company, USA.
[3]	DPX (distrene dibutyl phthalate xylene)	Spectrum Reagents and Chemicals Pvt. Ltd., Cochin, India.
[4]	DTNB [5,5′-dithiobis (2-nitrobenzoic acid)]	Himedia Laboratories, India.
[5]	Eosin Y	Kemphasol, Mumbai, India.
[6]	DNPH (2,4-dinitrophenyl hydrazine)	SRL Pvt. Ltd., Mumbai, India.
[7]	Nicotinamide adenine dinucleotide	Himedia Laboratories, India.
[8]	TSP (trimethylsilyl 2,2,3,3-tetradeuteropropionic acid)	Sigma Aldrich Chemical Company, USA.
[9]	Glutathione	LobaChemie Pvt. Ltd., Mumbai, India.
[10]	Nitroblue tetrazolium	SRL Pvt. Ltd., Mumbai, India.
[11]	Hematoxylin (Harris)	Himedia Laboratories, India.
[12]	Phenazine methasulphate	Himedia Laboratories, India.
[13]	Rat pellet (for feeding purposes)	VRK Nutritional Solutions, Pune, India.
[14]	All other reagents of analytical grade	Central store of KLECOP, Hubballi.

Table 14: List of instruments/equipment/software used in the study.

Sl. No.	Particulars	Company/Manufacturer
[1]	Erba Chem 7 semi-automated analyzer	Erba diagnostic, Mannheim, Germany.
[2]	Electronic balance	Sartorius, UK.
[3]	Hot air oven	Servewell Instruments Pvt Ltd., Bangalore, India.
[4]	GraphPad Prism	GraphPad Software Inc, USA.
[5]	Image J Software (Image J 2010), IJ 1.46r	Built by the National Institute of Health (NIH) of Bethesda, USA.
[6]	Inverted microscope (CKX41)	Olympus Microsystem, Japan.
[7]	Microcentrifuge	Genei Manufacturers.
[8]	Micropipettes and tips	Tarsons Products Pvt. Ltd., Kolkata, India.
[9]	NMR	JEOL advanced ECZ400S spectrometer, USA.
[10]	NMR software version delta 5.0.5.1.	Delta NMR software, JEOL Ltd. The USA.
[11]	Rotary microtome (RM2125 RTS)	Leica Microsystems IR GmbH.
[12]	UV 1800 spectrophotometer	Shimadzu, Japan.

2.1.2. Selection of laboratory animals and their housing conditions

Male albino Wistar rats measuring 150–200 g were considered for the experiment. They were kept in the central animal facility of the institute, where they were kept under a natural 12 h dark: 12 h light cycle at 27 ± 2°C and had direct access to regular rat pellet and water.

2.1.3. Animal ethical consideration

The experiment was carried out after the Institutional Animal Ethics Committee (IAEC) of KLE College of Pharmacy, Vidyanagar, Hubballi, Karnataka, India, gave

their permission (Approval No. 07/KLEU'SCOPH/16). All the experimental procedures were conducted following the Committee for the Purpose of Control and Supervision of Experiments on Animals (CPCSEA).

2.1.4. Handling of hepatocarcinogen (Diethylnitrosamine)

The carcinogenic material diethylnitrosamine (DEN) procured was handled carefully, as suggested by the supplier. The DEN-containing vial was taken to the fume hood, and a diaper was placed over the work area before dispensing the DEN. The required amount of DEN was carefully transferred through a syringe and used for the experimental purpose. The DEN-containing vial was placed in a plastic bag and stored in the freezer. Further, the contact materials were disposed off in the infectious/biohazard waste, and the unused solutions were disposed off according to the material safety data sheet and incinerated.

2.1.5. Preparation of inducing and test agents

2.1.5.1. Preparation of streptozotocin (STZ)

The STZ was prepared freshly by dissolving it in a citrate buffer solution of 0.05 M and maintaining the pH constant at 4.5 with 1M citric acid. The citrate buffer solution was prepared by mixing tri-sodium citrate dihydrate and citric acid of 0.05 M.[173]

2.1.5.2. Preparation of diethylnitrosamine (DEN)

The DEN was prepared freshly by dissolving in NaCl solution of 0.9 % w/v.[174]

2.1.5.3. Preparation of α-and β-asarone

The asarone was freshly prepared by dissolving it in a 1:1 ratio in 0.5 % w/v sodium carboxymethyl cellulose.[29,164]

2.1.5.4. Preparation of metformin HCl

The metformin HCl was prepared by dissolving in water at a concentration of 250 mg/1.5 ml.[24]

2.1.6. Induction of diabetes and hepatocarcinoma

A pre-standardized single dose of streptozotocin (55 mg/2 ml/kg b.w. *i.p.*) was administered to induce diabetes in 6 to 8 h fasting rats. To prevent severe hypoglycemia, the rats were given a sucrose water solution (10 % w/v) for one day after receiving STZ.[173] A single dose of diethylnitrosamine (200 mg/ml/kg b.w. *i.p.*) was administered to induce HCC in rats.[174]

2.1.7. Experimental study design

The acclimatized animals were divided into two experimental study designs assigned as I and II either at 12-weeks and 18-weeks.

- **Study design I** (Figure 5)**:** The effect of STZ-induced hyperglycemia on the development of DEN-induced HCC were examined for 12 weeks in this study design. As seen in Table 15, the rats in this experiment were randomly divided into four groups, each with eight animals (n=8). The blood/serum was obtained following mild ether anesthesia, and tissue samples were collected after the animals were humanely sacrificed to evaluate different parameters.

Table 15: Experimental study design I for a duration of 12-weeks.

Groupings	Treatment
I	Normal control (NC) group and received 0.9% w/v NaCl (1 ml/kg b.w. *i.p.*).
II	The diabetogenic (STZ) group was administered with a single dose of streptozotocin (Section 2.1.5.1 and 2.1.6).
III	The hepatocellular carcinoma (DEN) group was administered with

	a single dose of diethylnitrosamine (Section 2.1.5.2 and 2.1.6).
IV	The diabetic-hepatocellular carcinoma (STZ+DEN) group was administered with a single dose of STZ followed by DEN two weeks later after confirming the elevated glucose levels.

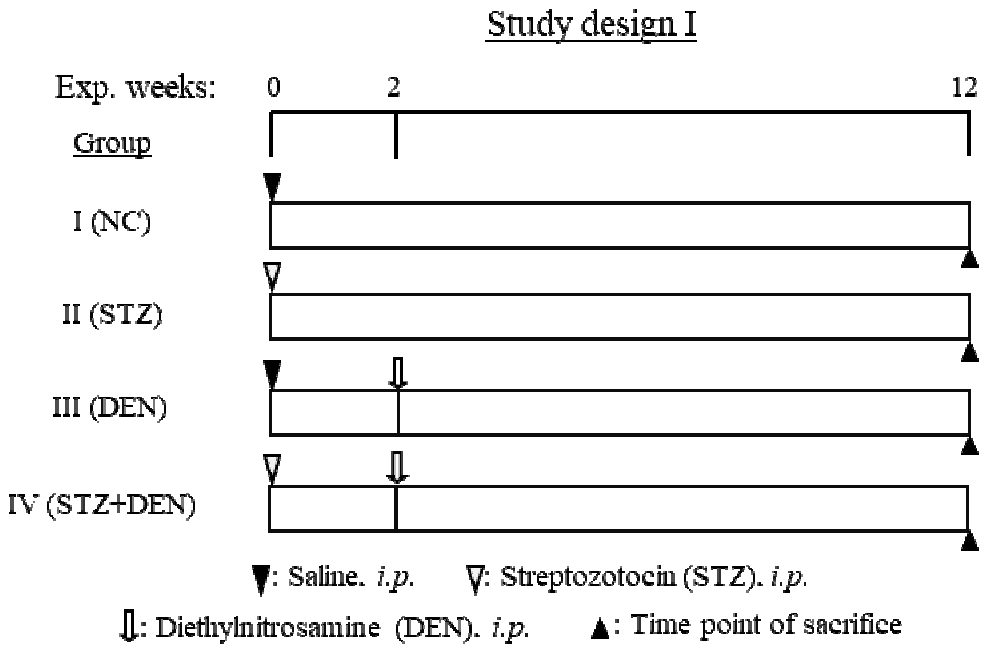

Figure 5 (Study design I)**:** The diabetes mellitus was confirmed in the second week after the administration of the streptozotocin (STZ). The diethylnitrosamine (DEN) was administered two weeks later to the administration of STZ to induce the HCC in diabetic rats. The total duration of the study was for the period of 12-weeks.

❖ **Study design II** (Figure 6)**:** The combination of α-and β-asarone and metformin HCl was examined separately on STZ+DEN rats for 18 weeks period in this study design. As seen in Table 16, the rats in this experiment were randomly divided into five groups, each with eight animals (n=8). The blood/serum was obtained following mild ether anesthesia, and tissue samples were collected after the animals were humanely sacrificed to evaluate different parameters.

Table 16: Experimental study design II for a duration of 18-weeks.

Groupings	Treatment
I & II	Similar to the study design I.
III	Served as diabetic-hepatocellular carcinoma (STZ+DEN) group and was similar to group IV of study design I.
IV	Served as a treatment group that was administered with a combination dose of α-and β-asarone. The asarone (50 µg/1.5 ml/kg b.w., *p.o.*) prepared in 0.5% w/v sodium carboxymethyl cellulose were given in the ratio of 1:1 for five days per week after two weeks of STZ+DEN injections.[29,164]
V	Similar to group IV except that the freshly prepared metformin HCl (250 mg/1.5 ml/kg b.w.) replaced the asarones.[24]

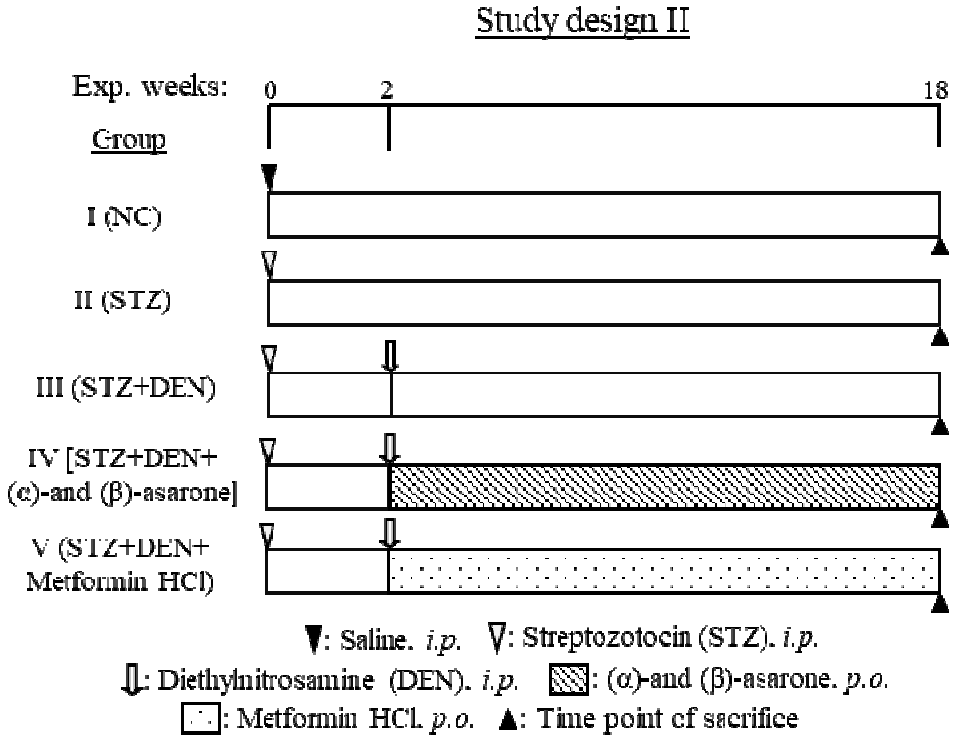

Figure 6 (Study design II)**:** The STZ and DEN were injected the same way as in study design I. For 18 weeks, the asarone and metformin were used as a treatment to study their effect on the diabetic-HCC condition.

2.1.8. Collection of blood, serum and liver specimens

Blood was drawn via retro-orbital sampling technique in a collection tube without any anticoagulant. The serum sample taken after two weeks was used to assess if STZ had caused hyperglycemia. All other biochemical tests were determined using the blood obtained at the end of the experiment. For measuring glycosylated hemoglobin (HbA_1c), a portion of the blood was kept in EDTA tubes. Another portion of the blood was kept at room temperature for 30 minutes before being taken for centrifugation (2500 rpm; 10 min) to collect the serum for analysis of different parameters. Following that, the rats were sacrificed, and tissue samples were collected, washed from the blood, cleaned in ice-cold normal saline solution, and measured. One portion of the liver was mixed with a 0.15 M Tris-HCl buffer of pH 7.4 to make a homogenate (10% w/v), taken for centrifugation at 4℃ (10,000×g; 10 min) for anti-oxidant activity. Another portion was preserved in formalin solution (10% v/v) and processed to study histopathological features of the liver with different stains.

2.1.9. Assessment of parameters

2.1.9.1. General observation

The daily food and water intake, and weekly body weight variations, were noted. The change in weight and consumption of food and water between weeks was calculated by subtracting the average weight of week 0 from the subsequent weeks. The results were measured as comparative food and water intake per week for 100 g of the rat. The liver weight of each rat in each group was measured at the end of the experiment, and the relative liver weight (g %) was determined by dividing the liver weight by the bodyweight of each rat.

2.1.9.2. Study of liver morphology (nodule incidence, multiplicity and size)

The liver specimens were examined for apparent nodules or tumors and graded into three types: less than 1, 1 to 3 and more than 3 mm. The number of the tumors-bearing liver (nodule incidence) and the total no. of tumors/nodule incidence (nodule multiplicity) were noted in all tumor-bearing groups.[175]

2.1.9.3. Measurement of biochemical parameters

The fasting glucose level in serum for all the experimental groups was measured by Trinder's method (glucose oxidation-peroxidase)[176] using Erba kit, liver dysfunction markers [such as alkaline phosphatase (ALP),[177] aspartate aminotransferase (AST),[178] and alanine aminotransferase (ALT)[179] was estimated by kinetic method, total and direct bilirubin (TB and DB) by Diazo method,[180] total protein (TP) by biuret method[181] and albumin (ALB) by Bromo cresol green method[182] using Erba kit], lipid profile levels [triglycerides (TG) was estimated by glycerol-3-phosphate oxidase (GPO)-Trinder method,[183] total cholesterol (TC) was determined by cholesterol oxidase-glycerol-3-phosphate oxidase enzymatic (CHOD-PAP) method[184] using Erba kit, high-density lipoprotein cholesterol (HDL-c) was estimated by polyethylene glycol methyl ether and polyvinylsulfonic acid (PEGME-PVS) coupled precipitation method[185] using Erba kit by Erba Chem 7 semi-automated analyzer (Erba diagnostic, Mannheim, Germany). Friedewald's method was used to quantify the low and very-low-density lipoprotein cholesterol (LDL-c/VLDL-c).[186] It was estimated as:

$$\mathrm{LDL} = \mathrm{TC} - (\mathrm{HDL} + \mathrm{VLDL})$$

$$\mathrm{VLDL} = \mathrm{TG}/5$$

Further, the tumor biomarker gamma-glutamyl transferase (GGT) was determined by the kinetic colorimetric method[187] using the Erba kit with the help of

Erba Chem 7 semi-automated analyzer (Erba diagnostic, Mannheim, Germany). The HbA_1c level was measured with a NycoCard™ (HbA_1c) reagent kit and examined in a NycoCard™ scanner as per the manufacturer's protocol. The company's instructions were followed to determine the quantitative assessment of the liver tumor bio-marker AFP[188] and serum insulin[189] using the enzyme-linked immunosorbent assay (ELISA) methodology.

2.1.9.4. Serum metabolites by ^{1}H-NMR spectroscopy and acquisition of spectra

The ^{1}H-NMR spectroscopy technique was employed to characterize and quantify the changes in the serum metabolites for all the samples of study design II. For analysis, a JEOL advanced ^{1}H-NMR spectrometer (ECZ400S) operating at 400 MHz proton frequency and a 5 mm TH5 direct broadband probe was used for the study. Briefly, for the study, 300µl of serum sample was mixed with 200µl of deuterium oxide (D_2O) in a co-axial sealed capillary NMR tube (5-mm; clean and dried). On the other hand, trimethyl silyl-propanoic acid (TSP; 30µl) containing salts of sodium ions was mixed with D_2O in a recyclable NMR tube before running the test samples. The TSP used in the study acts as an external standard and a chemical shift reference to measure the metabolites, while the D_2O acts as a filed-frequency lock. All the acquired ^{1}H-NMR spectra were carried out through water suppression in a 1-D Carr Purcell-Meiboom-Gill (CPMG) pulse order as it helped remove broad signals from the macromolecules, protein, or lipids.

❖ **Typical parameters and software used for obtaining the ^{1}H-NMR spectra:**

Spectral width	: 15 ppm
Number of scans	: 256
Dummy scans	: 4

Domain data points	: 16-times
Relaxation delay	: 5s
Receiver gain value	: 60
Pulse angle	: 90^{o}
Tau interval	: 0.172ms
Software	: NMR delta version 5.0.5.1. [It was used for the baseline and phase correction and for obtaining the area under the curve (AUC) value].

This technique identified and characterised the small metabolites such as pyruvate, lactate, creatine, acetate, valine, alanine, and glutamine. The ^{1}H-NMR spectroscopy technique was carried out by utilizing the instrument facilities of the University Scientific and Instruments Center (USIC), Karnatak University, Dharwad, Karnataka, India, for recording the spectra.

❖ **Metabolomic processing of the data**

The concentration of the detected metabolites was estimated over the processed data by utilizing the integral values (AUC) of definite signals for a known concentration of the TSP. The following formula was used for the estimation of the metabolite:

$$C\mathit{metabolite}(\mathrm{mmol}) = (\mathrm{Ax} \times \mathrm{Mx} \times \mathrm{Nr} \times \mathrm{Wr}/\mathrm{Ar} \times \mathrm{Mr} \times \mathrm{Nx} \times \mathrm{V}) \times 1000$$

Where, Ax denotes the integral area of the metabolite.

Mx signifies the molecular weight of metabolite.

Nr signifies the number of protons of TSP (standardized at 0.0 ppm for assignment of the metabolites).

Wr denotes the weight of TSP taken in the NMR tube.

Ar signifies an integral area of TSP.

Mr signifies the molecular weight of TSP, and

Nx represents the number of protons of the metabolite.

❖ **Functional significance of the analyzed metabolites associated with the metabolic pathways**

The changes related to the identified metabolites in study design II between the different experimental groups were linked with the metabonomic database. The functional significance of the identified metabolites concerning its pathway during the disease progression was determined using the following databases:

1. The HMDB (Human Metabolome Database; https://hmdb.ca/metabolites) and
2. The KEGG (Kyoto Encyclopedia of Genes and Genomes; https://www.genome.jp/kegg/pathway.html).

2.1.9.5. Anti-oxidant activity

Quantitative assessment of superoxide dismutase (SOD):

The SOD levels were measured utilizing the procedure of Kakkar *et al.*[190] as explained with the help of a flow chart (Figure 7).

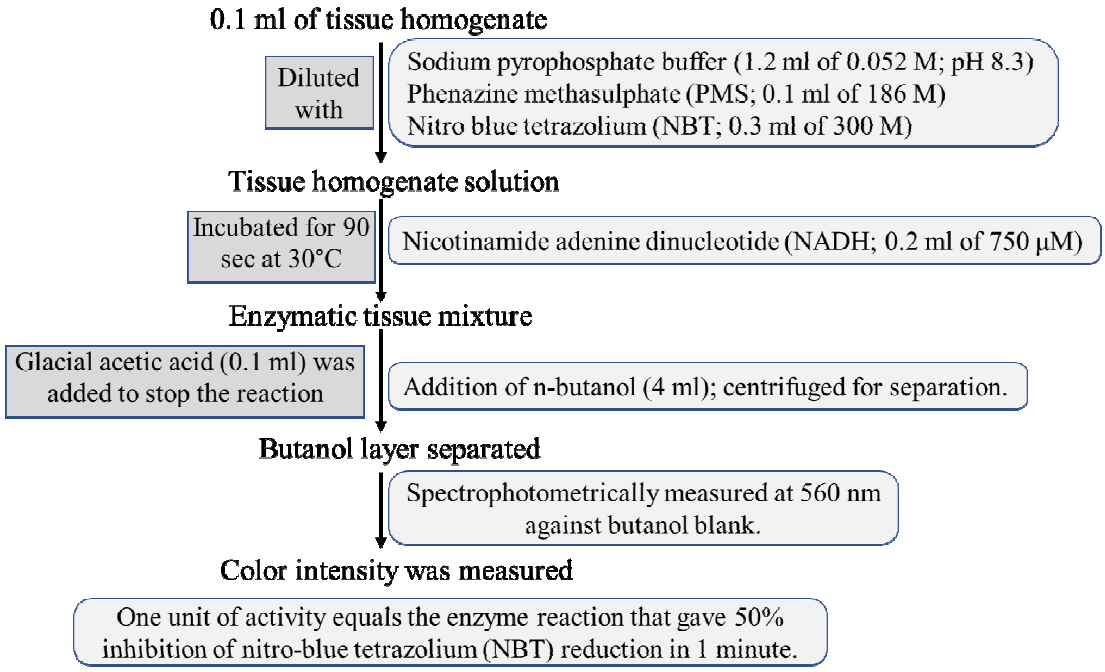

Figure 7: Flow chart for the quantitative assessment of superoxide dismutase (SOD).

Quantitative assessment of catalase (CAT):

The CAT levels were measured utilizing the procedure of Sinha AK[191] as explained with the help of a flow chart (Figure 8).

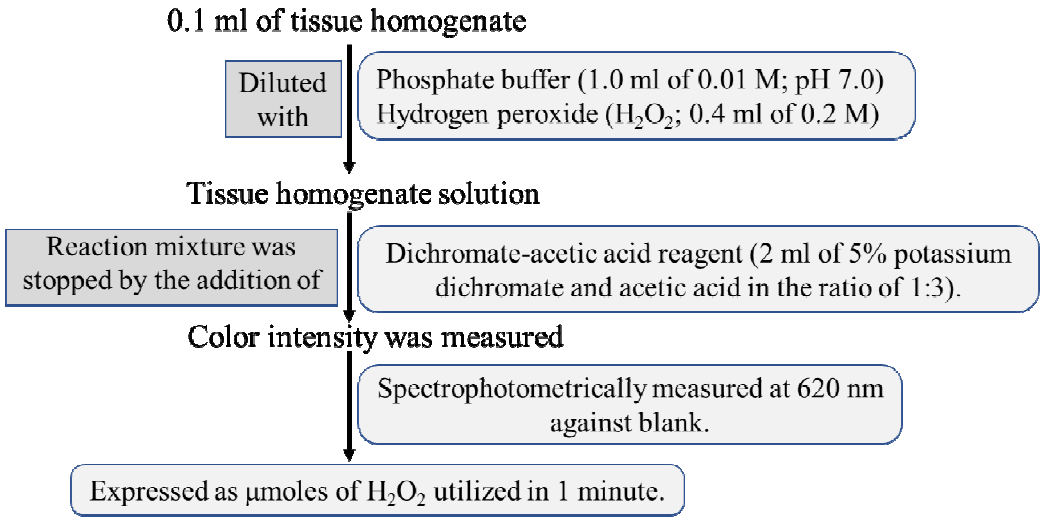

Figure 8: Flow chart for the quantitative assessment of catalase (CAT).

Quantitative assessment of lipid peroxidation (LPO):

The LPO levels were measured utilizing the procedure of Niehaus *et al.*, Jiang *et al.*, and Ohkawa *et al.*[192-194] as explained with the help of a flow chart (Figure 9).

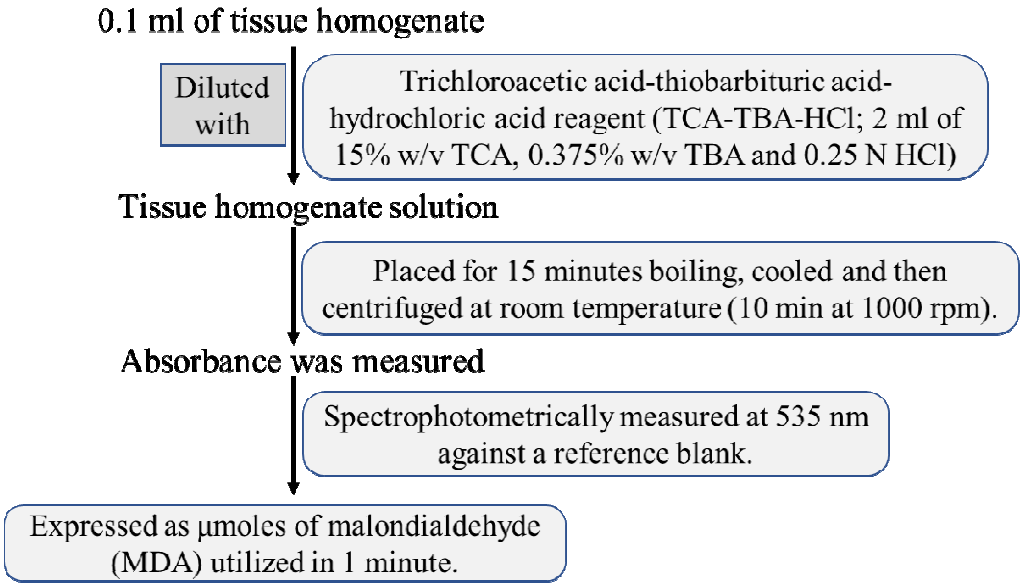

Figure 9: Flow chart for the quantitative assessment of lipid peroxidation (LPO).

Quantitative assessment of glutathione peroxidase (GPx):

The GPx levels were evaluated utilizing the method of Rotruck *et al.*[195] as explained with the help of a flow chart (Figure 10).

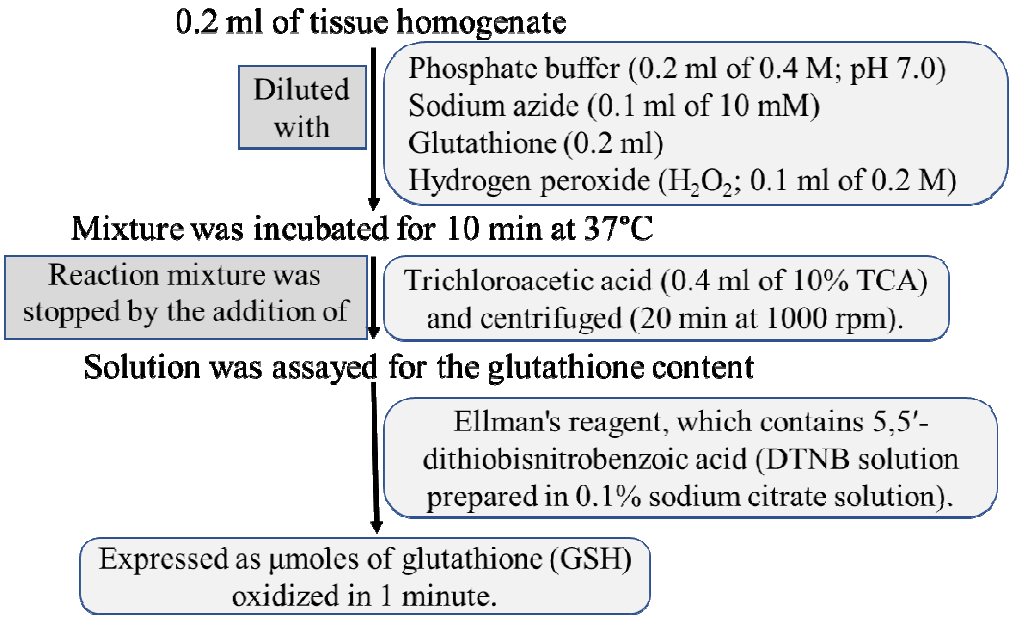

Figure 10: Flow chart for the quantitative assessment of glutathione peroxidase (GPx).

Quantitative assessment of reduced glutathione (GSH):

The GSH levels were measured utilizing the procedure of Ellman GL.[196] as explained with the help of a flow chart (Figure 11).

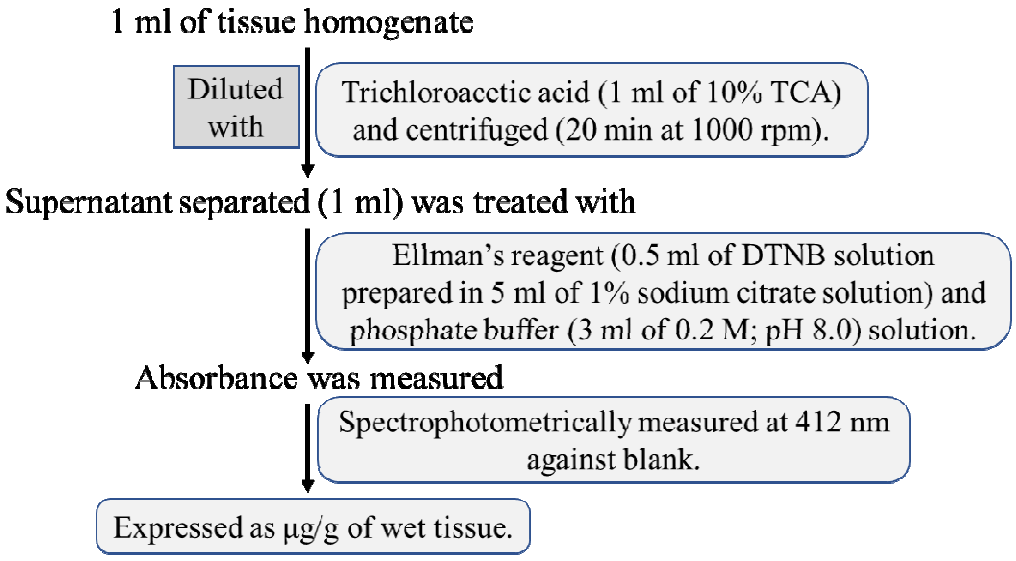

Figure 11: Flow chart for the quantitative assessment of reduced glutathione (GSH).

Quantitative assessment of Vitamin-C:

The Vitamin C levels were measured utilizing the procedure of Omaye *et al.*[197] as explained with the help of a flow chart (Figure 12).

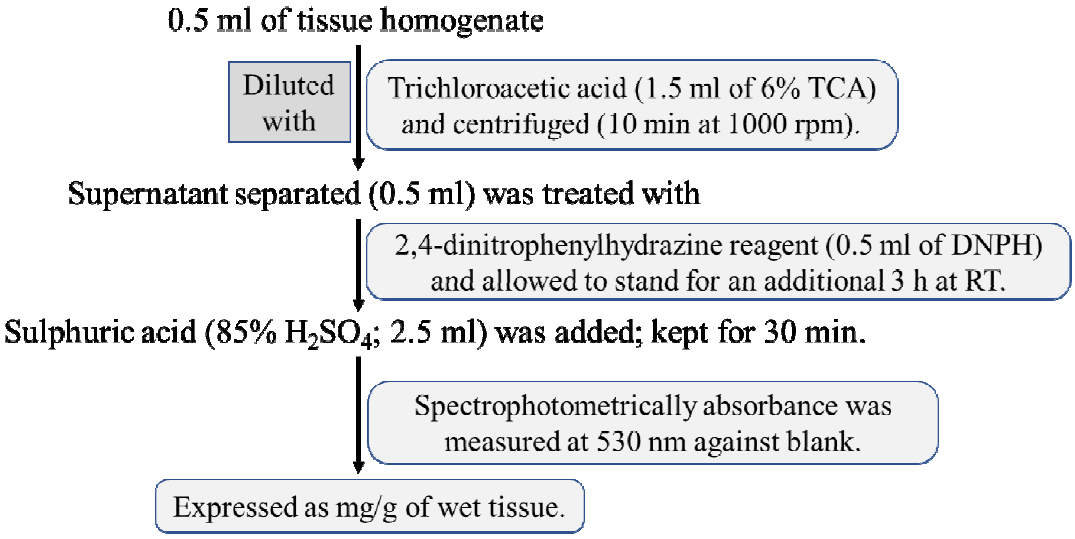

Figure 12: Flow chart for the quantitative assessment of Vitamin C.

2.1.9.6. Liver histopathology (H and E; Sirius red)

The formalin-fixed liver tissues were dehydrated by passing them through an increasing concentration of isopropyl alcohol (from 60 to 100%; to avoid excessive distortion of the tissues), followed by acetone and clearing agent (xylene) for de-alcoholization and were finally submerged in paraffin. A microtome was used to obtain 5 μm thick paraffin-embedded portions of the liver, which were stained. The histopathological changes in the liver sections were examined using Hematoxylin and Eosin (H and E) and Sirius red or Direct red 80 for staining.

Hematoxylin (H) stains the nucleus or the negatively charged structures like DNA, eliciting a blue-purplish color. Whereas, Eosin (E) imparts a pink-orange color by staining the cytoplasm. Sirius red is one of the best staining techniques for assessing hepatic fibrosis. It is obligatory to incorporate two dyes to obtain contrasting colors for staining the cellular structures. The Sirius red staining procedure was similar to the H and E staining, except the freshly prepared Sirius red, replaced the Eosin Y. Briefly, the rehydrated liver section slides (rehydrated with decreasing concentration of ethanol from 100 to 70%) were treated with Hematoxylin (Harris) for three minutes, followed by water-wash for three minutes. Further, the cytoplasm was cleared off from the hematoxylin by washing with 1% acid alcohol solution for two seconds, following water-wash for three minutes. The liver section slides were then treated with Eosin Y for 30 seconds, followed by water-wash for three minutes. The Sirius red stain (prepared in statured aqueous picric acid solution) was used instead of the Eosin Y. Finally, it was dehydrated (95% ethanol) and passed through a clearing agent (xylene) for one minute, and mounted in distrene dibutyl phthalate xylene (DPX) medium for observations. The photomicrographs were

captured from the stained slides with the help of a microscope (CKX41, Olympus Microsystem, Japan).

2.1.9.7. Sirius red positive area calculation

Image J software was used to calculate the relative hepatic fibrosis area. A definite area (190×190 μm^2) of six identical squares was measured from each observation and expressed as % Sirius red +ve area. Further, the results (% of Sirius red positive area) were copied to the GraphPad Prism software for subsequent analysis and represented as mean ± SEM for each observation.

The following sequence was adopted for the captured Sirius red-stained images:

1. A Sirius red-stained image was opened using the menu *File* > *Open* tool, and the scale was converted to pixels (Figure 13).

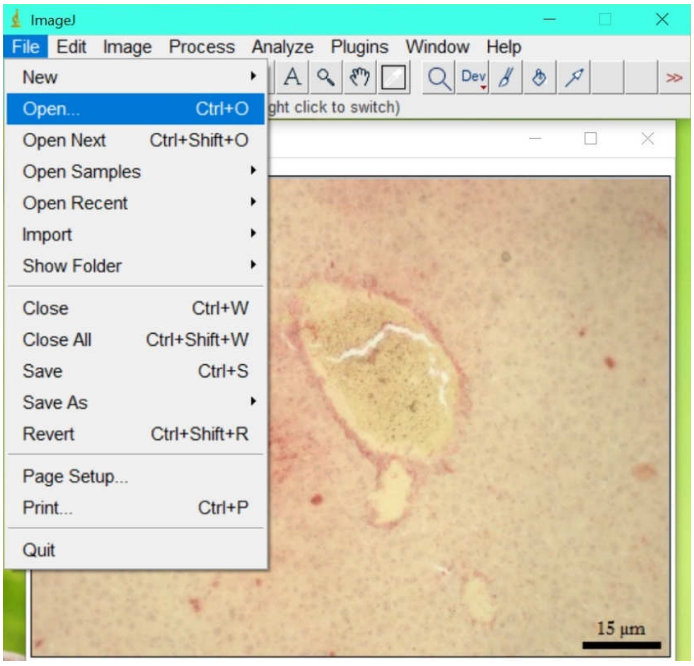

Figure 13: A Sirius red-stained image used for calculating the percentage (%) Sirius red positive area.

2. The conversion of the scale to µm was done using *Analyze* > *Set Scale* tool. The conversion ratio of 0.8 pixels/µm was used for all the captured images (Figure 14).

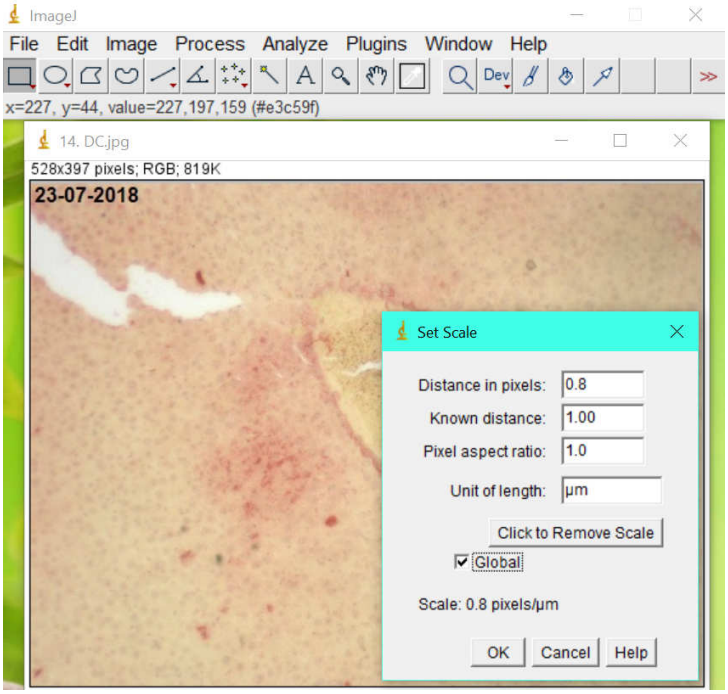

Figure 14: The scale of measurement was changed from pixels to µm (clicking global).

3. The stained image was then converted to grayscale by dividing the photo into red, green, and blue channels with the *Image* > *Type* > *8-bit* stack order. The image was stacked in grayscale for measuring the threshold level (Figure 15).

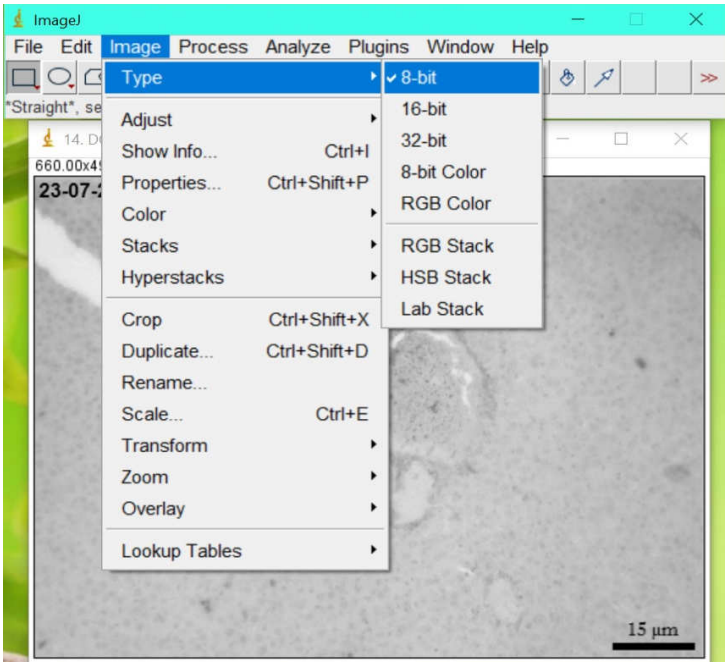

Figure 15: The conversion of the stained Sirius red image to grayscale.

4. The grayscale image was adjusted for threshold from the Menu bar using the *Image* > *Adjust* > *Threshold* tool. The threshold level was adjusted manually using the upper and lower limit of the 'Threshold tool' (Figure 16).

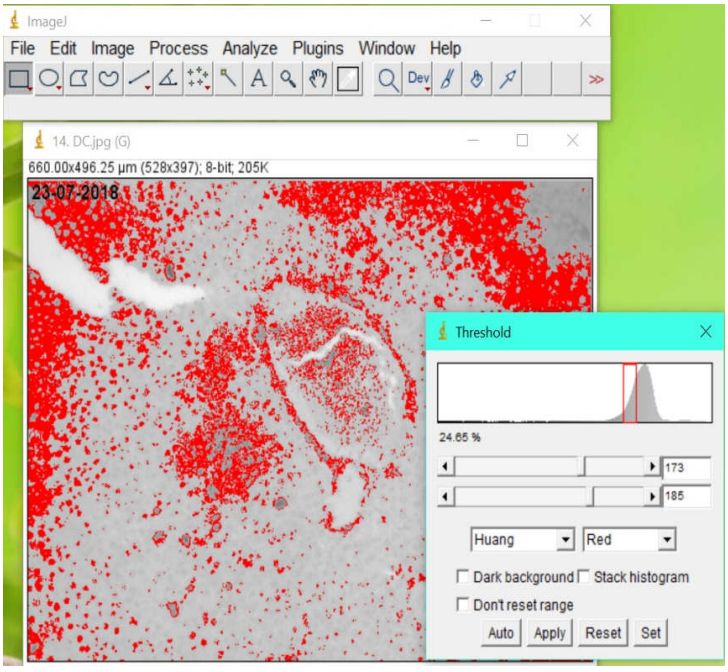

Figure 16: The threshold tool was used for reflecting the accurate staining.

5. Further, selecting the parameters to quantify for area and % area was used by selecting the *Analyze* > *Set Measurements* dialog box (Figure 17).

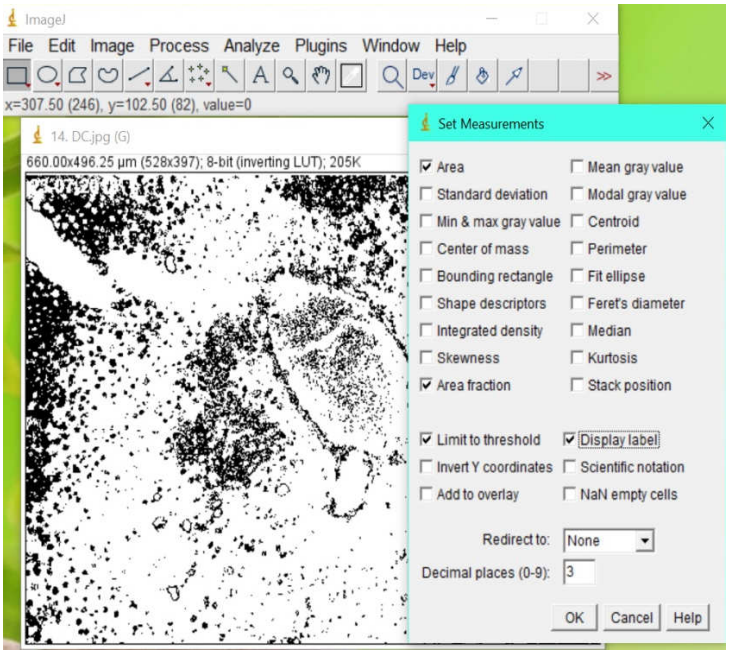

Figure 17: The selection of parameters to quantify the area and % area. The following settings were clicked as Area, Area fraction, Limit to the threshold, and Display label to measure the percentage of the selected stained area.

6. A square of 190×190 μm^2 was drawn using the rectangle selection method in Image J software. These specific dimensions were drawn on the stained grayscale image to measure the threshold within six identical sized areas to quantify the area. After drawing the square, the *Analyze* > *Measure* command was selected to display the area and % area in the '*Results*' window (Figure 18).

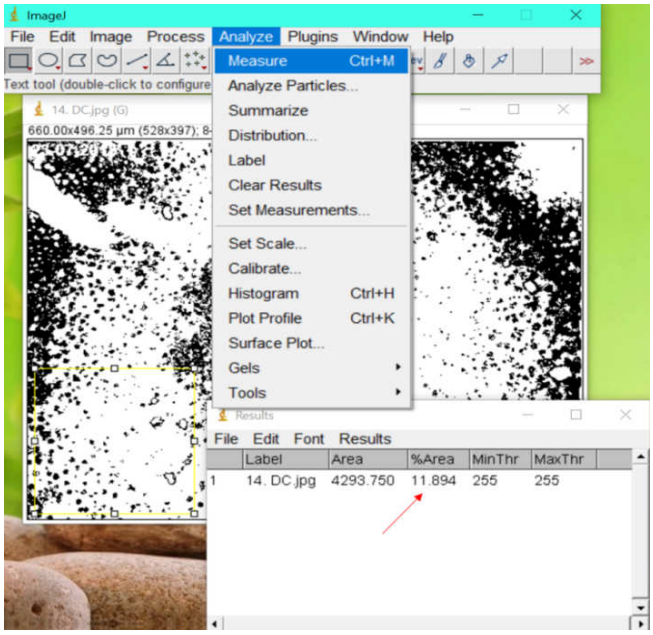

Figure 18: The squares of the definite area were measured from each stained image. The red arrowhead indicates the % area calculation for one square.

7. Finally, the area of six identical squares was measured. These results were copied to the GraphPad Prism software for subsequent analysis and expressed as the mean ± SEM (Figure 19).

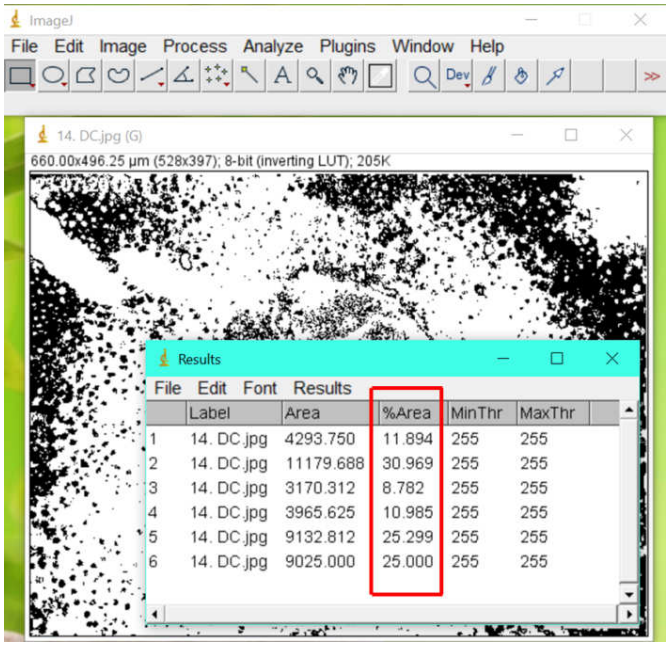

Figure 19: The red box represents the % area of six identical squares in the stained Sirius red slide.

2.1.9.8. Scoring of hepatic fibrosis, inflammation and hepatocyte ballooning

The scoring/stages of liver fibrosis were graded F1 to F3 based on the staining of the Sirius red, as explained in the Table 17.

Table 17: Scoring/stages of liver fibrosis.

F1	Fibrosis spreading over few portal areas without septa.
F2	Most portal areas have severe fibrosis expansion, with a frequent portal to portal (P–P) bridging.
F3	Fibrosis expansion in nearly all portal regions, with a portal to portal (P–P) and portal to central (P–C) bridging.

In addition, the number of inflammatory foci found in the H and E-stained slides was ranked from 0 to 3 as explained in the Table 18.

Table 18: Scoring of inflammatory foci.

Score 0	Normal, < 0.5 foci
Score 1	Slight, 0.5–1.0 foci
Score 2	Moderate, 1.0–2.0 foci
Score 3	Severe, > 2.0 foci

Finally, hepatocyte ballooning was also graded on a scale of 0 to 2 depending on the number of balloon cells observed in H and E-stained slides, as explained in the Table 19.

Table 19: Scoring of hepatocyte ballooning.

Score 0	No balloon cells.
Score 1	Scattered balloon cells.
Score 2	Panacinar balloon cells.

2.1.10. Data analysis

The data for various parameters was statistically calculated using the software program version 6.0 of '*GraphPad Prism*' and represented as mean ± SEM. The student's t-test or 1-way ANOVA following Bonferroni multiple as a post hoc statistical tool was used to determine the statistical significance, considering $p < 0.05$ as the limit of the significance.

2.2. *In-vitro* study

2.2.1. List of chemicals and instruments/equipment used in the study

Table 20: List of chemicals/cell line/antibodies used in the study.

Sl. No.	Particulars	Company/Manufacturer
[1]	Phosphate-buffered saline without calcium and magnesium (CMF-PBS), Trypsin-EDTA digestion solution 1X, Dulbecco's modified eagle's medium (DMEM), Methyl thiazolyl tetrazolium (MTT), Heat-inactivated fetal bovine serum (FBS)	HiMedia Laboratories Pvt. Ltd., Mumbai, India.
[2]	Dimethyl sulfoxide (DMSO)	Sigma-Aldrich Chemical Company, USA.
[3]	HepG2 Human hepatocellular carcinoma cells (ATCC® HB-8065™)	American Type Culture Collection (ATCC), USA.
[4]	Streptomycin (100 µg/ml) and Penicillin (100 U/ml)	Sigma-Aldrich Chemical Company, USA.
[5]	Polyclonal FITC (Fluorescein isothiocyanate) goat anti-rabbit secondary antibody IgG (Catalog No. 554020)	BD Biosciences, USA.
[6]	Primary rabbit polyclonal IgG antibody Akt: Catalog No. orb159889 AMPK α1: Catalog no. orb10076 PCK-2: Catalog no. orb5876 SREBP-1: Catalog no. orb11415	Biorbyt Ltd., Cambridge, UK.
[7]	Propidium iodide (PI)-RNase staining solution (Catalog No. 550825)	BD Biosciences, USA.

Table 21: List of instruments/equipment/software used in the study.

Sl. No.	Particulars	Company/Manufacturer
[1]	CO_2 incubator	Labwit Scientific Pty Ltd., Australia.
[2]	Cytomics FC500 flow cytometer equipped with CXP software (FlowJo software version 10.0.7.)	Beckman-Coulter, USA.
[3]	Microplate reader	Biobase® EL-10A, China
[4]	Inverted microscope (CKX41)	Olympus Microsystem, Japan.

2.2.2. Cell culture conditions

The human HepG2 carcinoma cell line used for the study was cultured according to the standard protocol of the supplier, as explained with the help of a flow diagram (Figure 20).

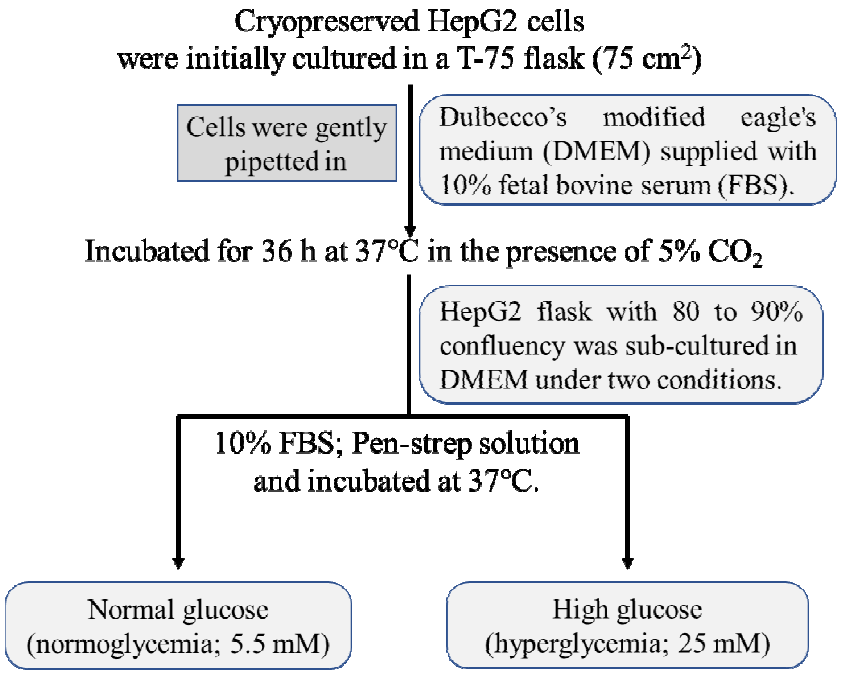

Figure 20: Protocol for the culture of HepG2 carcinoma cell line. Pen-strep solution, 100 U/ml Penicillin- 100 µg/ml Streptomycin solution.

2.2.3. Cell count (Trypan blue dye method)

The HepG2 cells were counted to monitor growth rates (during the experiment) or for further sub-culture or cryopreservation at a known concentration. For calculating the viable cells, the trypan blue dye method was adopted using the Neubauer hemocytometer. The viable unstained cells can be counted through this method as it doesn't uptake the trypan blue dye, appearing clear bright in color. Briefly, 20µl of HepG2 cells was gently combined to trypan blue (20µl; 0.4% v/v) in a 1:1 ratio. Further, from the trypan blue-treated cell suspension mixture, 20µl of the sample was carefully withdrawn and loaded to the clean hemocytometer. The cell suspension was gently applied underneath a coverslip, thus allowing it to be drawn through capillary action and viewed under a microscope (×20) for the viable cell count (in the four sets of 16 squares). The number of viable cells/ml was calculated by taking the average cell count from each set of 16 squares. Further, it was multiplied by a conversion factor of 10,000 ($\times 10^4$) and a dilution correction factor (for the trypan blue dye) for deriving the final viable cells/ml in the cell suspension.

$$\text{Number of viable cells/ml} = \text{Average cell count} \times 10{,}000 \times \text{dilution factor}$$

$$\text{Average cell count} = \text{Cell count for } (S1 + S2 + S3 + S4)$$

Here, S1-4: Sets of 16 corner squares from 1 to 4.

2.2.4. Cytotoxicity by methyl thiazolyl tetrazolium (MTT) assay

A colorimetric-based MTT assay was used to predict the cytotoxicity of metformin HCl, α-asarone, and β-asarone on the HepG2 cell line.[198] Briefly, the HepG2 cells were grown at a concentration of 10,000 cells/well (200µl) in a 96-well microtiter plate (flat-bottom received from Nunc™ MicroWell™, Thermo Fisher Scientific Inc., USA) and permitted to adhere in a CO_2 incubator (37^0C; 5% CO_2 and 95% humidity

for 24 h). Before the experiment, the cell count was verified by the trypan blue dye method (*Section 2.2.3.*). After the completion of 24 h of incubation, the medium was replaced with 200µl of fresh DMEM and treated with different concentrations of the test compounds (α-and β-asarone; 0.12 to 1.92 mM and metformin HCl; 1.6 to 25.6 mM). At the same time, cells containing only culture medium and devoid of any treatment served as a control for this experiment. These cells were further incubated at 37^0C for 48 h. After incubation, the drug-treated medium was replaced with MTT solution (200µl; prepared at a strength of 0.5 mg/ml in phosphate buffer solution) and kept for another three hours incubation at 37^0C. Finally, the medium was aspirated. The formazan-formed crystals were mixed with dimethyl sulfoxide (DMSO; 100µl) per well and the intensity of the purple color (due to solubilization of the formazan crystals) was recorded at 570 nm using a microplate reader. The corresponding equation was used to calculate the % of growth inhibition or cell viability:

$$\%\ Cell\ viability = \frac{Absorbance\ of\ treated\ cells}{Absorbance\ of\ untreated\ cells} \times 100$$

Finally, the IC_{50} (inhibitory concentration-50) result for HepG2 cells was calculated using the dose-response curve. The IC_{50} is the concentration of the test substances (asarone and metformin) needed to inhibit cell growth by 50%.

2.2.5. Cell proliferation assay and morphological observations

HepG2 cells were seeded at a concentration of 2×10^3/well in a microtiter plate of 96-well and permitted to adhere in a CO_2 incubator (37^0C; 5% CO_2 and 95% humidity for 24 h). The very next day, the HepG2 cells were deprived of glucose and serum for two hours. Subsequently, the cells were grown in a complete medium containing FBS (10%) for 48 and 96 hours under two glucose conditions:

1. Normoglycemic (NG; 5.5 mM) and
2. Hyperglycemic (HG; 25 mM).

Further, the changes in the percentage of cell proliferation were assessed by the MTT test (*Section 2.2.4.*) and represented as mean ± SEM in bar graphs. The morphological changes of the cell were observed with an inverted microscope after being cultured for 48 and 96 h under different glucose concentrations.

2.2.6. Experimental study design and treatment

Based on the IC_{50} values of the test compounds (asarone and metformin) derived through the colorimetric-based MTT assay (*Section 2.2.4.*), the concentration selected for the further study was one-half of the IC_{50}. Therefore, the HepG2 cells were categorized into four groups, as tabulated in Table 22.

Table 22: Experimental study design for the *in-vitro* study.

Groupings	Treatment
Normoglycemic (NG)	The HepG2 cells were cultured in 5.5 mM of normal glucose.
Hyperglycemic (HG)	The HepG2 cells were cultured in 25 mM of high glucose.
HG+Asarone (α+β)	The HepG2 cells were treated with a combination dose of 0.61 mM of α-asarone and 0.73 mM of β-asarone in HG condition.
HG+Metformin	The HepG2 cells were treated with 12.87 mM of metformin HCl in HG conditions.

2.2.7. Cell cycle analysis

An FC500 flow cytometer equipped with CXP software was used to investigate and collect data for the various stages of the cell cycle. As stated elsewhere, the percentage of ethanol-fixed HepG2 cells stained with propidium iodide (PI)-dye

method was determined.[199] Briefly, HepG2 cells were seeded at a concentration of 5 × 10^5 cells/well in a 6-well plate, permitted to adhere and incubated (37^0C; 5% CO_2 and 95% humidity for 24 h). The medium was removed after completion of 24 h of incubation, substituted with a complete growth medium containing a supplement of FBS (10%), and cultured under different conditions for the next 16 h (*Section 2.2.6.*; Table 22). Thereafter, the trypsinized cells (0.5 ml of trypsin-EDTA solution 1X) were washed with DPBS; 1X and immobilized with chilled ethanol (1000µl of 70% at 4^0C). The cells were rinsed in DPBS solution after 30 minutes of fixation and suspended in 400µl of staining solution (PI-RNase) for 30 minutes in the dark. Further, the ethanol-fixed PI-RNase-stained cells were harvested for analysis. The mixed samples were examined using the cytomics FC500 flow cytometer to collect the data. Data were evaluated using the FlowJo v10.0.7 software, and the histograms and plots depicted the proportion of cells for various stages of the cell cycle.

2.2.8. Intracellular markers evaluation of AMPKα1, Akt, PCK-2, and SREBP-1

The intracellular related markers AMPKα1, Akt, PCK-2, and SREBP-1, were analyzed quantitatively by a flow cytometer. Briefly, HepG2 cells were seeded at a concentration of 3 × 10^5 cells/2 ml in a 6-well plate and permitted to stay in a CO_2 incubator (37^0C; 5% CO_2 and 95% humidity for 24 h). After the completion of 24 h of incubation, the medium was discarded and washed with phosphate-buffered saline solution (1X PBS; 1000µl) and cultured under different conditions for 24 h (*Section 2.2.6.*; Table 22). At the same time, cells containing only culture medium and devoid of any treatment served as a control for this experiment. Thereafter, the medium containing the test compounds or control was transferred to a centrifuge tube (5 ml), and the wells were washed with PBS solution (500µl). The PBS was further aspirated from the wells and shifted to the same centrifuge tube. The plate containing the drug-

treated cells was treated with trypsin-EDTA solution (200µl) and incubated at 37^0C for 4 minutes. Then the incubated cells were finally collected into the same tube from the wells, centrifuged at 25^0C (at 300 × g; 5 min), and the cell-free supernatant was drained away. Thereafter, cells were treated with paraformaldehyde solution (PFA; 500µl of 2%) and incubated (20 min at RT). After 20 minutes of incubation, the PFA solution was diluted with PBS solution (1000µl), centrifuged at 25^0C (300 × g; 5 min), and drained off the supernatant. Further, the pellet-containing cells were permeabilized by adding Triton X-100 (500µl of 0.1%) and incubated (10 min at RT). Thereafter, bovine serum albumin solution (BSA; 1000µl of 0.5%) was added and mixed well for the settlement of the cells, centrifuged at 25^0C (200 × g; 5 min) and drained off the supernatant. Further, the primary antibody (Table 23) was prepared and mixed with the addition of BSA in PBS solution and incubated (1 h at 25^0C). Following incubation, the cells were washed with BSA solution, resuspended with BSA in PBS solution (500µl), and a secondary antibody was added (Table 23). Finally, the cells were incubated (1 h at 25^0C in a darkroom), centrifuged, decanted carefully, and mixed well with BSA solution (500µl) and analyzed with the help of a flow cytometer.

Table 23: List of the primary and secondary antibodies and their preparation process.

Antibody	**Preparation**
AMPKα1, Akt, PCK-2, and SREBP-1 (Primary antibody)	6µl of the primary antibody mixed with 0.5% BSA solution in 1X PBS (not exceeding the final volume of more than 100µl).
Polyclonal FITC goat anti-rabbit IgG (Secondary antibody)	6µl of secondary antibody added to each flow cytometer tube.

Table 24: Typical conditions and software used for the flow cytometer.

Phosphate-buffered saline solution	PBS solution of 1X.
Paraformaldehyde solution	PFA solution of 2%.
Bovine serum albumin solution	BSA solution of 0.5%.
Triton X-100	0.1%.
Primary antibody	Primary rabbit polyclonal IgG antibody. IgG (AMPKα1, Akt, PCK-2 and SREBP-1).
Secondary antibody	Polyclonal FITC goat anti-rabbit IgG.
Instrument	Cytomics FC500 flow cytometer.
Analysis software	FlowJo v10.0.7.
Data measurement approach	Geometric mean fluorescence intensity (GMFI) and peak.

Data processing:

Principle of gating: The FITC (Fluorescein isothiocyanate) stained cells were first gated for singlets for each observation through the CXP software. The data acquisition for the flow cytometer was carried out by selecting the following parameters viz., area, height, or width for the forward or side scatter. Finally, gating or regions (Figure 21) was achieved through drawing boundaries around the cell population of interest to characterize and quantify the number of cells for each marker observation.

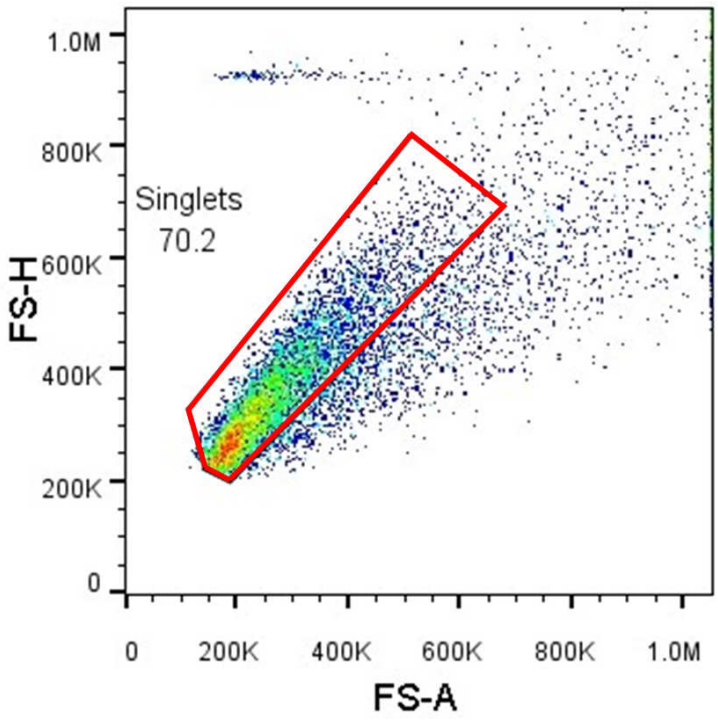

Figure 21: Flow cytometry gating data (The boundary represented in red was set for the populations of interest around the cells using the geometry gate).

Flow cytometric peak/histograms: After setting the principle of gating around the population of interest, the data was acquired by separating the cells into the percentage of positive and negative cells (Figure 22) for each marker analysis. The obtained data was estimated through FlowJo v10.0.7 software, and the peak or histogram events denote the % of cells. Further, the results were expressed as GMFI of FITC.

Note: The greater the magnitude of GMFI of the cells as a population, the greater the expression of particular markers (AMPK1, Akt, PCK-2, and SREBP-1).

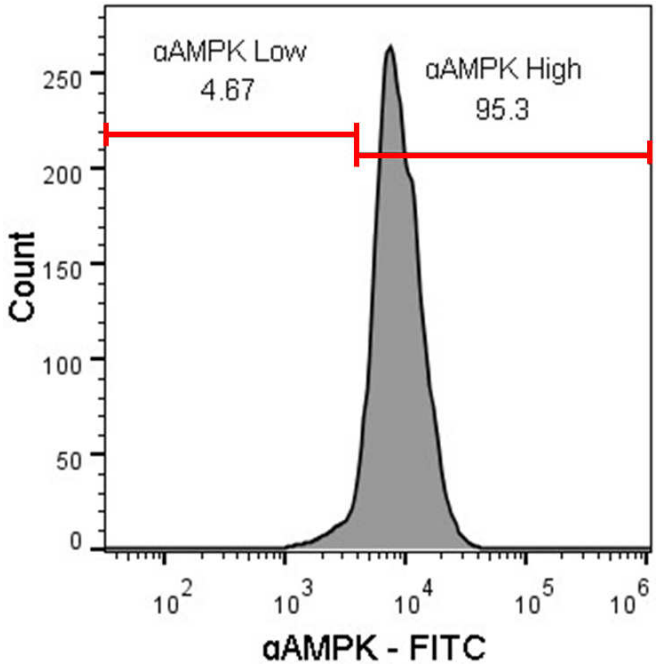

Figure 22: Flow cytometry peak/histogram data showing the percentage of the respective marker.

2.2.9. Data analysis

The data for various parameters was statistically calculated using the software program version 6.0 of '*GraphPad Prism*' and represented as mean ± SEM, performed in triplicate. The one-way ANOVA following Bonferroni multiple as a post hoc statistical tool was used to determine the statistical significance, considering $p < 0.05$ as the limit of the significance.

3. RESULTS

3.1. *In-vivo* study

3.1.1. Study design I

The effect of STZ-induced hyperglycemia on the development of DEN-induced HCC was examined for 12 weeks in this study design.

3.1.1.1. General observation (Weekly body weight, food and water intake and relative liver weight)

The body weight of the normal rats changed significantly on the 9^{th} ($p<0.01$) and from the 10^{th} to 12^{th} ($p<0.001$) week when compared at the start of the study with subsequent weeks. There was no statistical difference for the STZ and/or DEN treated rats within the group compared to the beginning of the study with subsequent weeks. On the other hand, the STZ and DEN administered rats alone showed a significant decrease ($p<0.001$) in body weight compared to normal rats. In comparison to DEN alone rats, the diabetic-hepatocellular carcinoma (STZ+DEN) rats exhibited a rise ($p<0.001$) in body weight (Figure 23). The difference in the absolute food and water consumption for each experimental group are illustrated in figure 24 and 25. The STZ treated rats exhibited a significant rise ($p<0.001$) in food and water intake compared to normal rats. Furthermore, compared to DEN rats, the STZ+DEN rats consumed significantly more food and water ($p<0.01$; $p<0.001$). The STZ and/or DEN rats showed a significant increase in relative liver weight (Table 25) compared to normal rats.

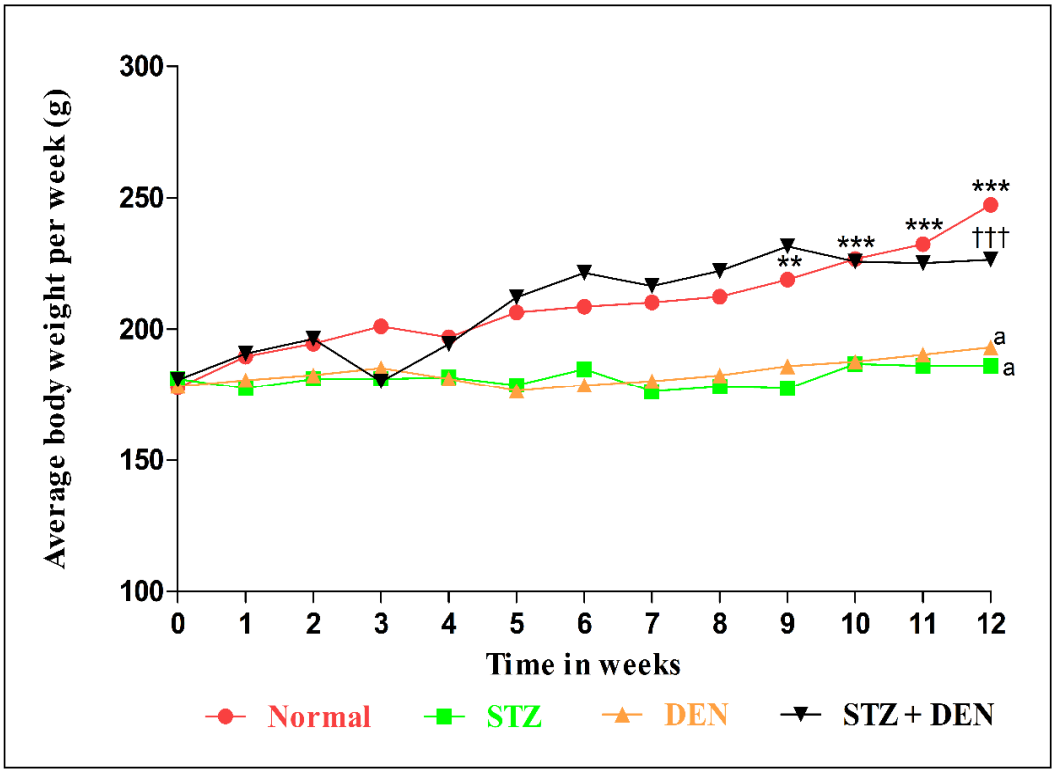

Figure 23 (Average body weight per week for study design I)**:** Values are expressed as average body weight per week (g), where ***p*<0.01, ****p*<0.001 in comparison at the start of the study with subsequent weeks for the normal group, [a]*p*<0.001 in comparison to the normal group and [†††]*p*<0.001 in comparison to DEN group.
STZ, Streptozotocin; DEN, Diethylnitrosamine.

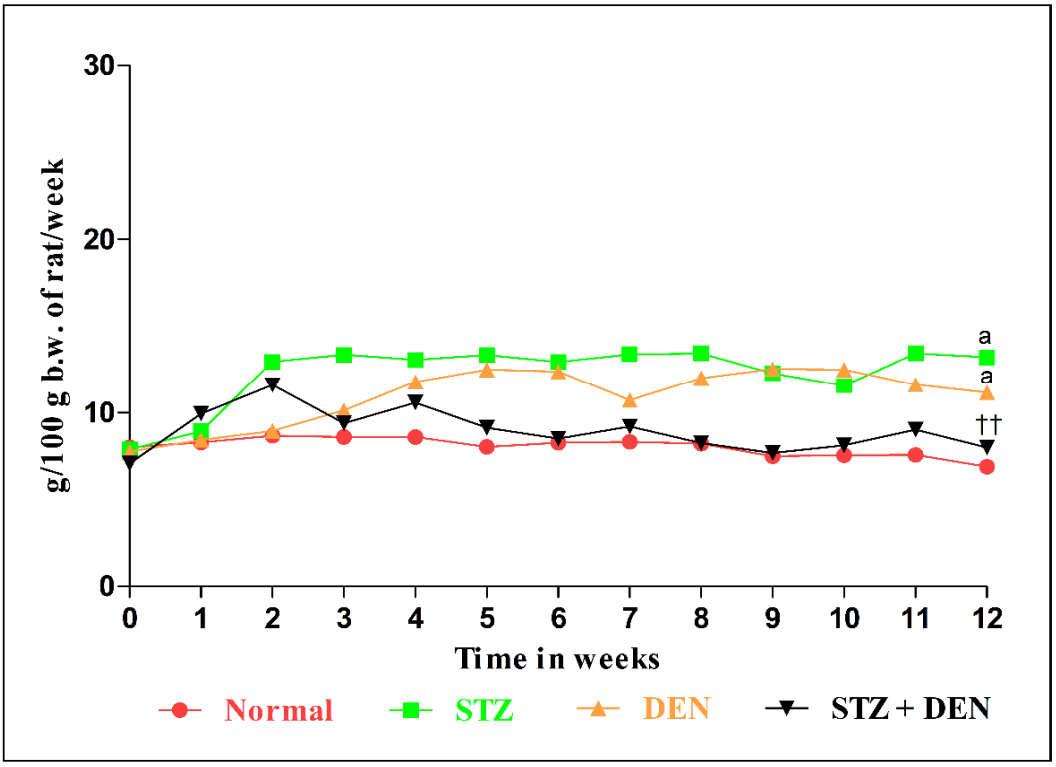

Figure 24 (Relative food consumption per week for study design I)**:** Values are expressed as relative food consumption per week (g/100 g *b.w.* of rat), where $^{a}p<0.001$ in comparison to the normal group and $^{††}p<0.01$ in comparison to DEN group.

STZ, Streptozotocin; DEN, Diethylnitrosamine.

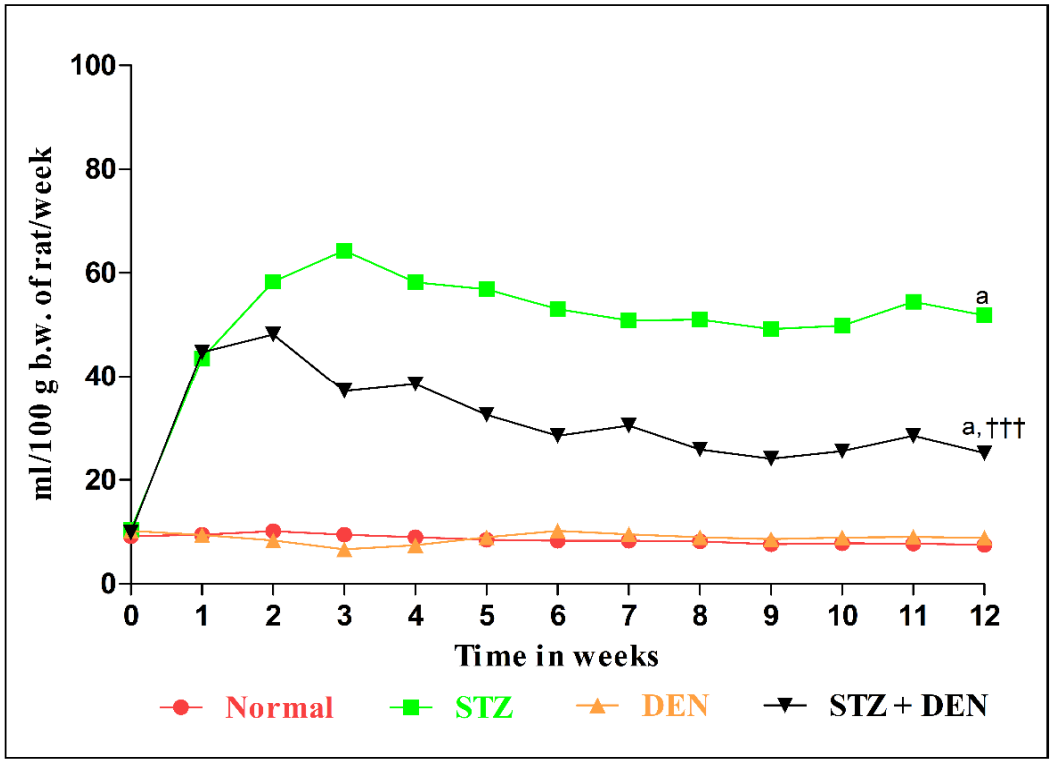

Figure 25 (Relative water consumption per week for study design I)**:** Values are expressed as relative water consumption per week (ml/100 g *b.w.* of rat), where $^{a}p<0.001$ in comparison to normal group and $^{\dagger\dagger\dagger}p<0.001$ in comparison to DEN group.

STZ, Streptozotocin; DEN, Diethylnitrosamine.

3.1.1.2. Study of liver morphology

The gross scale observation about the nodule incidence, multiplicity and size are summarized in table 26. There were no visible hepatocyte nodules in the livers of normal and STZ rats at the end of 12-weeks, whereas DEN alone and STZ+DEN administered groups had multiple carcinoma tumors. In comparison to DEN rats, the STZ+DEN rats had a higher incidence of nodule multiplicity ($p<0.05$) and size.

3.1.1.3. Biochemical parameters

Figure 26 illustrates the glucose levels in various groups either before (Day 0) or after streptozotocin (STZ) induction (weeks 2 and 12). The STZ-induced hyperglycemia was established by significantly elevated ($p<0.001$) glucose levels compared to normal rats at the end of the second week. In comparison to normal rats, STZ and STZ+DEN groups maintained an elevated ($p<0.001$) blood glucose level for the entire 12-weeks period.

As stated in table 25, the diabetic rats (STZ alone) exhibited a significant reduction in serum insulin and an elevation in glycosylated hemoglobin ($p<0.001$) in comparison to normal rats. Furthermore, as compared to normal rats, the STZ-induced rats had a substantial increase in the serum aminotransferases (AST and ALT; $p<0.05$) and phosphatase (ALP; $p<0.001$) along with serum lipid profile (TG, TC and LDL-c; $p<0.001$) as well as a decline ($p<0.001$) in HDL-c (Table 27 and 28). On the other hand, the serum liver dysfunction markers (TB, DB, total protein, albumin, and globulin) and liver-specific bio-markers (GGT and AFP) in the STZ-induced rats were not significantly different from normal rats. In comparison to normal rats, the hepatocellular carcinoma rats (DEN alone) had significantly higher levels ($p<0.001$) of serum aminotransferases and phosphatase except for no changes for albumin and globulin, along with an elevation in serum lipid profile ($p<0.001$) and liver-specific

bio-markers (GGT and AFP; $p<0.001$, $p<0.05$) as represented in table 27 and 28. The diabetic-hepatocellular carcinoma (STZ+DEN) rats reflect the characteristic manifestation of diabetes and cancer, but with a greater degree of severity in biochemical profiles and the number of hepatic nodules than the DEN group alone (Table 25 to 28).

Table 25: The relative liver weight, insulin, and glycosylated hemoglobin (HbA_{1c}) in rats of study design I.

Parameters	I (NC)	II (STZ)	III (DEN)	IV (STZ+DEN)
Relative liver weight (g%)	3.94±0.15	5.88±0.37**	5.76±0.08**	6.79±0.66***
Insulin (µU/ml)	16.11±0.26	5.80±0.20***	16.87±0.21	6.52±0.19***, a
HbA_{1c} (%)	5.30±0.13	8.43±0.24***	5.82±0.16	7.67±0.26***, a

Relative liver weight and the levels of insulin and glycosylated hemoglobin (HbA_{1c}) for study design I. Results are expressed as the mean ± SEM, where** $p<0.01$, *** $p<0.001$ compared to normal group and [a] $p<0.001$ compared to DEN group.

NC, Normal control; STZ, Streptozotocin; DEN, Diethylnitrosamine.

Table 26: Morphometric analysis (Nodule incidence, nodule multiplicity, and size of nodules) of study design I.

Group (Treatment)	Nodule incidence (%)	Nodule multiplicity	Relative nodular size (% of total numbers)		
			<1 mm (%)	1 to 3 mm (%)	>3 mm (%)
III (DEN)	37.5	1.66±0.33	5 (100)	--	--
IV (STZ+DEN)	87.5	5.28±0.68[c]	18 (48.7)	12 (32.4)	07 (18.9)

The gross scale observation (subcapsular greyish white nodules) expressed as nodule incidence, multiplicity and size in hepatocellular carcinoma rats (DEN alone) and diabetic-hepatocellular carcinoma rats (STZ+DEN) for study design I. Results for multiplicity are expressed as the mean ± SEM, where $^{c}p<0.05$ compared to the DEN group.

NC, Normal control; STZ, Streptozotocin; DEN, Diethylnitrosamine.

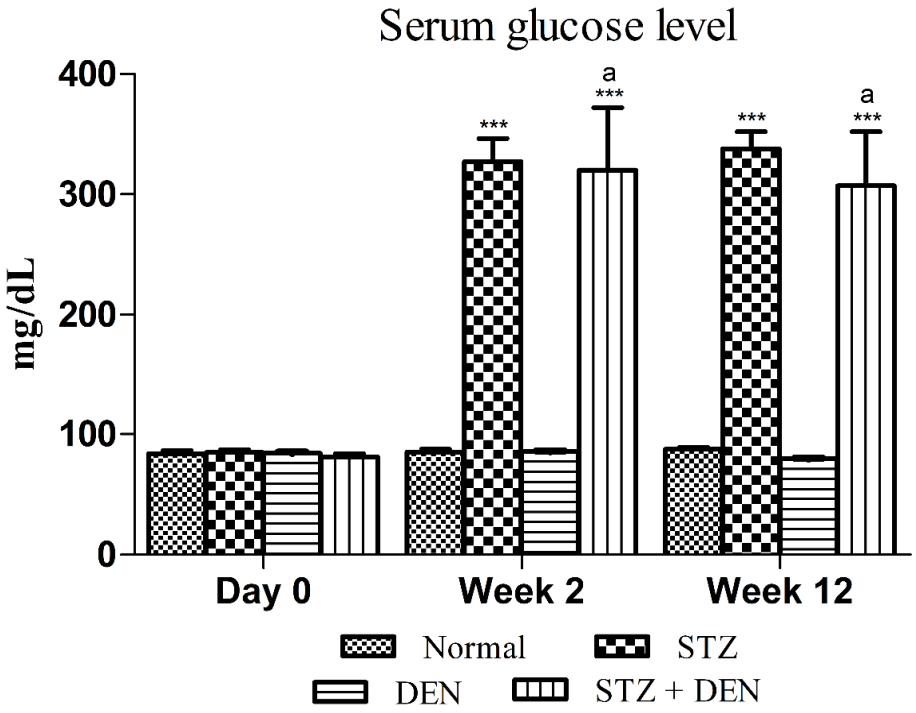

Figure 26 (Serum glucose level for study design I) The glucose level (mg/dL) either before (Day 0) or after streptozotocin (STZ) induction (week 2 and 12) for study design I. Results are expressed as the mean ± SEM, where $^{***}p<0.001$ in comparison to normal group and $^{a}p<0.001$ in comparison to the DEN group.

STZ, Streptozotocin; DEN, Diethylnitrosamine.

Table 27: The serum liver dysfunction markers in rats of study design I.

Parameters	I (NC)	II (STZ)	III (DEN)	IV (STZ+DEN)
AST (IU/L)	55.97±4.16	75.38±3.35*	88.10±3.56***	102.00±7.31***
ALT (IU/L)	47.17±1.81	58.88±3.13*	69.59±1.41***	82.86±3.97$^{***, c}$
ALP (IU/L)	96.11±2.10	163.60±14.50***	155.00±2.26***	178.30±5.36***
TB (mg/dl)	0.32±0.05	0.50±0.06	0.67±0.01***	0.84±0.04***
DB (mg/dl)	0.05±0.005	0.23±0.02	0.40±0.01***	0.50±0.11***
Total protein (mg/dl)	7.01±0.20	6.25±0.18	5.56±0.19***	5.32±0.15***
Albumin (mg/dl)	5.03±0.21	4.45±0.20	4.05±0.34	3.69±0.24**
Globulin (mg/dl)	1.98±0.33	1.80±0.16	1.50±0.32	1.62±0.31

Serum liver dysfunction markers for study design I. Results are expressed as the mean ± SEM, where $^{*}p<0.05$, $^{**}p<0.01$, $^{***}p<0.001$ in comparison to normal group and $^{c}p<0.05$ in comparison to DEN group.

NC, Normal control; STZ, Streptozotocin; DEN, Diethylnitrosamine; AST, Aspartate aminotransferase; ALT, Alanine aminotransferase; ALP, Alkaline phosphatase; TB, Total bilirubin; DB, Direct bilirubin.

Table 28: The serum lipid profile and tumor bio-markers (GGT and AFP) in rats of study design I.

Parameters	I (NC)	II (STZ)	III (DEN)	IV (STZ+DEN)
TG (mg/dL)	47.38±1.78	100.6±5.78***	103.4±3.85***	130.3±9.89$^{***, c}$
TC (mg/dL)	55.50±1.66	130.9±4.45***	135.2±2.38***	151.9±9.89***
HDL-c (mg/dL)	51.25±2.80	39.50±0.77***	35.75±1.14***	40.29±0.94***
LDL-c (mg/dL)	30.38±0.96	63.88±3.55***	66.75±1.59***	71.89±8.64***
GGT (IU/L)	28.85±1.38	37.38±1.14	48.25±2.19***	62.86±4.41$^{***, b}$
AFP (ng/ml)	0.33±0.02	0.37±0.03	0.60±0.01*	0.77±0.11***

Serum lipid profile and tumor bio-markers for study design I. Results are stated as the mean ± SEM, where $^{*}p<0.05$, $^{***}p<0.001$ in comparison to normal group and $^{c}p<0.05$, $^{b}p<0.01$ in comparison to DEN group.

NC, Normal control; STZ, Streptozotocin; DEN, Diethylnitrosamine; TG, Triglycerides; TC, Total cholesterol; HDL-c, High-density lipoprotein cholesterol; LDL-c, Low-density lipoprotein cholesterol; GGT, Gamma-glutamyl transferase; AFP, Alpha-fetoprotein.

3.1.1.4. Macroscopic and histopathological features (H and E; Sirius red)

Macroscopically, the livers of the hepatocellular carcinoma (DEN alone) and diabetic-hepatocellular carcinoma (STZ+DEN) receiving rats showed the presence of visible subcapsular greyish white nodules on the peripheral surface compared to normal and diabetic (STZ alone) rats, which revealed smooth surface without any nodules at the end of 12-weeks (Figure 27A-D).

The histopathological changes supported the biochemical and morphological differences at the end of the 12-week period. Following STZ injection, the liver architecture was slightly disrupted, with congestion in central vein and sinusoids and mild inflammation compared to normal hepatic architecture exhibiting well-preserved hepatocytes, intact globular nucleus, clear lobule margins and cytoplasm (Figure 27a, b). The un-inflamed portal triad depicting the hepatic artery (HA), bile duct (BD), and portal vein (PV) was evident in the normal liver rats compared to the initiation of congestion in the diabetic (STZ alone) administered rats (Figure 27e, f). On the other hand, the STZ+DEN administered rats unveiled marginally distorted hepatic architecture showing congestion in sinusoids, central vein (CV), and portal triad (PT), as well as mild inflammatory cells compared to DEN, treated rats (Figure 27c, d, g, h). Further, the severity of fibrosis in the STZ+DEN rats was increased as indicated by Sirius-red staining compared to DEN-only rats (Figure 28c, d). Quantitative estimate of the proportion of Sirius-red positive area increased significantly ($p<0.001$) for the STZ+DEN administered rats in comparison to DEN alone, which was then substantially higher ($p<0.001$) in comparison to normal rats (Figure 28).

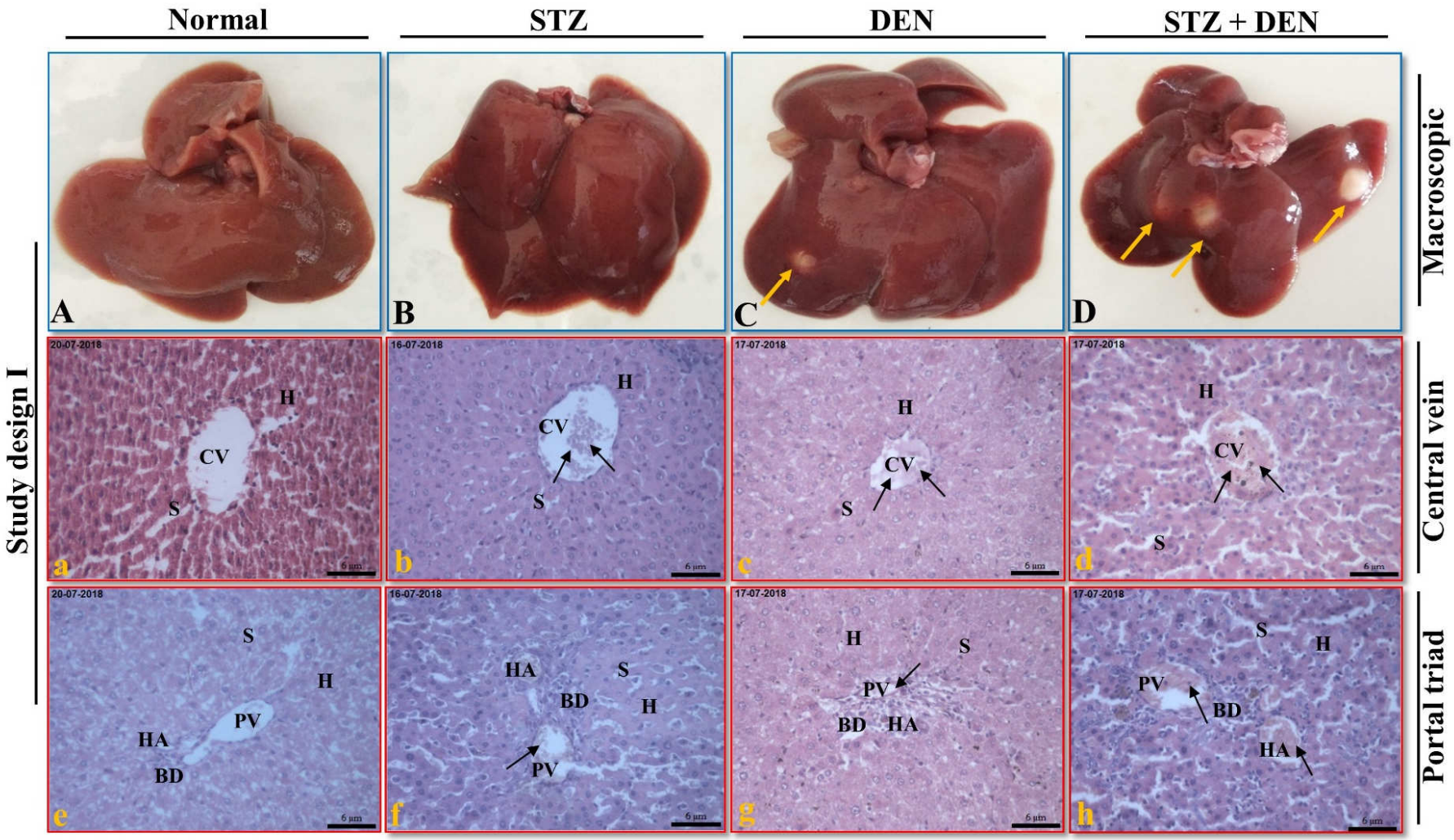
Normal
STZ
DEN
STZ + DEN
Study design I
Macroscopic
Central vein
Portal triad
A
B
C
D
a
b
c
d
e
f
g
h
20-07-2018
16-07-2018
17-07-2018
H
CV
S
HA
BD
PV
6 µm

Figure 27 (Macroscopic appearance and histological characteristics for study design I)**:** The upper panel depicts the liver's gross macroscopic appearance from normal (A), STZ-induced diabetes (B), DEN-induced hepatocellular carcinoma (C) and STZ+DEN-induced diabetic-hepatocellular carcinoma (D) groups after study, where the arrowheads indicate nodules. The middle and lower panel represents the photomicrographs of the liver specimens treated with H and E, which depicts the central vein (CV), sinusoids (S), plates of hepatocytes (H) and portal triad (PT) showing hepatic artery (HA), bile duct (BD), portal vein (PV). Here, the black arrowheads specify CV and PT congestion (Magnification: 200 for the photomicrographs a–h).

STZ, Streptozotocin; DEN, Diethylnitrosamine; CV, Central vein; PT, Portal triad; H, Hepatocytes; BD, Bile duct; S, Sinusoids; PV, Portal vein HA, Hepatic artery.

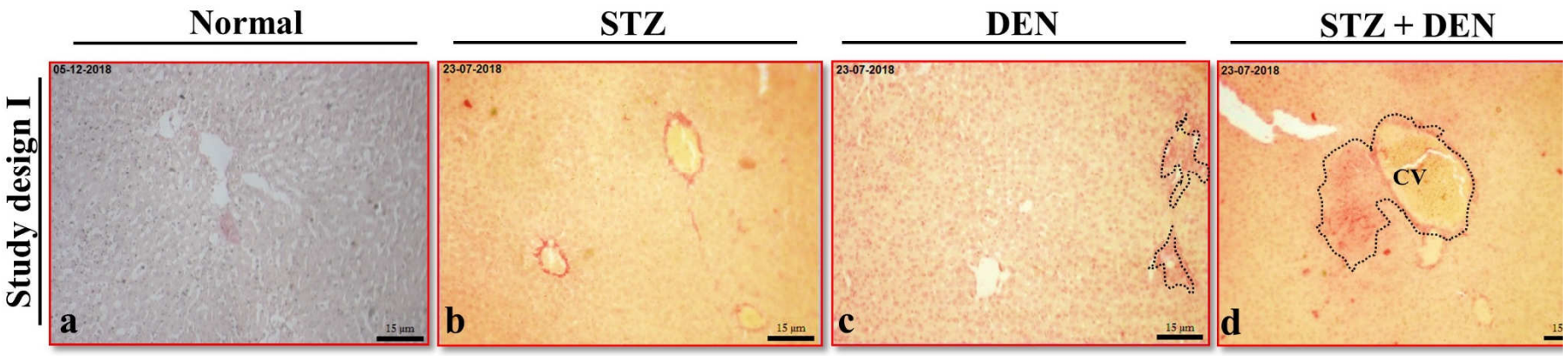
Normal
STZ
DEN
STZ + DEN
Study design I
05-12-2018
23-07-2018
23-07-2018
23-07-2018
a
b
c
d
15 µm
CV

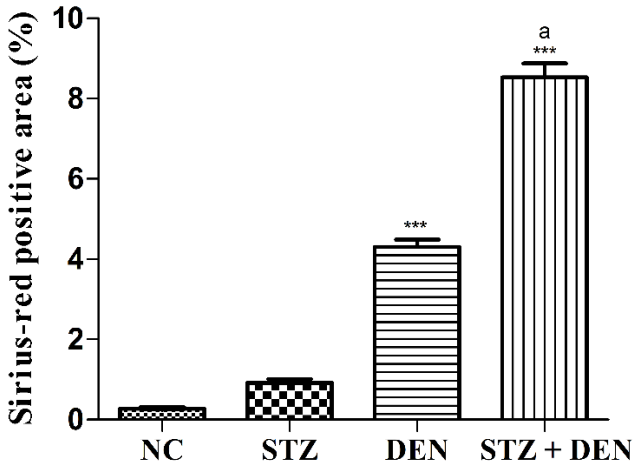
Sirius-red positive area (%)
10
8
6
4
2
0
a
***
***
NC
STZ
DEN
STZ + DEN

Figure 28 (Histological evaluation of hepatic fibrosis evaluated by Sirius red staining for study design I)**:** Representative photomicrographs of the liver sections stained with Sirius red were calculated as the % of Sirius red-positive area for every group with the help of a bar diagram. The hepatic fibrosis was significantly more in STZ+DEN-induced rats compared to DEN-induced rats at the end of 12-weeks. Results are expressed as the mean ± SEM, where $^{***}p<0.001$ compared to the normal group and $^{a}p<0.001$ compared to the DEN group. Here, the dotted lines in black in the photomicrographs 'c' and 'd' show the collagen deposition in the plates of hepatocytes (Magnification: 100 for the photomicrographs a–d).

STZ, Streptozotocin; DEN, Diethylnitrosamine; CV, Central vein.

3.1.2. Study design II

The combined role of α-and β-asarone was evaluated and compared to metformin HCl, a biguanide anti-diabetic agent, for 18 weeks against diabetic-HCC rats. Table 29 compares the effectiveness of the 18-weeks study to the 12-weeks; hereafter, the 18-weeks duration was preferred. The morphological and biochemical changes observed in the 18-weeks study were high in the STZ+DEN treated rats compared to the 12-week one. In addition, histological features between study design I and II reveal metastasis, ballooning hepatocytes, alterations in ground glass and hyperplasia of kupffer cells only during 18 weeks of study with a higher degree of severity.

Table 29: Comparative percentage (%) changes and histopathological characteristics between study design I and II.

Parameters	**STZ+DEN**	
	12-weeks	**18-weeks**
Relative liver weight	89.81	100
Nodule incidence	87.5	100
Nodules <1 mm in diameter	48.7	18.5
Nodules 1–3 mm in diameter	32.4	34.5
Nodules >3 mm in diameter	18.9	47.0
Average no. of nodules	45.67	100
GGT	86.31	100
AFP	28.51	100
Histological features/changes		
Metastasis	–	+
Ballooning hepatocytes	–	+++
Ground glass change	–	++
Kupffer cell hyperplasia	–	++

Comparative percentage (%) alterations (morphological, biochemical analysis, and histological characteristics) were observed in diabetic-HCC rats at the end of the 12- and 18-week duration. The histological features are scored as mild (+), moderate (++), severe (+++), and absent (–).

3.1.2.1. General observation (Weekly body weight, food and water intake and relative liver weight)

The normal rats showed significant changes in body weight on 9^{th} ($p<0.05$), 10^{th} ($p<0.01$), and 11^{th} to 18^{th} ($p<0.001$) week when compared at the start of the study with subsequent weeks. The bodyweight of diabetic alone and diabetic-HCC groups for this design was comparable to the 12-weeks period, where no statistical difference was observed within the group in comparison at the start of the study. However, asarone and metformin-treated groups showed significant changes in body weight on the 9^{th} ($p<0.01$) and from 10^{th} to 18^{th} ($p<0.001$) week when compared at the start of the study with subsequent weeks. On the other hand, the STZ and STZ+DEN administered rats exhibited a substantial decrease ($p<0.001$; $p<0.05$) in body weight compared to normal rats. Compared to STZ+DEN administered rats, both the asarone and metformin-treated groups didn't alter the bodyweight statistically (Figure 29).

The food and water intake alterations for each experimental group are illustrated in figure 30 and 31. The rats treated with STZ and STZ+DEN exhibited a considerable increase ($p<0.001$) in food and water intake compared to normal rats. There was no statistical difference in treatment groups except that water intake was significantly less in metformin-treated rats ($p<0.05$) compared to STZ+DEN rats.

The rats treated with STZ alone and STZ+DEN compared with the normal showed a considerable increase ($p<0.001$) in the relative weight of the liver. Whereas the asarone and metformin-treated groups, when compared with the STZ+DEN, exhibited a substantial decrease ($p< 0.01$; $p< 0.001$) in the relative weight of the liver (Table 30).

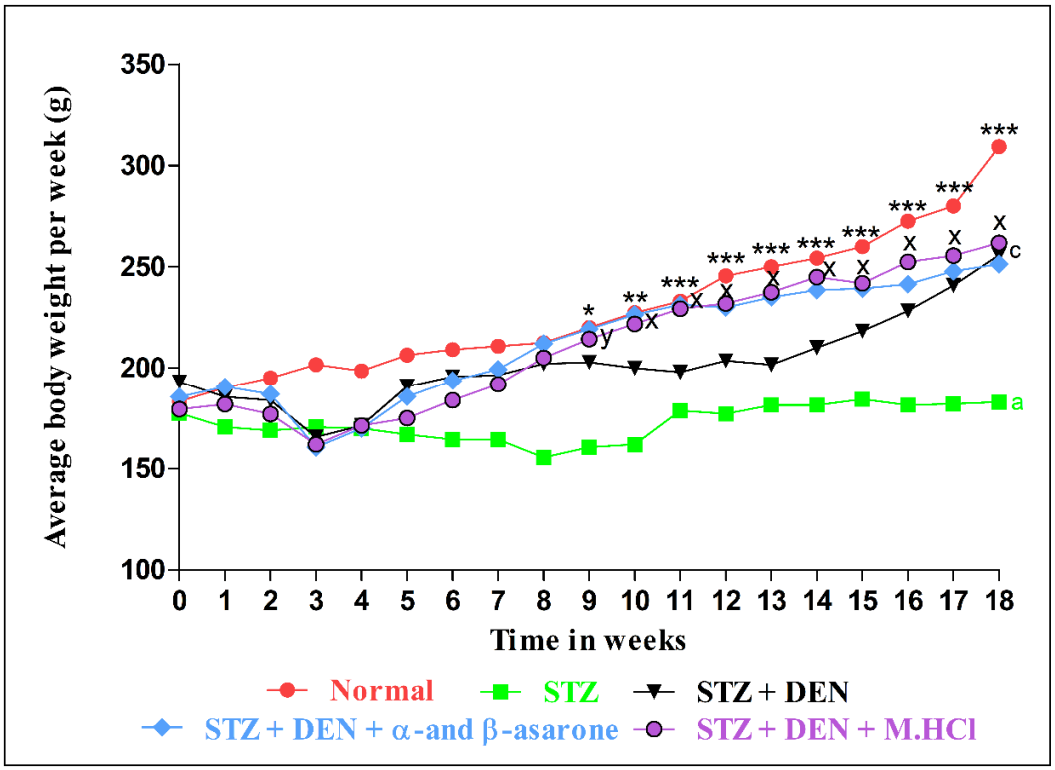

Figure 29 (Average body weight per week for study design II)**:** Values are expressed as average body weight per week (g), where *p<0.05, **p<0.01, ***p<0.001 for normal rats compared at the beginning of the study with subsequent weeks, ^{y}p<0.01 and ^{x}p<0.001 for both the treatment groups (Asarone and Metformin HCl) in comparison at the beginning of the study with subsequent weeks and ^{c}p<0.05 and ^{a}p<0.001 for STZ+DEN and STZ group compared to the normal group.

STZ, Streptozotocin; DEN, Diethylnitrosamine.

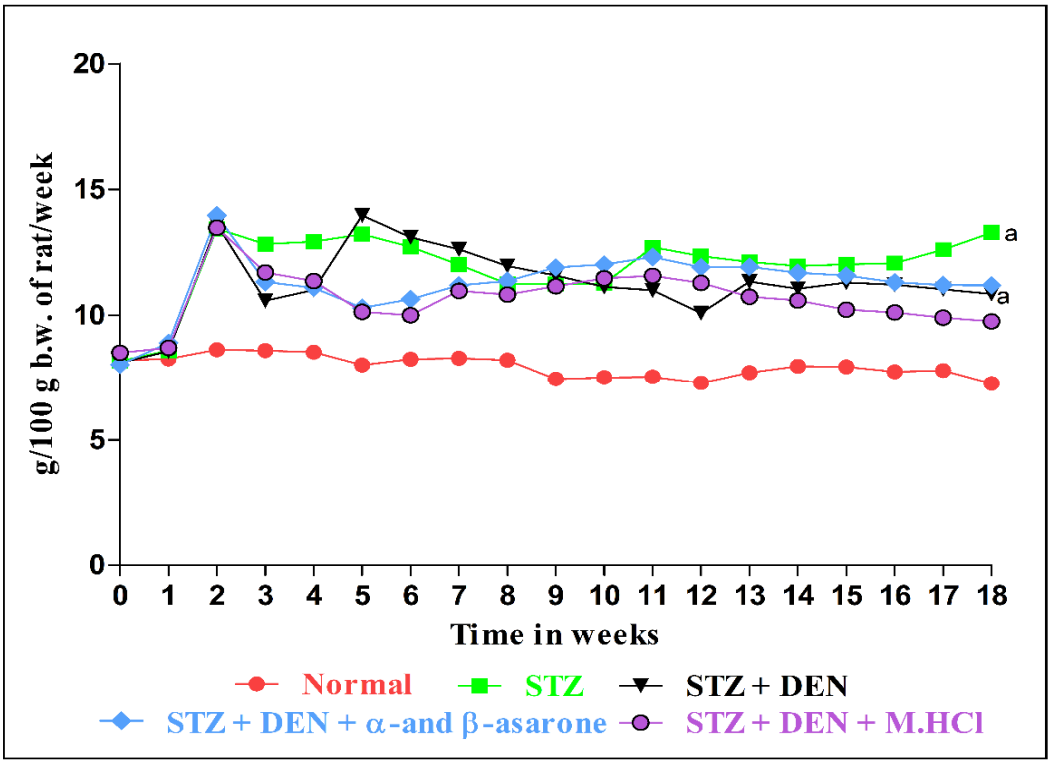

Figure 30 (Relative food consumption per week for study design II)**:** Values are expressed as relative food consumption per week (g/100 g *b.w.* of rat), where [a]*p*<0.001 for rats treated with STZ alone and STZ+DEN compared to the normal group.

STZ, Streptozotocin; DEN, Diethylnitrosamine.

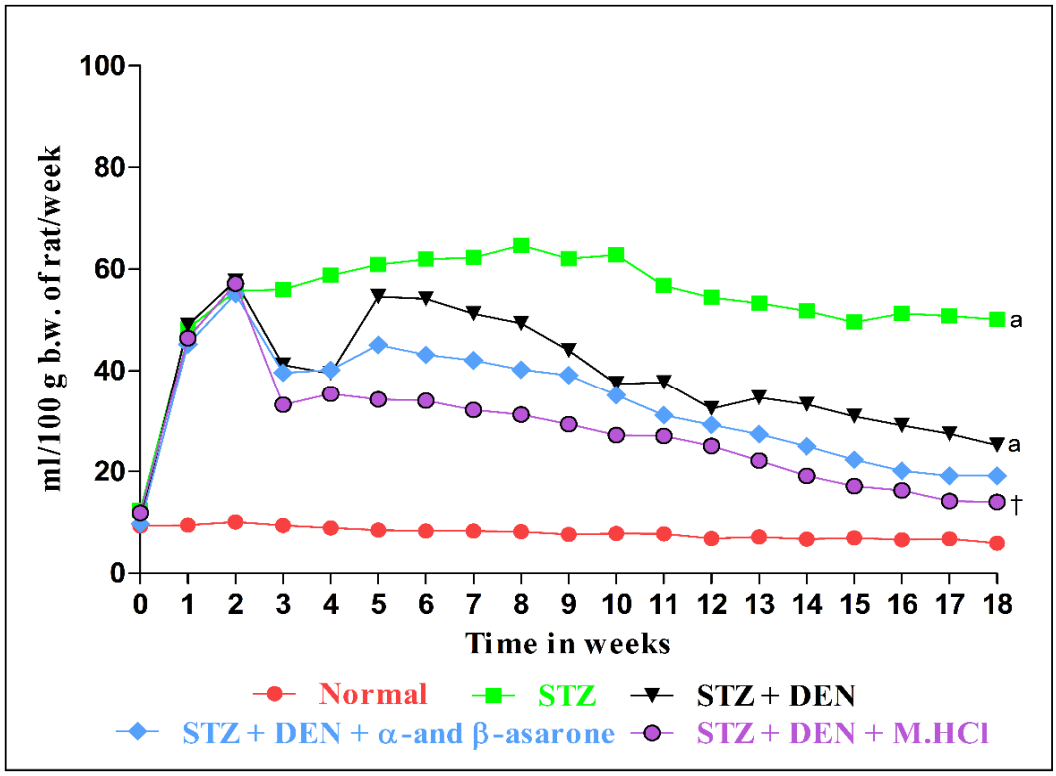

Figure 31 (Relative water consumption per week for study design II)**:** Values are expressed as relative water consumption per week (ml/100 g *b.w.* of rat), where [a]*p*<0.001 in comparison to normal rats and [†]*p*<0.05 in comparison to STZ+DEN rats. STZ, Streptozotocin; DEN, Diethylnitrosamine.

3.1.2.2. Study of liver morphology

Table 31 summarizes the gross scale observation about the nodule incidence, multiplicity and size. The STZ-induced diabetogenic rats did not show the incidence of any hepatocytic subcapsular nodules until the end of 18-weeks. Compared to normal and diabetogenic rats, several subcapsular greyish white nodules were seen in the rats treated with STZ+DEN and treatment groups. Nonetheless, compared to STZ+DEN treated rats, the asarone and metformin-treated groups reduced ($p<0.05$; $p<0.01$) the number and size of the nodules.

3.1.2.3. Biochemical parameters

As stated before, under *Section 3.1.1.3*, the induction of hyperglycemia was confirmed by the elevated levels of serum glucose due to the administration of STZ at the end of the 2nd week. This increase of glucose was sustained until the completion of the study in the animals treated with STZ alone and STZ+DEN. When compared to STZ+DEN-induced rats, the metformin-treated group was successful in controlling the serum glucose levels ($p<0.001$). Similarly, in comparison to STZ+DEN treated rats, the test substance, asarone ($p<0.001$), was also able to control the blood glucose level (Figure 32).

Table 30 shows that STZ alone and STZ+DEN rats had a marked decline ($p<0.001$) in serum insulin levels and a substantial increase ($p<0.001$) in glycosylated hemoglobin as compared to normal rats. Further, a significant increase ($p<0.001$) in the serum liver dysfunction markers such as AST, ALT, ALP, TB, DB, total protein, albumin along with the serum lipid profile such as TG, TC and LDL-c and a decline ($p<0.001$) in HDL-c was observed in the STZ alone and STZ+DEN-induced rats at the end of 18-weeks compared to normal rats (Table 32 and 33). The liver dysfunction marker globulin and HCC specific bio-markers GGT and AFP compared to normal

rats didn't display any significant variations in the STZ treated rats. But, only the STZ+DEN-induced rats showed a substantial increase ($p<0.001$) in HCC specific bio-markers (GGT and AFP) as compared to normal rats (Table 33). In contrast, the asarone and metformin-treated groups showed significant alterations in all the biochemical markers levels with a varying degree compared to the diabetic-hepatocellular carcinoma (STZ+DEN) group (Table 30-33).

Table 30: The relative liver weight, insulin, and glycosylated hemoglobin (HbA_{1c}) in rats of study design II.

Parameters	**I (NC)**	**II (STZ)**	**III (STZ+DEN)**	**IV (STZ+DEN+Asarone)**	**V (STZ+DEN+Metformin)**
Relative liver weight (g%)	3.35±0.08	6.56±0.24***	7.56±0.49***	6.06±0.08$^{***, b}$	4.90±0.12$^{***, a}$
Insulin (µU/ml))	16.57±0.26	4.63±0.18***	5.73±0.27***	10.03±0.49$^{***, a}$	12.60±0.33$^{***, a}$
HbA_{1c} (%)	5.50±0.09	8.90±0.15***	8.10±0.15***	6.89±0.28$^{***, b}$	5.88±0.24^{a}

Effect of Asarone and Metformin HCl on relative liver weight, insulin, and glycosylated hemoglobin (HbA_{1c}) for study design II. Results are expressed as the mean ± SEM, where*** $p<0.001$ in comparison with the normal group and $^{b}p<0.01$, $^{a}p<0.001$ compared to the STZ+DEN-induced group.

NC, Normal control; STZ, Streptozotocin; DEN, Diethylnitrosamine.

Table 31: Morphometric analysis (Nodule incidence, nodule multiplicity, and size of nodules) of study design II.

Group (Treatment)	Nodule incidence (%)	Nodule multiplicity	Relative nodular size (% of total numbers)		
			<1 mm (%)	1 to 3 mm (%)	>3 mm (%)
III (STZ+DEN)	100	10.13±0.71	15 (18.5)	28 (34.5)	38 (47.0)
IV (STZ+DEN+Asarone)	62.5	7.00±0.31[c]	7 (20.0)	12 (34.2)	16 (45.8)
V (STZ+DEN+Metformin)	50	5.75±0.75[b]	4 (17.3)	8 (34.8)	11 (47.9)

The gross scale observation (subcapsular greyish white nodules) expressed as nodule incidence, multiplicity and size, and the effect of Asarone and Metformin HCl for study design II. Results of multiplicity are expressed as the mean ± SEM, where [c]$p<0.05$, [b]$p<0.01$ in comparison to STZ+DEN-induced group.

STZ, Streptozotocin; DEN, Diethylnitrosamine.

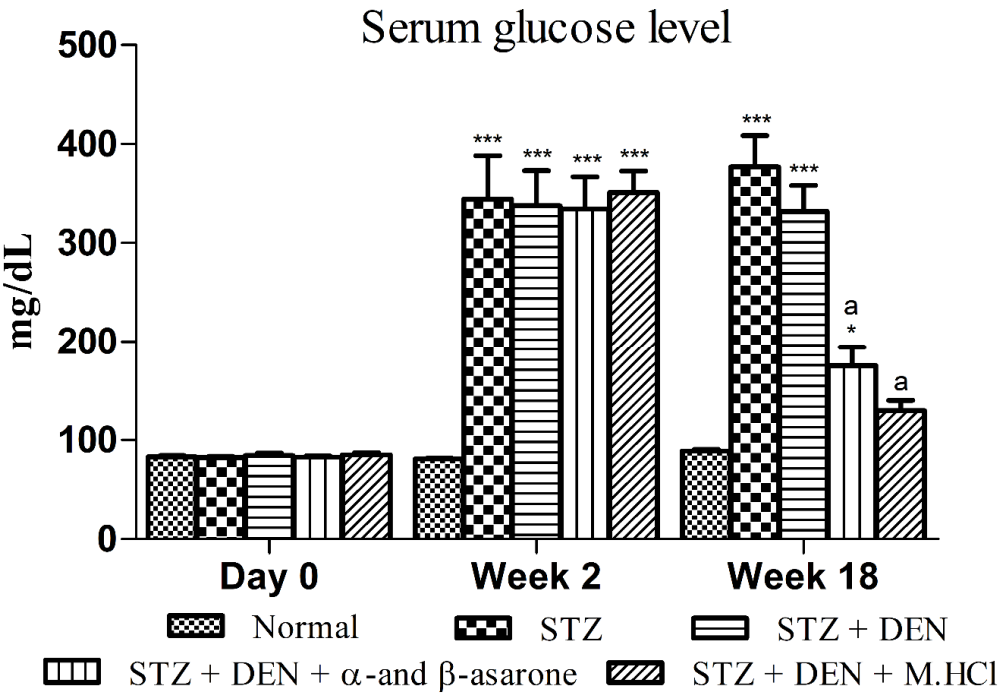

Figure 32 (Serum glucose level for study design II) The glucose level (mg/dL) either before (Day 0) or after streptozotocin (STZ) induction (week 2 and 18) and effect of Asarone and Metformin HCl for study design II. Results are expressed as the mean ± SEM, where *p<0.05, ***p<0.001 compared to the normal group and ^{a}p<0.001 compared to the STZ+DEN-induced group.

STZ, Streptozotocin; DEN, Diethylnitrosamine.

Table 32: The serum liver dysfunction markers in rats of study design II.

Parameters	I (NC)	II (STZ)	III (STZ+DEN)	IV (STZ+DEN+Asarone)	V (STZ+DEN+Metformin)
AST (IU/L)	55.51±0.93	78.09±0.72***	166.50±1.80***	71.40±1.91$^{***, a}$	68.78±1.66$^{***, a}$
ALT (IU/L)	46.62±1.84	64.88±1.55***	176.20±2.41***	65.16±2.05$^{***, a}$	56.01±3.20^{a}
ALP (IU/L)	93.09±0.91	164.80±2.24***	263.70±3.33***	128.70±2.11$^{***, a}$	110.20±5.33$^{**, a}$
TB (mg/dl)	0.33±0.01	0.58±0.01***	1.07±0.04***	0.39±0.04^{a}	0.35±0.02^{a}
DB (mg/dl)	0.07±0.006	0.27±0.01***	0.97±0.02***	0.35±0.01$^{***, a}$	0.14±0.01$^{*, a}$
Total protein (mg/dl)	8.84±0.19	7.18±0.06***	4.76±0.17***	6.32±0.16$^{***, a}$	7.20±0.08$^{***, a}$
Albumin (mg/dl)	5.63±0.16	4.22±0.27***	2.14±0.14***	4.09±0.04$^{***, a}$	4.57±0.12$^{***, a}$
Globulin (mg/dl)	3.33±0.06	2.87±0.11	2.27±0.14***	2.86±0.11^{c}	3.00±0.13^{b}

Effect of Asarone and Metformin HCl on serum dysfunction markers of the liver for study design II. Results are expressed the mean ± SEM, where $^{*}p<0.05$, $^{**}p<0.01$, $^{***}p<0.001$ in comparison to normal group and $^{c}p<0.05$, $^{b}p<0.01$, $^{a}p<0.001$ in comparison to STZ+DEN-induced group. NC, Normal control; STZ, Streptozotocin; DEN, Diethylnitrosamine; AST, Aspartate aminotransferase; ALT, Alanine aminotransferase; ALP, Alkaline phosphatase; TB, Total bilirubin; DB, Direct bilirubin.

Table 33: The serum lipid profile and tumor bio-markers (GGT and AFP) in rats of study design II.

Parameters	I (NC)	II (STZ)	III (STZ+DEN)	IV (STZ+DEN+Asarone)	V (STZ+DEN+Metformin)
TG (mg/dL)	49.00±1.61	103.60±1.91***	138.50±2.91***	105.30±5.30$^{***, a}$	90.50±4.00$^{***, a}$
TC (mg/dL)	57.13±2.03	129.90±1.80***	156.70±2.15***	125.90±3.31$^{***, a}$	94.57±8.24$^{***, a}$
LDL-c (mg/dL)	31.25±0.52	65.20±2.14***	75.67±1.86***	60.79±1.60***	51.24±7.91$^{*, b}$
HDL-c (mg/dL)	57.75±1.50	38.29±0.96***	37.50±0.95***	41.57±0.81***	45.50±2.25$^{***, b}$
GGT (IU/L)	29.50±1.41	35.86±1.59	72.83±2.52***	44.60±3.08$^{***, a}$	38.88±2.72^{a}
AFP (ng/ml)	0.34±0.02	0.42±0.02	2.70±0.10***	1.31±0.02$^{***, a}$	0.99±0.03$^{***, a}$

Effect of Asarone and Metformin HCl on serum lipid profile and tumor bio-markers for study design II. Results are expressed as the mean ± SEM, where $^{*}p<0.05$, $^{***}p<0.001$ in comparison to normal group and $^{b}p<0.01$, $^{a}p<0.001$ in comparison to STZ+DEN-induced group.

NC, Normal control; STZ, Streptozotocin; DEN, Diethylnitrosamine; TG, Triglycerides; TC, Total cholesterol; HDL-c, High-density lipoprotein cholesterol; LDL-c, Low-density lipoprotein cholesterol; GGT, Gamma-glutamyl transferase; AFP, Alpha-fetoprotein.

3.1.2.4. Serum metabolites by ^{1}H-NMR spectroscopy

The characteristic ^{1}H-NMR spectra obtained from the serum samples of different experimental groups are illustrated in figure 33 and 34. These spectra permit the measurements of several metabolites from the region showing strong resonances ranging from 0.0 to 5.3 ppm. In this study, the small metabolites related to glucose, lipid, and amino acid metabolisms such as pyruvate, lactate, creatine, acetate, valine, alanine, and glutamine were quantified to extract more details. The alterations in the metabolite levels detected by ^{1}H-NMR serum analysis present an association with their relevant pathways, as depicted in a schematic diagram (Figure 35).

As shown in table 34, the diabetic animals (STZ alone) showed a substantial reduction in pyruvate ($p<0.05$), alanine ($p<0.01$) and glutamine ($p<0.001$) levels, as well as a rise ($p<0.001$) in acetate levels in comparison to normal animals. Although the STZ-treated group had lower lactate, creatine, and valine levels, the difference was insignificant. Besides, in comparison to the normal rats, the diabetic-HCC rats (STZ+DEN) had elevated levels of pyruvate ($p<0.01$), lactate ($p<0.05$), creatine ($p<0.05$) and acetate ($p<0.001$) as well as decrease levels of alanine ($p<0.05$) and glutamine levels ($p<0.001$). The levels of valine in the STZ+DEN treated rats were not statistically significant compared to normal rats. On the other hand, treatment groups showed significant alterations in the levels of the metabolites with a varying degree compared to the STZ+DEN-induced group. But no such significant changes were observed for alanine in asarone treated, creatine in metformin-treated, and valine for both the treatment groups compared to STZ+DEN-induced rats.

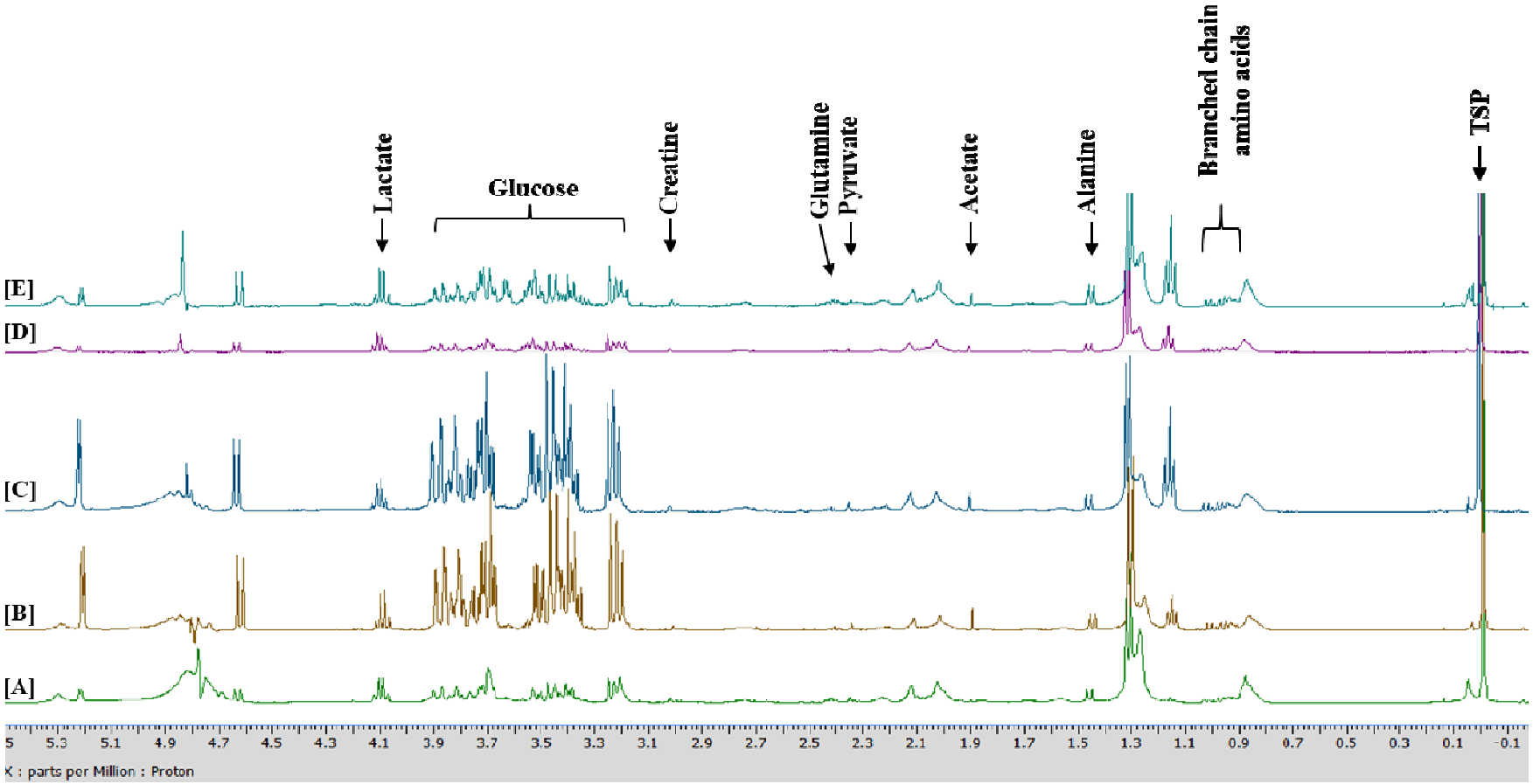

Figure 33 (The ^{1}H-NMR spectra for study design II)**:** Representative spectra produced by 400 MHz 1D (^{1}H-NMR) from the serum samples of normal (A), STZ (B), STZ+DEN (C), STZ+DEN+Asarone (D) and STZ+DEN+Metformin (E). The arrow mark indicates the respective metabolites in each NMR spectra. STZ, Streptozotocin; DEN, Diethylnitrosamine; TSP, Trimethylsilyl 2,2,3,3-tetradeuteropropionic acid.

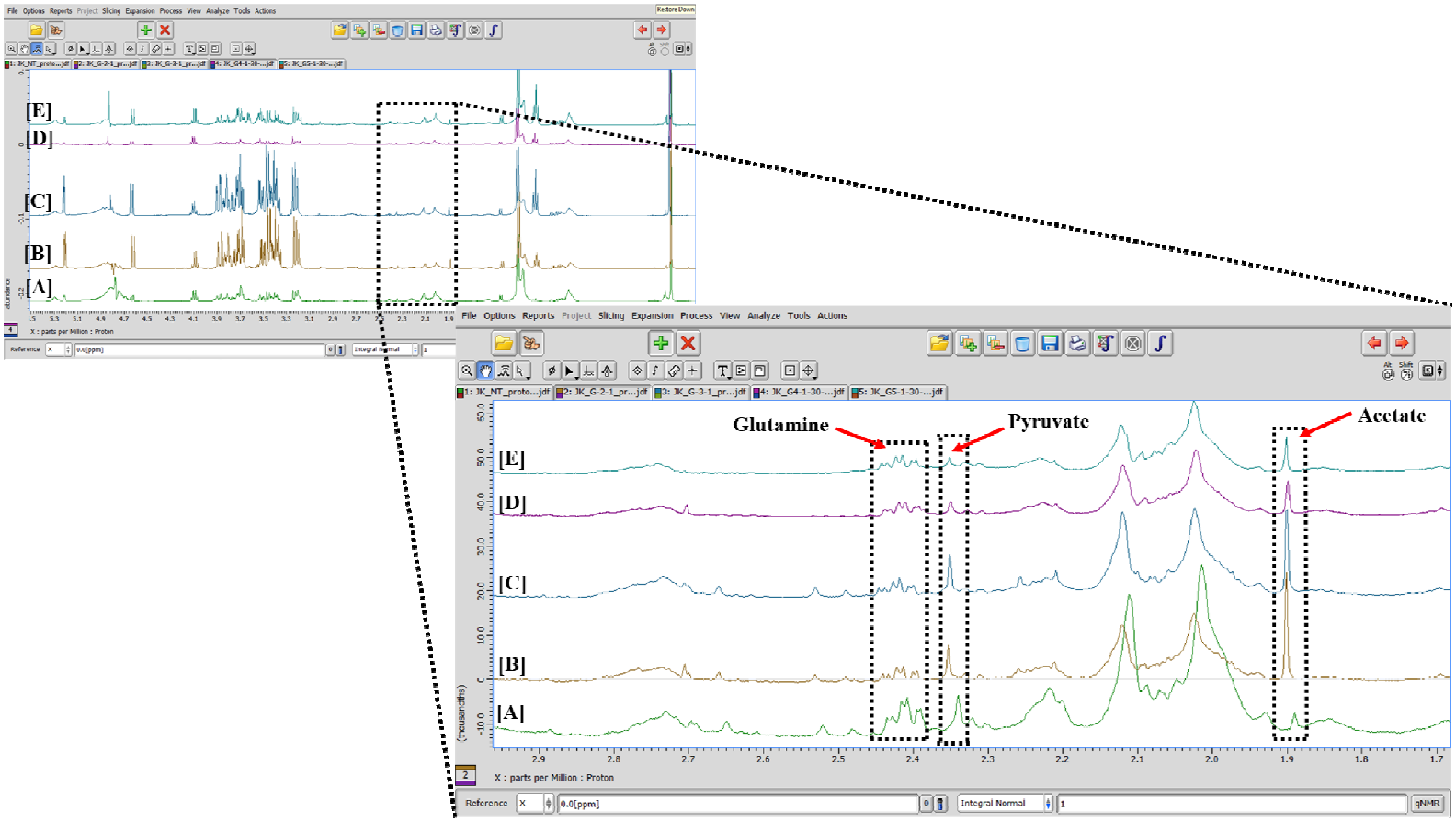

Figure 34 (The extended ^{1}H-NMR spectra for study design II)**:** Representative extended spectra for glutamine, pyruvate and acetate from the serum samples of normal (A), STZ (B), STZ+DEN (C), STZ+DEN+Asarone (D) and STZ+DEN+Metformin (E). STZ, Streptozotocin; DEN, Diethylnitrosamine.

Table 34: The serum metabolites in rats of study design II.

Metabolites/Groups	I (NC)	II (STZ)	III (STZ+DEN)	IV (STZ+DEN+ Asarone)	V (STZ+DEN+ Metformin)	HMDB	KEGG
Energy metabolism							
Pyruvate	1.33±0.03	0.97±0.11*	1.79±0.09**	0.57±0.07$^{***, a}$	0.66±0.02$^{***, a}$	HMDB00243	C00022
Lactate	42.33±1.49	35.50±5.01	74.00±9.17*	46.39±3.46^{c}	44.88±8.76^{c}	HMDB00190	C00186
Creatine	1.27±0.13	0.85±0.05	2.61±0.55*	1.30±0.16^{c}	1.36±0.31	HMDB00064	C00300
Lipid metabolism							
Acetate	0.22±0.02	1.88±0.34***	1.71±0.23***	0.73±0.13^{c}	0.48±0.12^{b}	HMDB00042	C00033
Amino acid metabolism							
Valine	1.60±0.13	1.01±0.32	1.12±0.08	1.47±0.21	1.19±0.17	HMDB00883	C00183
Alanine	6.45±0.27	4.02±0.39**	4.51±0.29*	5.94±0.35	6.78±0.62^{b}	HMDB00161	C00041
Glutamine	8.03±0.16	4.99±0.36***	4.81±0.25***	8.69±0.18^{a}	7.44±0.59^{a}	HMDB00641	C00064

Effect of Asarone and Metformin HCl on different serum metabolites (match with the HMDB and KEGG database) levels for study design II. Results are expressed as the mean ± SEM, where $^{*}p<0.05$, $^{**}p<0.01$, $^{***}p<0.001$ in comparison to normal group and $^{c}p<0.05$, $^{b}p<0.01$, $^{a}p<0.001$ in comparison to STZ+DEN-induced group.

NC, Normal control; STZ, Streptozotocin; DEN, Diethylnitrosamine; KEGG, Kyoto Encyclopedia of Genes and Genomes; HMDB, Human Metabolome Database.

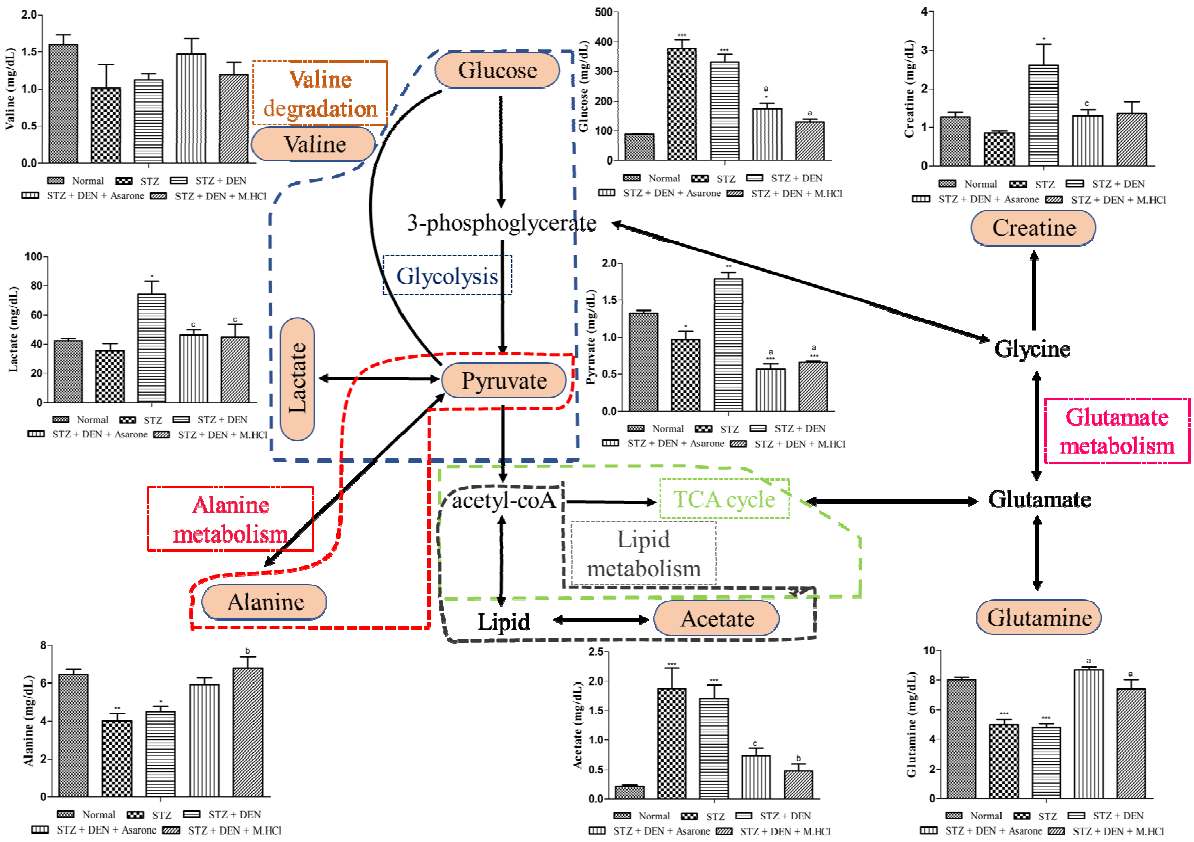

Figure 35 [The metabolic pathway (represented in the dotted boxes) in hepatocarcinogenesis during diabetic condition]: The graphic representation of metabolic pathways (as obtained from the KEGG and HMDB database) with the changes in the levels of metabolites detected (demonstrated in the orange box) by ^{1}H-NMR serum analysis presents the association in diabetic-HCC condition. The changes of the metabolites were quantified and results were expressed in bar diagrams as mean ± SEM, where $^{*}p<0.05$, $^{**}p<0.01$ and $^{***}p<0.001$ in comparison with the normal group and $^{c}p<0.05$, $^{b}p<0.01$, $^{a}p<0.001$ in comparison to STZ+DEN-induced group.

STZ, Streptozotocin; DEN, Diethylnitrosamine; TCA cycle, Tricarboxylic acid cycle.

3.1.2.5. Anti-oxidant activity

As shown in table 35, diabetic rats (STZ alone) had significantly lower levels of SOD, CAT, GSH ($p<0.001$), GPx and Vitamin-C ($p<0.01$), along with an increase ($p<0.001$) in the levels of LPO compared to normal rats. Furthermore, in contrast to normal animals, the STZ+DEN-induced rats exhibited a substantial reduction ($p<0.001$) in SOD, CAT, GPx, GSH, and Vitamin-C levels and an elevation ($p<0.001$) in LPO levels. On the contrary, the asarone and metformin-treated groups showed significant changes in the enzymatic and non-enzymatic anti-oxidants levels with a varying degree compared to the diabetic-hepatocellular carcinoma (STZ+DEN) group.

Table 35: The anti-oxidant enzymes in rats of study design II.

Parameters	**I (NC)**	**II (STZ)**	**III (STZ+DEN)**	**IV (STZ+DEN+Asarone)**	**V (STZ+DEN+Metformin)**
SOD (units/min/mg protein)	8.11±0.05	4.05±0.07***	3.85±0.24***	6.21±0.14$^{***, a}$	6.74±0.29$^{***, a}$
CAT (µmol/min/mg protein)	47.38±1.56	28.79±1.09***	20.39±0.74***	37.71±1.63$^{***, a}$	39.55±0.84$^{***, a}$
LPO (µmol/min/mg protein)	2.49±0.16	6.22±0.19***	7.55±0.16***	4.70±0.13$^{***, a}$	3.93±0.16$^{***, a}$
GPx (µmol/min/mg protein)	2.55±0.12	1.94±0.10**	0.99±0.09***	2.03±0.05$^{*, a}$	2.17±0.11^{a}
GSH (µg/g wet tissue)	21.17±0.39	14.17±0.93***	11.19±0.43***	13.89±0.48$^{***, c}$	15.67±0.19$^{***, a}$
Vitamin-C (mg/g wet tissue)	0.77±0.02	0.62±0.03**	0.33±0.02***	0.50±0.03$^{***, b}$	0.60±0.02$^{**, a}$

Effect of Asarone and Metformin HCl on enzymatic and non-enzymatic anti-oxidants for study design II. Results are expressed as the mean ± SEM, where $^{*}p<0.05$, $^{**}p<0.01$, $^{***}p<0.001$ in comparison to normal group and $^{c}p<0.05$, $^{b}p<0.01$, $^{a}p<0.001$ in comparison to STZ+DEN-induced group. Units are as follows: SOD= 1 unit of activity equals the enzyme reaction that gave 50% inhibition of nitro-blue tetrazolium (NBT) reduction in 1 minute, CAT= µmoles of H_2O_2 utilized in 1 minute, LPO= µmoles of malondialdehyde (MDA) formed in 1 minute, GPx= µmoles of glutathione (GSH) oxidized in 1 minute.

3.1.2.6. Histopathological assessment

The streptozotocin (STZ) induced diabetic livers of the rats appeared dark in color with no visible subcapsular greyish white tumors upon its peripheral surface compared to the normal liver of rats, which revealed a smooth surface without any discoloration at the end of 18-weeks. In contrast, the livers of diabetic-hepatocellular carcinoma (STZ+DEN) rats exhibited growth and the presence of foci on the outermost layer as well as numerous subcapsular greyish white tumors, which are typical hallmarks of hepatocarcinoma. Furthermore, compared to STZ+DEN-induced rats, the treatment groups showed a reduced occurrence of hepatic nodules (Figure 36A-E).

The normal rat's liver histology exhibited characteristic hepatic structure, including well-preserved hepatocytes described by the presence of central vein (CV), clear lobule margins and cytoplasm along with intact globular nucleus and an un-inflamed portal triad (PT) that included portal vein (PV), bile duct (BD) and hepatic artery (HA) (Figure 36a, f). The single intra-peritoneal injection of STZ in the diabetic group revealed a moderately disturbed hepatic architecture showing congestion in CV, PT, and sinusoids (Figure 36b, g) with severe inflammation (Figure 37a). This further prompt necrosis (Figure 37e), ensuing in the accumulation and infiltration of lymphocytes as observed between the plates of hepatocytes. Furthermore, stage 1 fibrosis was evident and confirmed through Sirius red staining, where the expansion of fibrosis was observed into a few portal areas without any septa in the STZ injected group (Figure 36l).

On the other hand, the diabetic-HCC rats (STZ+DEN) showed complete loss of the hepatic architecture with deformed cellular boundaries. In addition, the rats exhibited severe congestion in the CV, sinusoids, and PT (Figure 36c, h) along with

the signs of inflammation (Figure 37b), resulting in the infiltration of leukocytes, hemorrhage, necrosis (spotty) (Figure 37f) and fibrosis (Figure 36m) alike to STZ alone with increased intensity. Nevertheless, histologically, the incidence of numerous neoplastic cells (confirmed HCC), ballooning hepatocytes (Figure 38d), cellular hyperplasia (Figure 39b) along with the presence of bridging necrosis (Figure 38a), changes in the ground glass (Figure 39a), cholestasis, growth of the kupffer cell (Figure 39b), and centrilobular degeneration were more prominent at 18-weeks in the STZ+DEN-induced rats. Furthermore, the stages of fibrosis patterns (F1 to F3) identified from the tumor, and non-tumor sections of the STZ+DEN-induced group were assessed through Sirius red staining (Figure 39c-e). This progressive fibrosis followed by cirrhosis (Figure 39f) lastly develops HCC, where the presence of a cluster of satellite tumoral cells with irregular hepatocytes was observed and confirmed with H and E staining in STZ+DEN-induced rats (Figure 39g).

The extent of the toxic effect of histopathological architecture in STZ+DEN-induced rats was decreased in asarone and metformin-treated groups (Figure 36, 37, and 38). In contrast to STZ+DEN-induced rats, the presence of few histopathological features was reversed following treatment with asarone and metformin. They were alterations in the ground glass, growth of the kupffer cell, and metastasis (as metastasis towards the lung as observed in few cases of STZ+DEN-induced rats). Besides these, all the other histopathological hallmarks of hepatocarcinoma were significantly decreased following treatment with metformin and, to a lesser extent, following treatment with asarone (Table 36).

Additionally, the quantitative estimation of fibrosis (expressed as a percentage of Sirius-red positive area; assessed by Sirius-red staining) in comparison to normal rats was statistically elevated for the STZ alone ($p<0.05$) and STZ+DEN-induced

(p<0.001) animals. On the contrary, the percentage of Sirius-red positive area was significantly decreased (p<0.001) in the asarone and metformin-treated groups when compared to STZ+DEN administered rats (Figure 36). Furthermore, the increased inflammation score (score out of 3) in the STZ+DEN-induced rats was significantly reduced (p<0.05; p<0.01) when treated with the test compounds asarone and metformin (Figure 37). The histologically observed ballooning hepatocytes prominent at 18-weeks of study in the STZ+DEN-induced rats were quantified, where the increase in the ballooning score (score out of 2) was significantly decreased (p<0.05) only in the metformin-treated rats (Figure 38).

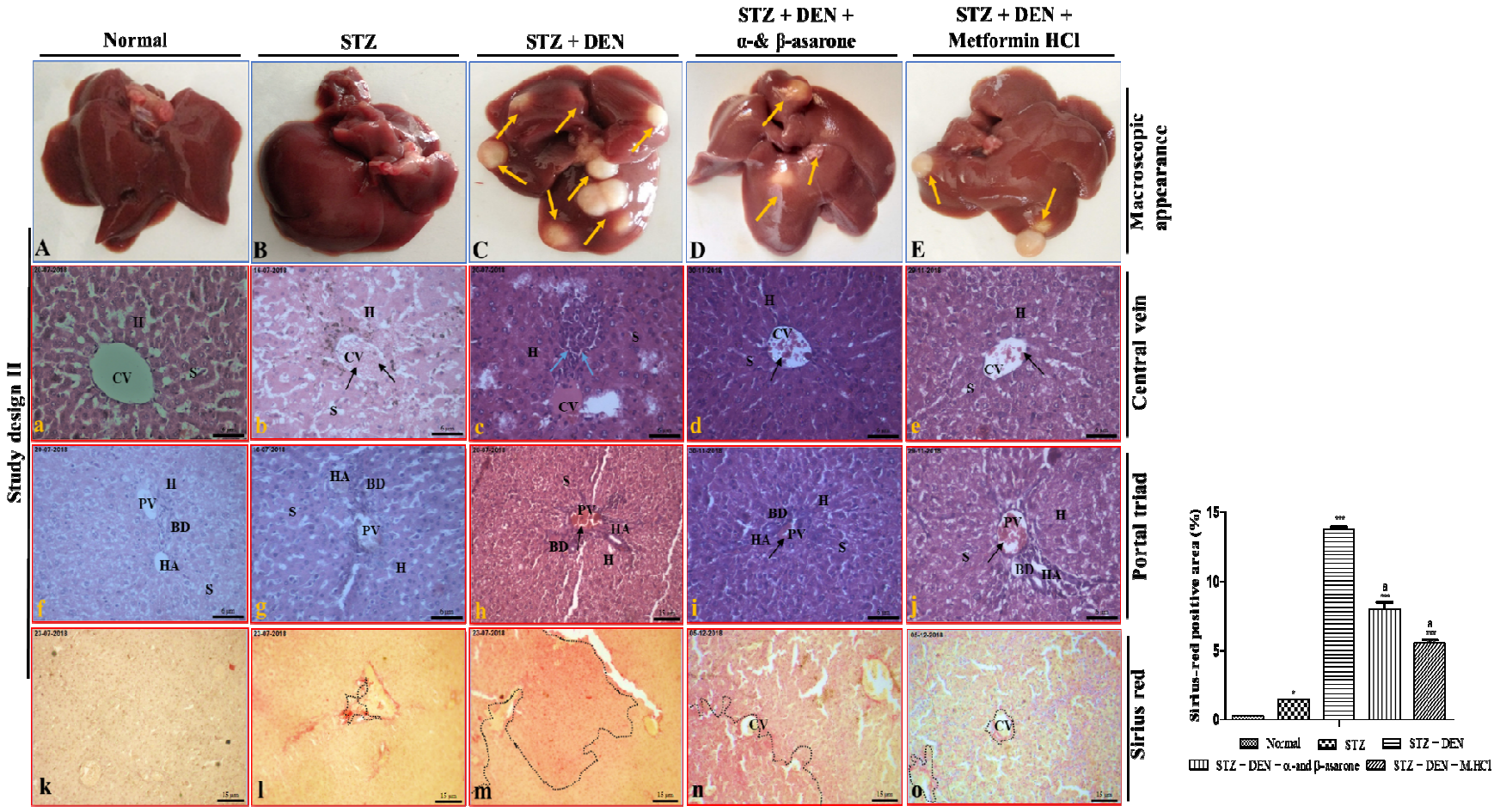
Normal
STZ
STZ + DEN
STZ + DEN + α-& β-asarone
STZ + DEN + Metformin HCl
Study design II
Macroscopic appearance
Central vein
Portal triad
Sirius red
A
B
C
D
E
a
b
c
d
e
f
g
h
i
j
k
l
m
n
o
H
CV
S
PV
BD
HA
Sirius-red positive area (%)
Normal
STZ
STZ – DEN
STZ – DEN – α-and β-asarone
STZ – DEN – M.HCl

Figure 36 (Macroscopic appearance and histological characteristics for study design II)**:** Macroscopic and histopathological features of different experimental groups for study design II. The top panel of the collage represents the overall morphological aspects of normal rat liver (A), STZ-induced diabetic rat liver (B), STZ+DEN-induced diabetic-hepatocellular carcinoma rat liver (C), STZ+DEN+Asarone treated rat liver (D), and STZ+DEN+Metformin treated rat liver (E) after 18-weeks experiment (arrowheads designates nodules). The two mid horizontal panels (a–j) represents the hematoxylin-eosin (H and E) stained liver sections, which depict the central vein (CV) showing sinusoids (S) and hepatocytic plates (H) as well as a portal triad (PT) depicting the bile duct (BD), hepatic artery (HA), and portal vein (PV). Here, the black arrowheads represent the CV and PT congestion, whereas the blue arrowheads indicate lymphocytic cell aggregation and invasion as well as necrosis. The Sirius red-stained liver sections (k–o) in the lowermost horizontal row indicate hepatocytic plates. The collagen deposition is shown by the black dotted lines in the photomicrographs (l–o). (Magnification: 200 for the photomicrographs a–g, i & j; Magnification: 100 for the photomicrographs h, k–o). The hepatic fibrosis was calculated as the percentage of Sirius red positive area as shown in the bar diagram. Results are expressed as the mean ± SEM, where $^{*}p<0.05$, $^{***}p<0.001$ compared to the normal group and $^{a}p<0.001$ compared to STZ+DEN-induced group.

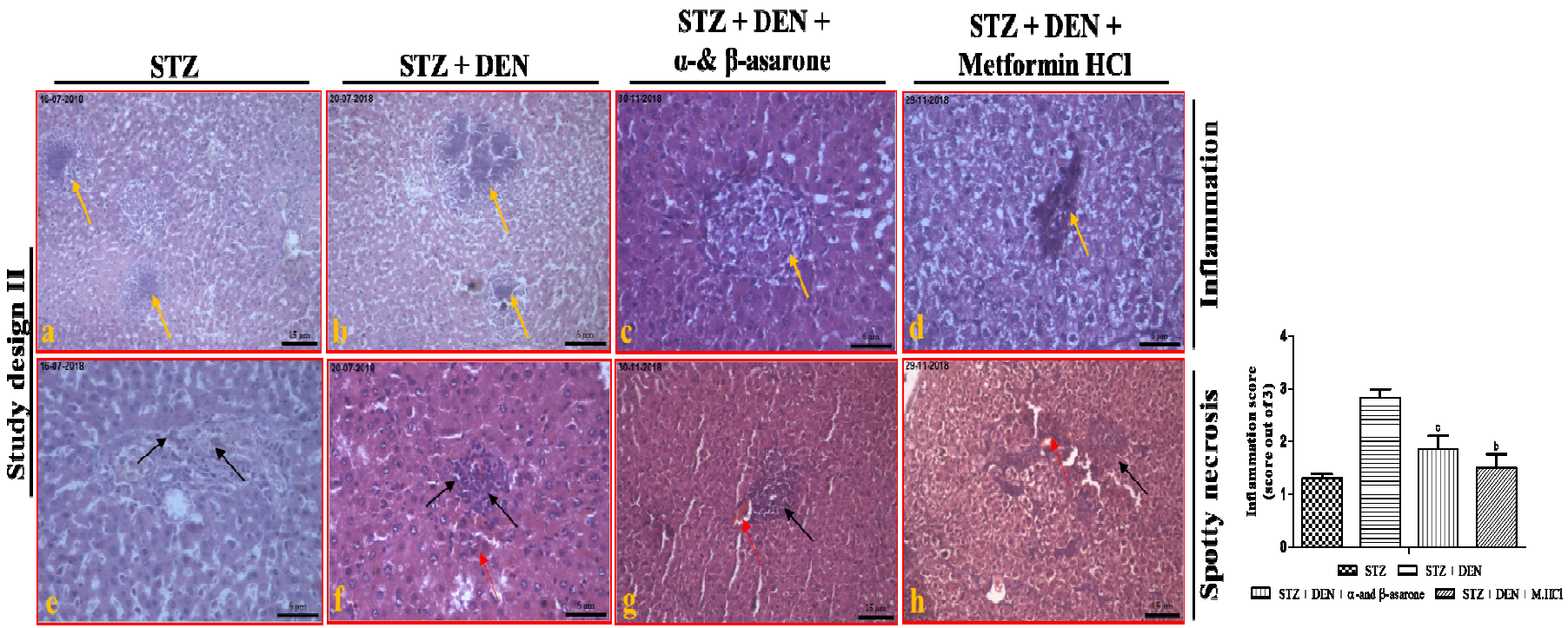

Figure 37 (Histology of non-tumor region for study design II)**:** Representative H and E staining photomicrographs from the non-tumor sections of liver showing inflammation and spotty necrosis for study design II. The yellow arrowheads depict cellular infiltration leading to inflammation; the black arrowheads depict spotty necrosis, and the red arrowheads represent focal hemorrhage. (Magnification: 100 for the photomicrographs a, g & h Magnification: 200 for the photomicrographs b–f). Further, the inflammation score was calculated and represented as the mean ± SEM, where $^{c}p<0.05$ $^{b}p<0.01$ in comparison to the STZ+DEN-induced group.

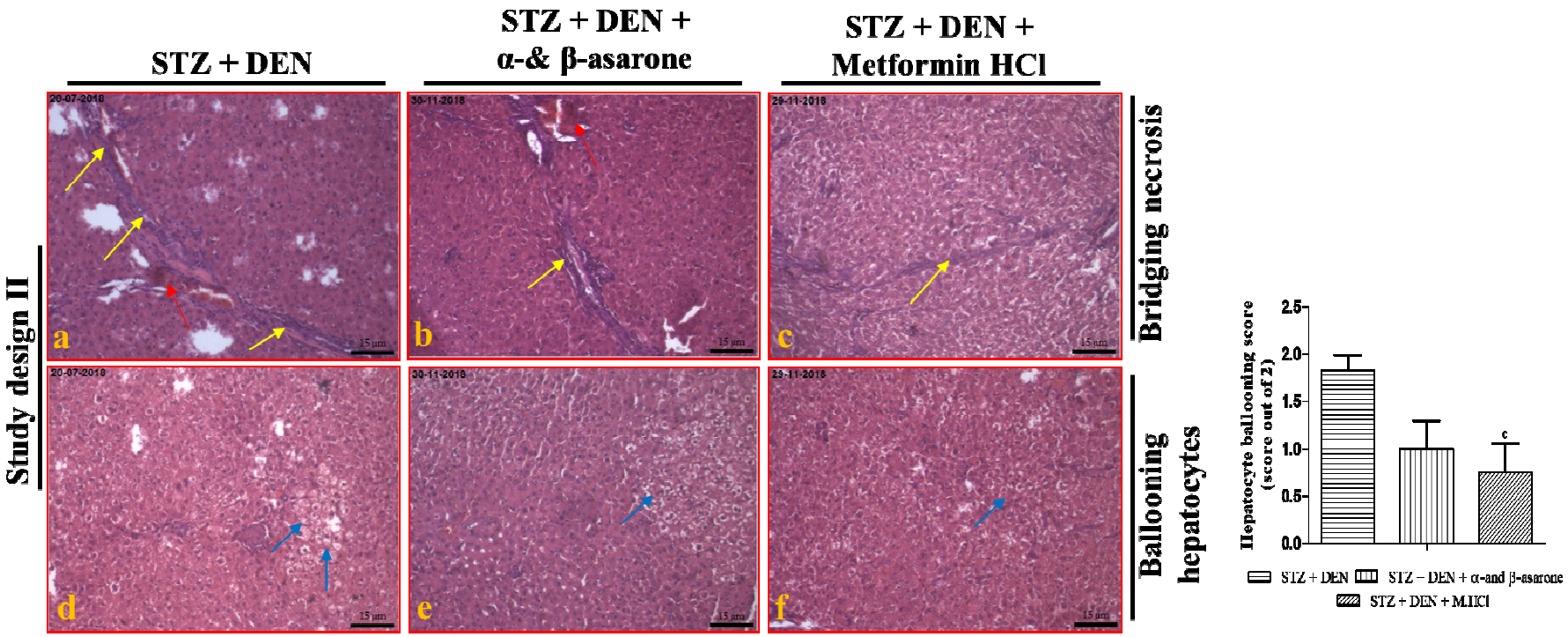

Figure 38 (Histology of tumor region for study design II)**:** Representative H and E staining photomicrographs from the tumor sections of liver showing bridging necrosis and ballooning hepatocytes for study design II. Here, the yellow arrowheads depict bridging necrosis; the red arrowheads depict focal hemorrhage, and the blue arrowheads represent enlarged and round hepatocytic cells showing ballooning hepatocytes with clear cytoplasm. (Magnification: 100 for the photomicrographs a–f). Further, the ballooning hepatocytes score was calculated and represented as the mean ± SEM, where $^{c}p<0.05$ compared to the STZ+DEN-induced group.

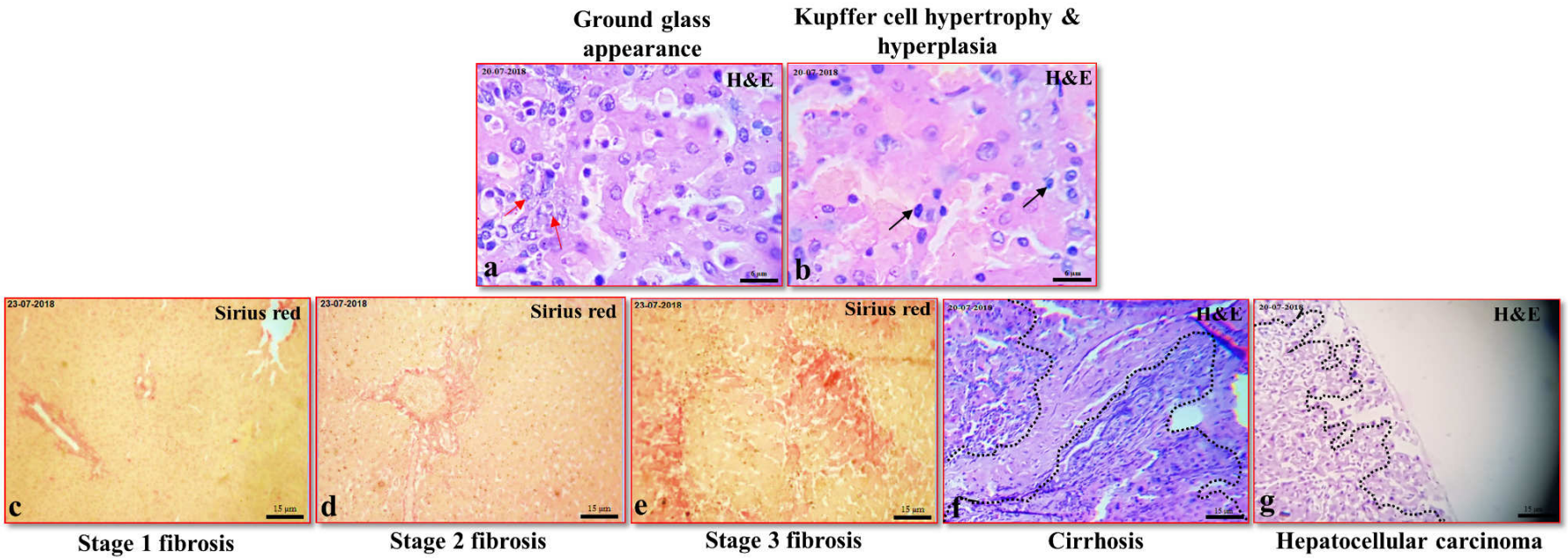

Figure 39 (Fibrosis, cirrhosis, and HCC features for study design II)**:** Representative H and E staining photomicrographs from the tumor and non-tumor sections of diabetic-HCC livers. The photomicrographs show the different stages of fibrosis (Stage 1 to 3), cirrhosis and hepatocellular carcinoma (HCC) sequentially. Here, the red arrowheads depict ground glass appearance; the black arrowheads depict the growth of kupffer cells, and the dotted lines in black exhibited well-defined cirrhosis (f) and the presence of a cluster of satellite nodular cells with asymmetrical hepatocytic cells (g). (Magnification: 200 for the photomicrographs a & b; Magnification: 100 for the photomicrographs c–g).

Table 36: Histopathological characteristics of the liver of study design II.

Histological features/changes	II (STZ)	III (STZ+DEN)	IV (STZ+DEN+Asarone)	V (STZ+DEN+Metformin)
Stage (F1/F2/F3)	6/1/0	1/1/4	2/2/3	4/2/2
Metastasis	–	+	–	–
Central vein & sinusoidal congestion	++	+++	+	+
Inflammation	++	+++	++	++
Focal hemorrhage	++	+++	+	+
Ballooning hepatocytes	–	+++	+	+
Altered hepatic foci	–	+++	+	+
Spotty necrosis	+	+++	++	+
Portal triaditis	+	+++	+	+
Ground glass change	–	++	–	–
Kupffer cell hyperplasia	–	++	–	–
Cirrhosis	–	++	+	+
Hepatocellular dysplasia	–	+++	+	+
Hepatocellular carcinoma	–	+++	++	+

The severity of different histological characteristics was scored based on absent (–), severe (+++), moderate (++), and mild (+). The scoring/stage of liver fibrosis as assessed by Sirius red staining are based on the following criteria where F1: the growth of fibrosis into a few portal areas without the presence of septa; F2: the growth of fibrosis in most of the portal areas with an infrequent portal to portal (P–P) bridging and F3: the growth of fibrosis in almost all of the portal areas with clear portal to central (P–C) and portal to portal (P–P) bridging.

3.2. *In-vitro* study

3.2.1. Cytotoxicity assay

The HepG2 cells were treated with various concentrations of α and β-asarone (0.12 to 1.92 mM), as well as metformin HCl (1.6 to 25.6 mM) for 48-h and cytotoxicity evaluated by the MTT assay. Based on the concentrations (0.12 to 1.92 mM) of the α-asarone, significant inhibition of cell viability was observed compared to untreated cells (Figure 40A). For β-asarone, it exhibited marked inhibition of cell viability with concentrations from 0.48 to 1.92 mM compared to untreated cells (Figure 40B). Furthermore, metformin HCl significantly reduced the viability of HepG2 cells in a dose-dependent manner (1.6 to 25.6 mM) compared to untreated in the 48-h treatment (Figure 40C).

Figure 41A-D shows the comparative morphology of HepG2 cells in the untreated and treatment groups (α-asarone, β-asarone, and metformin). The HepG2 cells cultured for 48-h in the untreated group had a high concentration with adherent properties aggregating in small cellular colonies. It was also observed that few HepG2 cells in the untreated group build up, forming a multi-layered appearance. However, the cell morphology in the treatment groups showed a characteristic dose-dependent decrease in density with a small round body owing to cellular shrinkage. In addition, the presence of detached non-viable HepG2 cells was observed as the concentration increases in the treatment groups. The morphology of the cells exposed to asarone and metformin supported the results showing cell cytotoxicity and growth inhibition. Henceforth, these results indicate that asarone and metformin reduce viability and modifies the morphology of HepG2 cells.

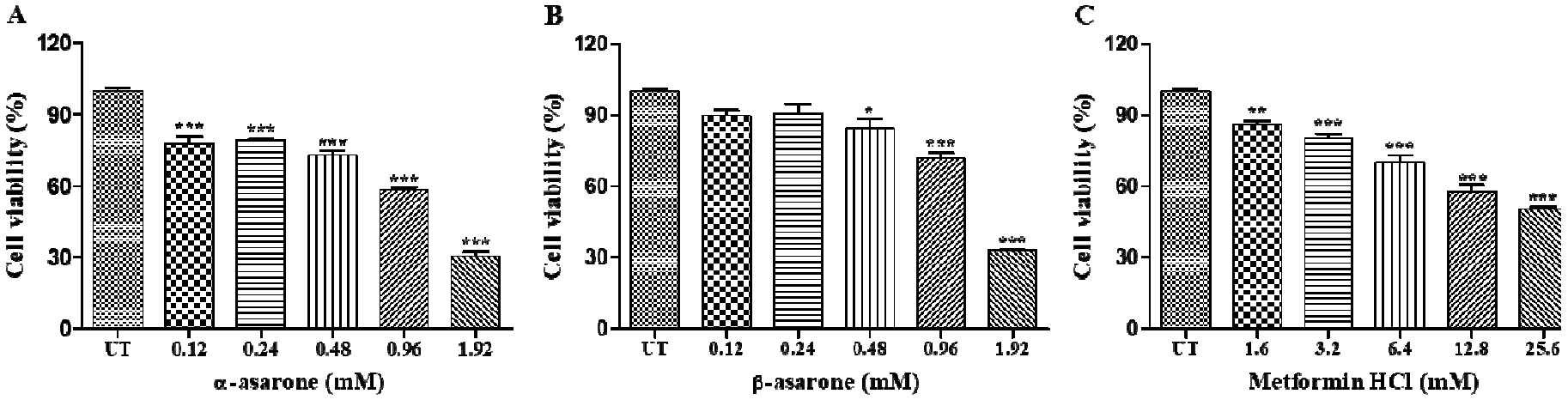

Figure 40 (Asarone and Metformin inhibit the viability of human HepG2 cells): (A-C) Cells were treated with an indicated drug concentration of α-asarone, β-asarone and metformin HCl for 48-h. The results were calculated and expressed as mean ± SEM for triplicate experiments, where $^{*}p<0.05$, $^{**}p<0.01$, $^{***}p<0.001$ in comparison to untreated (UT) group.

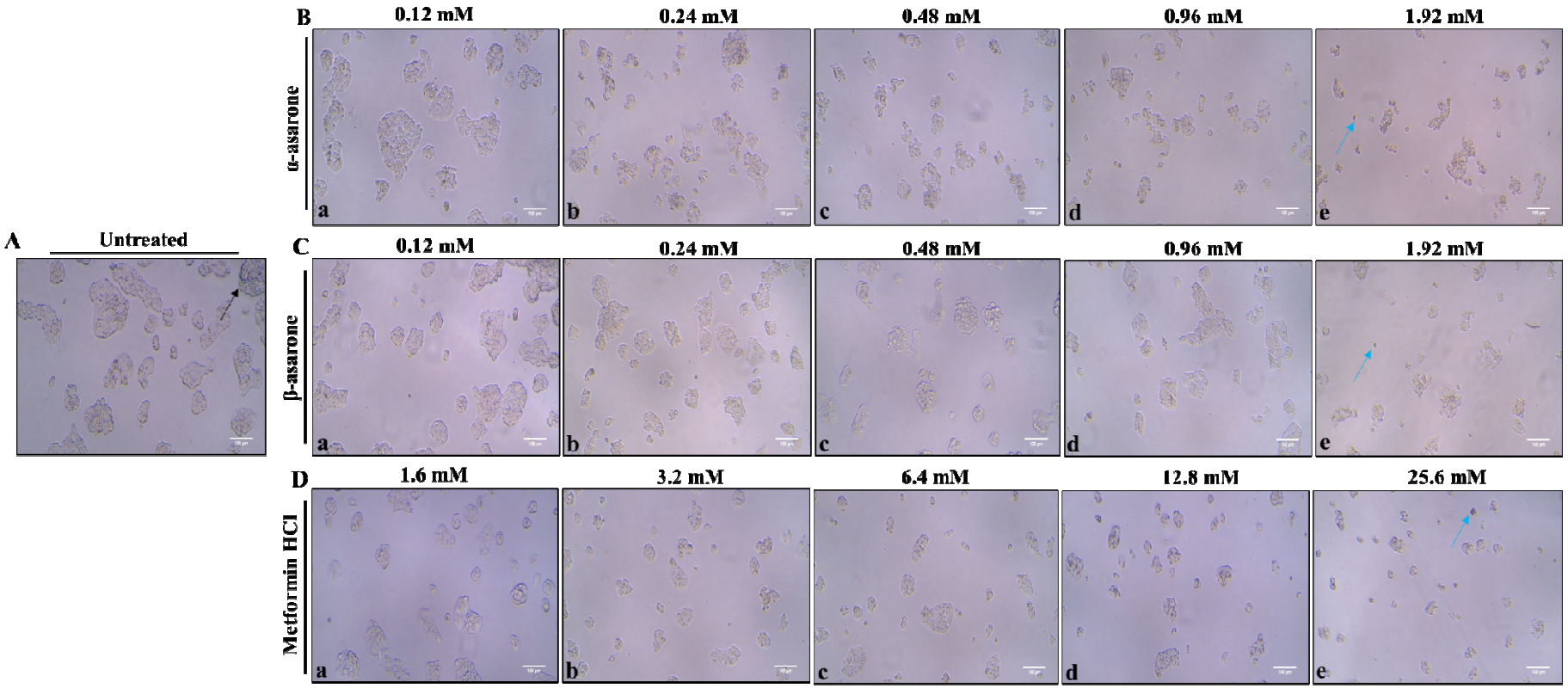

Figure 41 (Asarone and Metformin modify the morphology of human HepG2 cells)**:** The changes of HepG2 cell morphology shown as representative images were observed by an inverted microscope (100 µm). (A) Untreated group, the cells had a high concentration with adherent properties showing epithelial-like morphology (black arrowhead indicates multi-layered appearance). Whereas the cells in the treatment groups, asarone (B, C), and metformin (D) were round (small body), low density, and presence of detached non-viable cells (blue arrowhead) as the concentration increases (a-e).

3.2.2. Cell proliferation assay

The effect of glucose on HepG2 cell growth was examined by measuring changes in percentage proliferation. For this, the HepG2 cells were cultured under different glucose conditions for 48 and 96-h. A time-dependent elevation in growth or viability of the HepG2 cells was found when incubated with a high glucose concentration (25 mM) compared to the cells cultured in normal glucose (5 mM) as measured by MTT assay. In addition, the HepG2 cells in high glucose concentration exhibited the formation of adherent cell colonies as detected under an inverted microscope (Figure 42). These findings suggest that a high-glucose environment promotes HepG2 cell growth.

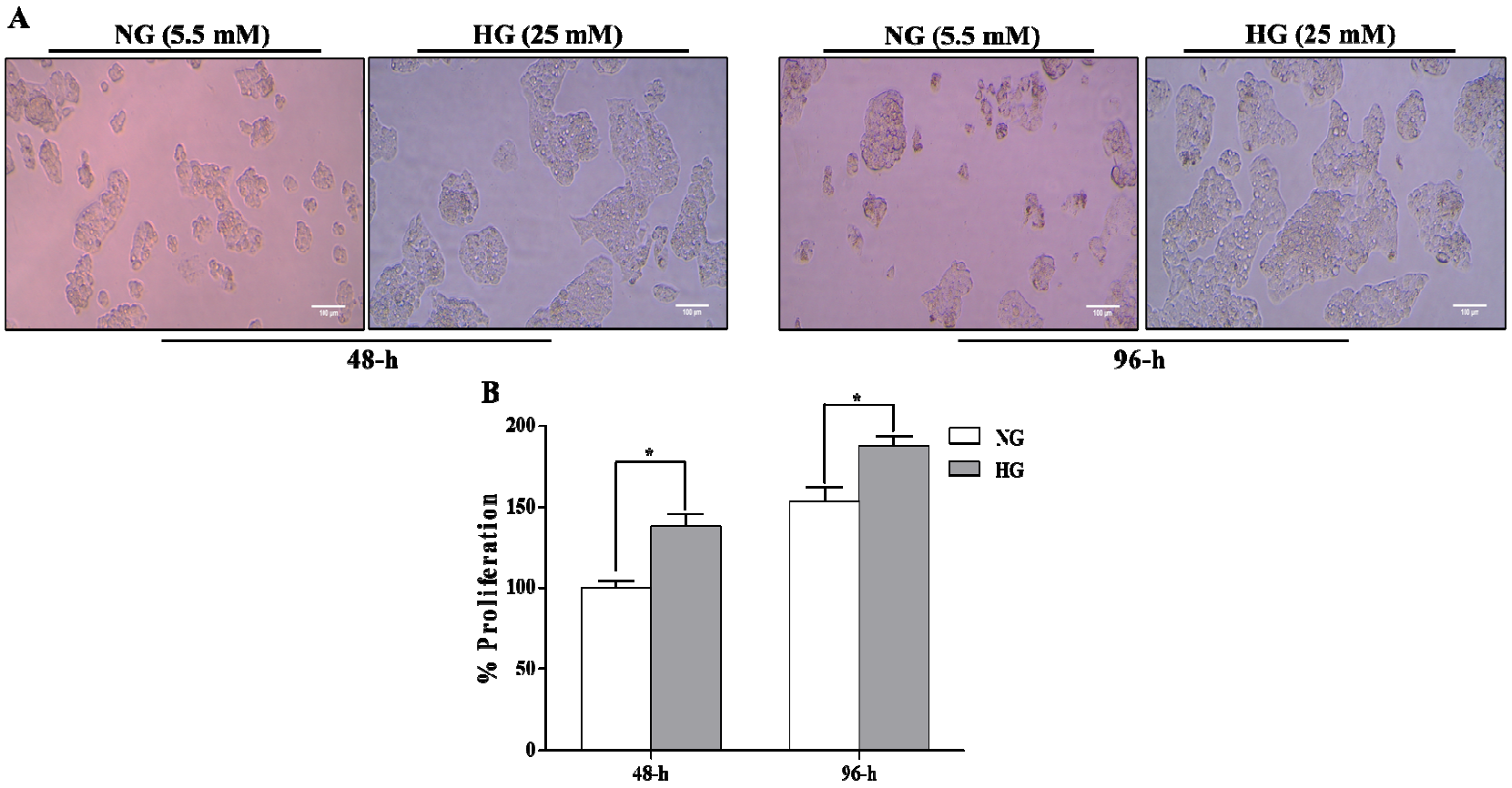

Figure 42 (HepG2 cells proliferate more in a hyperglycemic condition)**:** (A, B) HepG2 cells were grown for 48 and 96 hours in normal and high glucose conditions (NG; 5.5 mM, HG; 25 mM). Afterwards, the changes in the percentage of proliferation were determined by MTT assay. The results were calculated and expressed as mean ± SEM for triplicate experiments, where $^{*}p<0.05$ compared as indicated.